MTG16, A TARGET OF THE t(16;21), CONTRIBUTES TO MURINE LYMPHOID DEVELOPMENT

By

Aubrey Ann Salvino Hunt

Dissertation

Submitted to the Faculty of the

Graduate School of Vanderbilt University

in partial fulfillment of the requirements

for the degree of

DOCTOR OF PHILOSOPHY

in

Biochemistry

May, 2013

Nashville, Tennessee

Approved:

Professor Scott W. Hiebert

Professor Bruce Carter

Assistant Professor Utpal Davé

Professor Luc Van Kaer

To Colin, Luke, and Sam, for late nights, short weekends, and unending patience.

To Morgann, my mom Beth, and my dad Frank, for walking me to the car, no matter what time of the night.

ACKNOWLEDGEMENTS

I would like to thank my mentor, Dr. Scott Hiebert, for my education as a scientist and, perhaps more importantly, his support and patience throughout the many stages of my graduate career. I would like to extend that gratitude to past and current members of the Hiebert laboratory, all of who played an integral role in my growth. A special thank you to Dr. Mike Engel, who sparked my interest in Myeloid Translocation Genes, and Dr. Isabel Moreno-Miralles, who taught me all about mouse hematopoietic techniques; without these two, I would have been lost as I began my graduate career. Drs. Amy Moore, Srividya Bhaskara, Laura DeBusk, Chris Williams, and Alyssa Summers answered many technical questions and provided immense support at various stages of my education. Ryan Ice, Jialing Yuan, and Steven Pierce provided valuable technical support and helped make it possible for me to work, even when the centrifuge wouldn't open or my computer was acting funny. Finally, I would like to acknowledge my fellow graduate students, Sarah Knutson, Tiffany Farmer, Christina Wells, Jonathan Kaiser, and particularly Melissa Fischer, who has been my partner throughout the past five years. Melissa contributed the most significantly to my work, often sharing reagents, her time, and a sympathetic ear. My graduate career would have been very different without her.

Thank you to the members of my thesis committee, Dr. Utpal Dave, Dr. Luc Van Kaer, Dr. Zu-Wen Sun, and Dr. Bruce Carter, for all their advice and important questions. Thank you also to members of the Dave lab, who have been an important source of technical advice and reagents. In particular, I would like to acknowledge Dr. Susan

Cleveland who always has time to help; she has become an important mentor and friend. I would also like to thank other member laboratories of the Leukemia Interest Group, many of whom have provided important insight and reagents.

I would like to thank the various core facilities at Vanderbilt who have made my work possible. In particular, I would like to acknowledge the Vanderbilt Flow Cytometry Core and David Flaherty and Brittany Mortlock. Dave and Brittany had a hand in many of these experiments and became great friends along the way.

I would like to thank the Vanderbilt MSTP and the director, Terry Dermody, for giving me the opportunity to pursue this education. I would also like to thank the MSTP Leadership team and support staff for facilitating all of the aspects of my education. I would like to thank the Department of Biochemistry, including our administrator Marlene Jayne, the Director of Graduate Studies Dr. Dave Cortez and particularly our grants administrator Robert Dortch for his help in writing and funding my F30.

On a personal note, I would like to thank my friends and family for all of their support over the last seven years. To my MSTP colleagues, Britney, Katy, Ali, Erin, Mica, and Elizabeth, for your support in good times and bad. To my network of Vanderbilt friends, especially Allison, Chandni, and Melissa, for years of support even from far away. To Colin, for everything. And last but not least to my parents, who are my reason for being here. Thank you to you all.

Financially, this work was supported by NIH grants T32 GM07347 (Medical Scientist Training Program), F30 HL093993, RO1 CA64140, and RO1 HL088494.

TABLE OF CONTENTS

LIST OF TABLES

Table Page

LIST OF FIGURES

LIST OF ABBREVIATIONS

AD	Activation Domain
ALL	Acute Lymphocytic Leukemia
AML	Acute Myeloid Leukemia
Bcl6	B-cell Lymphoma 6
bHLH	basic-Helix-Loop-Helix
CBF	Core Binding Factor
CFU-S	Colony Forming Unit Spleen
ChIP	Chromatin Immunoprecipitation
CLP	Common Lymphoid Progenitor
CMP	Common Myeloid Progenitor
CSL	CBF1-Supressor of Hairless-Lag
DN	Double Negative
DP	Double Positive
EBF1	Early B-cell Factor
ETO	Eight-Twenty-one
ETP	Early Thymocyte Progenitor
FLT3	fms-Like Tyrosine Kinase 3
Gfi1	Growth-factor Independent 1
GMP	Granulocyte-Monocyte Progenitor
HAT	Histone Acetyltransferase
HDAC	Histone Deacetylase

HEB	HeLa E-box Binding Factor
ID	Inhibitor of Differentiation
IgH	Immunoglobulin Heavy Chain
IgL	Immunoglobulin Light Chain
IL7R	Interleukin 7 Receptor
Lin	Lineage
LMPP	Lymphoid Primed Multipotent Progenitor
LSK	$Lineage^{neg}sca\text{-}1^{+}c\text{-}kit^{+}$
LTC-IC	Long-term culture Initiating Cell
LT-HSC	Long-term Hematopoietic Stem Cell
MEL	Murine Erythroid Leukemia
MEP	Megakaryocyte-erythrocyte Progenitor
MLL	Mixed Lineage Leukemia
MPP	Multipotent Progenitor
MTG	Myeloid Translocation Gene
NCoR	Nuclear receptor corepressor
NHR	Nervy Homology Region
NICD	Notch Intracellular Domain
PAX5	Paired Box gene 5
PLZF	Promyelocytic leukemia zinc finger
RAG	Recombination activating gene
RHD	Runt homology domain
Runx1	Runt-related Transcription Factor

shRNA	short hairpin RNA
SMRT	Silencing mediator for retinoid and thyroid hormone receptors
ST-HSC	Short-term Hematopoietic Stem Cell
Tal1/SCL	T-cell acute lymphocytic leukemia 1/Stem Cell leukemia
TCF4	Transcription Factor 4
TCR	T-cell Receptor

CHAPTER I

INTRODUCTION

Leukemia, perhaps more than any other cancer, is often associated with the aberrant function of transcriptional regulators resulting from chromosomal translocations. These chromosomal translocations frequently target genes that are required for normal hematopoiesis, including Mixed lineage leukemia (MLL), Runt-related transcription factor 1 (RUNX1), T-cell acute lymphocytic leukemia 1/stem cell leukemia (TAL1/SCL), E2A, B-cell Lymphoma 6 (BCL6), and the Notch receptor [1-8]. While these factors were first identified through their respective translocations, knockout mouse models and biochemical studies have shown important functions for these proteins beyond leukemia. In fact, they all regulate multiple stages of hematopoiesis, not just the population targeted for cancer transformation. Furthermore, many of these factors interact with and/or regulate the expression of each other, creating a network of critical modulators of hematopoiesis[9,10]. Mutation of these targets may disrupt hematopoietic lineage allocation, cell growth, and survival, ultimately leading to leukemia.

The Myeloid Translocation Gene (MTG) family was first discovered through the (8;21) translocation that leads to Acute Myeloid Leukemia (AML)[4]. This translocation fuses nearly all of Myeloid Translocation Gene 8 (MTG8, also known as Eight-Twenty-one or ETO) to an N-terminal portion of RUNX1, also known as Acute Myeloid Leukemia 1 (AML1) containing the DNA-binding Runt homology domain (RHD), thus redirecting the normal function of MTG8 as a transcriptional co-repressor[4,11]. The t(8;21)

accounts for 12-15% of de novo AML, which is of the M2 subtype. Two other MTG family members have since been identified: Myeloid Translocation Gene 16 (MTG16 or ETO2 or CBFA2T3) and Myeloid Tumor Gene Related-1 (MTGR1 or CBFA2T2), both of which are implicated in leukemia[12-14]. MTG16 is a target of the t(16;21) that, like the t(8;21), fuses MTG16 to AML1 to produce AML, though this rare translocation develops primarily in response to therapy. While not a direct target of a chromosomal translocation, MTGR1 is frequently deleted in myelodysplastic syndrome and in 3-10% of AML. In addition to their well-studied roles in myeloid leukemia, MTG family members have been implicated in other cancers as well: *MTG8* is mutated in colorectal carcinoma, breast, and lung cancer while *MTG16* is mutated in ovarian, breast and colorectal cancer[15-18].

Given the precedence for targets of leukemia-related chromosomal translocations acting as critical regulators of hematopoiesis, we generated an *Mtg16*$^{-/-}$ knock-out mouse model to better understand how Mtg16 functions in normal development and, ultimately, cancer[19]. In the absence of *Mtg16*, B- and T-cell development were decreased, particularly after stress such as a competitive bone marrow transplant. Both early B- and T-cell development were perturbed *in vitro* and these developing *Mtg16*$^{-/-}$ cells showed altered cell growth and survival, though different mechanisms contributed to the B- and T-cell phenotypes. *Mtg16* deletion also negatively affected mature B-cell mediated immune responses.

Hopefully, basic development information generated from the *Mtg16*$^{-/-}$ mouse can be translated to disease, leading to a better understanding of how both the AML1-ETO fusion protein and the more rare AML1-Mtg16 fusion protein produce leukemia. The

work presented here highlights the importance of Mtg16 in regulating multiple stages of hematopoiesis, and provides a framework for future studies on how the loss of normal Mtg16 function may contribute to phenotypes seen in AML. Additionally, this work provides a new understanding for the importance of the interactions between Mtg16 and the Notch-intracellular domain, Bcl6, and E2A, which are all master regulators of hematopoiesis that are mutated in leukemia.

Myeloid Translocation Genes

MTG family members function as transcriptional co-repressors by binding to a variety of DNA binding transcription factors and recruiting histone deacetylases (HDACs) and other transcriptional co-repressors such as mSin3a and the nuclear receptor co-repressor (N-CoR) and silencing mediator for retinoid and thyroid hormone receptors (SMRT) and to repress transcription (Fig. 1)[20-24]. The list of transcription factors that regulate hematopoiesis and that also recruit MTG family members includes the mediator of Notch signaling CSL (CBF1-Suppressor of Hairless-Lag1), growth factor independence (Gfi)-1, Gfi-1B, Promyelocytic Leukemia Zinc Factor (PLZF), Bcl-6, Transcription Factor 4 (Tcf4), Tal/Scl, GATA1, and the basic Helix-loop-helix E-proteins E2A, HeLa E-box binding factor (HEB), and E2-2[25-32]. These transcription factors are critical during specific stages of hematopoiesis, and function in part by recruiting MTGs to repress transcription, suggesting that MTG family members can directly regulate hematopoiesis. Roles for Mtg16 in hematopoiesis are becoming

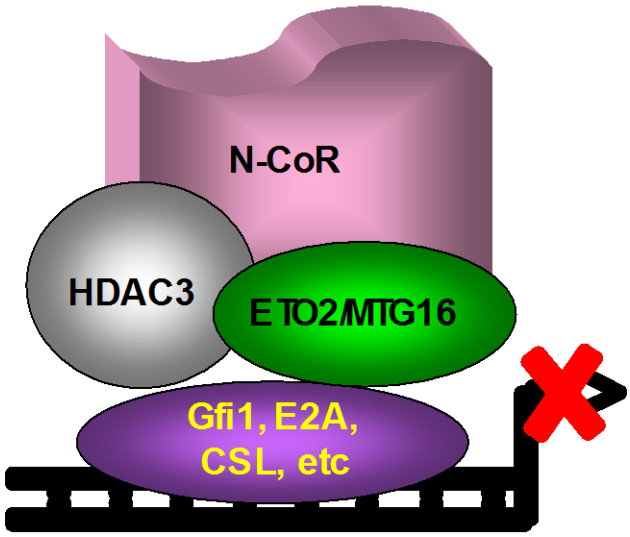

Figure 1. Myeloid Translocation Genes Function as Transcriptional Corepressors Myeloid Translocation Genes (MTGs) do not bind DNA, but instead bind DNA binding transcription factors such as GFI1, E2A, and CSL and recruit corepressors such as Histone Deacetylases (HDACs) and NCoR to repress downstream transcription.

more apparent and will be covered in more detail later in this introduction. Chapters III and IV will introduce new information on Mtg16's function in lymphoid development.

In addition to regulating hematopoiesis, MTG family members also regulate stem cell populations in the gut and nervous system through many of these same transcription factors[33-35]. In particular, Mtgr1 affects self-renewal and lineage allocation of stem cells of the small intestine, at least in part through Tcf4[28,33,34]. While neural phenotypes have not been well characterized after deletion of MTG family members, MTG proteins are well expressed in the nervous system[36]. MTG function is necessary to terminate specific stages of neurogenesis in concert with the basic-Helix-Loop-Helix (bHLH) factors Neurog2 and E47[35,37]. With their ability to regulate multiple different transcription factors in a given cell and the importance of these transcription factors in stem and progenitor cell populations, MTGs can potentially serve as master regulators of development.

Structure and Function of MTG Family Members

The mammalian MTG family members are closely related and conserved with a single *Drosophila* homologue, *Nervy* (Fig. 2)[38]. The homology between the mammalian and fly counterparts is concentrated within four domains termed Nervy Homology Regions, or NHRs[38]. Nervy homology region 1 (NHR1) has some similarities to a domain in hTAF110 and contacts many DNA binding transcription factors including E-proteins such as E2A[26,31,39]. NHR2 is a tetramerization domain that can also contact other proteins such as mSin3A[22,40,41]. MTGs can homo- and hetero-dimerize and MTGR1 was the most robust interacting partner for ETO by immunoprecipitation[31].

	NHR1	NHR2	NHR3	NHR4
Mtg16	98%	88%	84%	90%
Mtgr1	95%	79%	66%	97%
Nervy	50%	51%	46%	70%

Figure 2. Structure and Homology of MTG family Members The three Myeloid Translocation Gene (MTG) family members, Mtg8, Mtg16, and Mtgr1 are highly homologous with the drosophila protein Nervy in four regions, titled Nervy Homology Regions (NHRs). Two proline/serine/threonine (PST) rich regions exist at the N-terminus. Adapted from Davis et al 2003 [38]

NHR3 is the least conserved of the 4 domains and binds to Protein kinase A and CSL[42,43]. NHR4 forms a ring finger motif and is the weaker of the two binding sites for the nuclear hormone co-repressors N-CoR and SMRT [22,40].

When MTGs are expressed as Gal fusion proteins and thus tethered to the promoter of a luciferase construct driven by a Gal-thymidine kinase (Gal-TK) promoter, they repress downstream luciferase expression[20,22]. Transcriptional repression by MTGs is contingent upon histone deacetylase (HDAC) function, as treatment of cells with the HDAC inhibitor trichostatin A (TSA) abrogates the ability of MTGs to repress transcription[43,44]. In the context of Gal-fusion transcriptional reporter assays, NHR4 and a domain between NHR1 and NHR2 (which is the major contact point for N-CoR) contribute to transcriptional repression, and NHR2 contributes in a stochiometric manner in that deletion of this domain has a 2-4-fold effect [22,41].

While all three family members generally have similar binding partners, some unique contacts exist. For example, mSin3a interacts with MTGR1 and MTG8 but not MTG16[33]. Additionally, the effect of different MTG family members binding to the same proteins may vary in degree. While all three MTG family members can repress E47 mediated transcription, Mtg16 is more effective than Mtg8 or Mtgr1 by luciferase assay[37]. Given that MTG family members have similar binding capacities, it is possible that they can perform some compensatory functions in knockout mouse models and that deletion of more than one family member will reveal new functions for MTGs. In fact, double deletion of *Mtg16* and *Mtgr1* leads to a novel embryonic lethality by an undefined mechanism (Moore et al, in prep).

Targeting of each MTG family member's function relies in part upon patterns of expression. Generally, MTG family members are widely expressed[38]. By Northern blot, *Mtg8* is well expressed in murine brain, lung, heart, testis, ovary, and developing gut[11,45]. *Mtg16* is expressed in heart, brain, lung, skeletal muscle, and hematopoietic lineages[12]. The final MTG family member, *Mtgr1*, is expressed at the highest levels in the heart, brain, and skeletal muscle, and at lower levels in several other tissues[46]. *Mtg8* and *Mtgr1* are both expressed in the developing gut, while *Mtg16* is not well expressed in this tissue[33]. All three family members are expressed in the nervous system, though the timing of each family member's activation is unique and tightly regulated[36]. In hematopoiesis, expression of MTG proteins is varied: *Mtg8* is not expressed at detectable levels in any population except for erythroid progenitors; *Mtgr1* is expressed at low levels through hematopoiesis; and *Mtg16* is the most highly expressed family member and is expressed at the highest levels in early stem and progenitor populations[47,48].

Hematopoiesis

Gene targeting studies have implicated MTGs in regulation of stem cell populations, and the stem cell phenotypes generated by loss of *Mtg* family members reflect their diverse patterns of expression. Specifically, *Mtg8*$^{-/-}$ and *Mtgr1*$^{-/-}$ mice have defects in the gut. *Mtg8*$^{-/-}$ germ line deletion yielded perinatal lethality with an associated deletion of the midgut[45]. The *Mtgr1* knockout also produced an intestinal phenotype: most notably, these mice have a decrease in the cells of the secretory lineage (goblet and paneth cells) and increased proliferation of undifferentiated stem/progenitor cells in the

crypts[33]. Interestingly, no defects in hematopoiesis have been reported in either mouse model.

In contrast, *Mtg16*$^{-/-}$ mice have striking defects in hematopoiesis, implicating Mtg16 as the critical family member in this system[19]. *Mtg16*$^{-/-}$ mice have profound defects in erythropoiesis, particularly in response to stress such as treatment with phenylhydrazine, an erythrolytic drug. Furthermore, they have defects in lineage allocation as well as changes to stem cell function, phenotypes that have influenced the work presented in Chapters III and IV. As hematopoiesis is a complex and specialized developmental process, a framework is presented here to enable interpretation of the data in Chapters III and IV. Additionally, the function of MTG interacting partners and gene expression targets in hematopoiesis will be highlighted.

Hematopoietic Stem and Progenitor Cell Development

Hematopoiesis is the classic stem cell system, and has served as the model for subsequent work on tissue specific stem cells and cancer stem cells[49,50]. Early hematopoietic models depicted a common stem cell giving rise to two different arms of hematopoietic cells, namely myeloid cells and lymphoid cells[49]. This model, which persisted for years, showed one common early branch point for myeloid versus lymphoid cell fate decisions, then development within a myeloid framework to develop erythroid cells, megakyocytes, granulocytes, and monocytes, or a lymphoid framework, to develop B- and T-cells. Within the lymphoid framework, common B and T-cell progenitors remained in the bone marrow to give rise to B cells or traveled through the circulation to seed the thymus and develop into T-cells. This model has undergone significant revision

in recent years, adding layers of complexity with multiple early branch points and increasing lineage plasticity[51-54]. The current models are still under intense debate and consensus has not been definitively reached, but a summary is presented (Fig. 3.)

The one constant to all models of hematopoiesis is that hematopoietic cells begin in the bone marrow as long-term hematopoietic stem cells (LT-HSC) $Lin^{neg}Sca\text{-}1^{+}c\text{-}Kit^{+}Flt3^{-}$). These cells have self-renewal capacity as well as the pluripotent ability to differentiate into all hematopoietic lineages. LT-HSCs are functionally defined by their ability to repopulate lethally irradiated recipient mice for at least 16 weeks, though stringent conditions suggest true LT-HSCs should be assessed at greater than 6 months post transplant[55]. These stem cells will gradually lose their self-renewal potential, becoming pluripotent short-term hematopoetic stem cells (ST-HSC) ($Lin^{neg}Sca\text{-}1^{+}c\text{-}Kit^{+}Flt3^{lo}$) that can repopulate after transplant for several weeks, but do not have long-term capacity[56,57].

From this point, models of hematopoiesis begin to diverge. While alternate versions exist, generally stem cells lose self-renewal capacity and become multipotent progenitor cells (MPP) ($Lin^{neg}Sca\text{-}1^{+}c\text{-}Kit^{+}Flt3^{+}$). MPP can then follow one of several hypothesized pathways through intermediate progenitor populations. All of these progenitor populations are lineage restricted, but not lineage committed, and thus have potential to develop into some types of hematopoietic cells but not others. For example, one model suggests that MPP cells will lose their ability to give rise to megakaryocytes and erythrocytes and gain high expression of the transmembrane receptor fms-like tyrosine kinase 3 (Flt3), becoming lymphoid-primed multipotent progenitor cells (LMPP) ($Lin^{neg}Sca\text{-}1^{+}c\text{-}Kit^{+}Flt3^{hi}$) that have granulocyte/monocyte and lymphocyte potential[51].

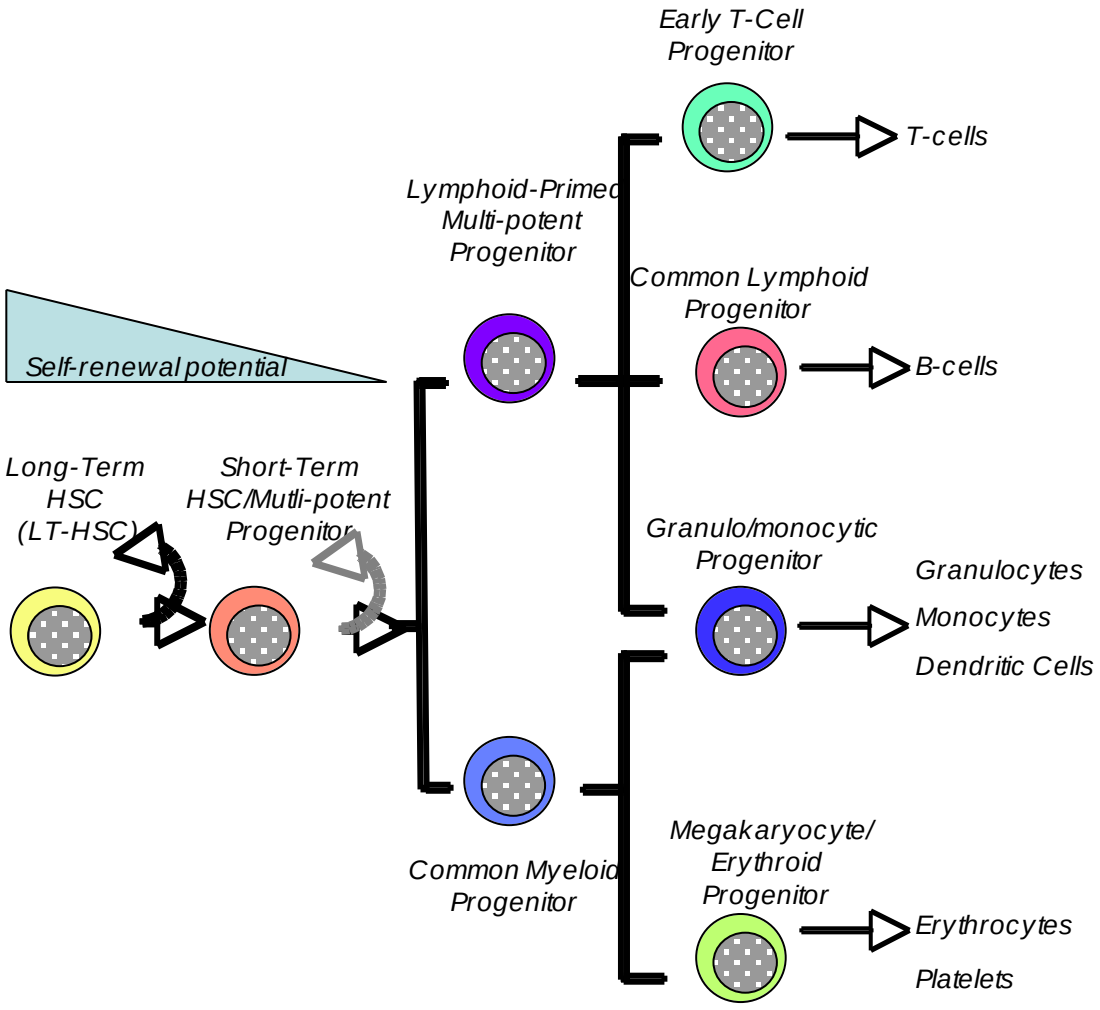

Figure 3. Model for Hematopoietic Progenitor Development Hematopoetic cells begin in the bone marrow as Long-term hematopoietic stem cells (LT-HSC) that self-renew and differentiate to form all the lineages of the blood. As self renewal decreases, lineage commitment begins. Cells can become Lineage Primed Multipotent Progenitors (LMPPs) with granulocyte/monocyte and lymphoid potential or Common Myeloid Progenitors (CMPs) with megakaryocyte/erythrocyte and granulocyte/monocyte potential.

As part of this lineage potential, LMPP cells can give rise to granulocyte/monocyte progenitor cells (GMP), common lymphoid progenitor cells (CLP), and early thymocyte progenitor cells (ETP). Alternatively, MPP cells can lose lymphoid lineage potential and give rise to common myeloid progenitor cells (CMP) that have granulocyte/monocyte potential as well as megakaryocyte/erythrocyte potential[58]. These intermediate CMP cells can then develop into GMP and megakaryocyte/erythrocyte progenitor cells (MEP).

During and after lineage commitment, cells undergo various stages of lineage specific development before becoming mature functional hematopoietic cells. Many of the changes we see in the absence of *Mtg16* are located in these early stem and progenitor populations, as this is the location of the highest levels of *Mtg16* expression[47]. Additionally, the work presented in Chapters III and IV focuses on early lymphocyte development. Therefore, in addition to this overview of stem and progenitor pathways, T- and B-cell development will be covered in more detail, while the development of other lineages is beyond the scope of this work.

Early Lymphocyte Development

Early B and T-cell development share many common features and precursor populations. Like all hematopoietic cells, both B- and T-cells begin as long-term hematopoietic stem cells and travel through short-term hematopoetic stem cell and MPP cell populations. Lymphoid lineage development begins with the production of LMPP cells. These cells have both myeloid and lymphoid, but not megakaryocytic or erythroid, lineage potential and are the first cells where lymphoid associated gene expression is initiated[51,59]. Loss of the LMPP population leads to a complete less of B- and T-cells;

this result is shown in *Hdac3*$^{-/-}$ mice that have no LMPP cells and no B or T-cells as a result (Summers et al, in prep). Flt3 expression and signaling is a functionally important characteristic of LMPP cells in lymphoid lineage development, and contributes to the upregulation of IL7-Receptor expression, the critical cytokine receptor for early lymphoid development[60]. In fact, loss of *Flt3-ligand* expression in mouse models and thus loss of Flt3 receptor mediated signaling leads to a decrease in both early B cells and early T cells[61].

Lineage plasticity and myeloid skewing are hallmarks of the LMPP population[51,59]. Granulocyte/monocyte specific genes, such as *Colony stimulating factor 3 receptor* (*Csf3r)* and *SFFV proviral integration 1* (*Sfpi1),* are expressed throughout the course of early hematopoietic differentiation and into the LMPP population. By contrast, early lymphoid specific genes, such as *Recombination activating gene 1 (Rag1)* and *2 (Rag2),* are only upregulated within the LMPP population. Lymphoid expression programs are not completely activated at this early stage, though, and genes that are expressed only in committed lymphoid cells, such as *Paired box gene 5* (*Pax5)* and *Cd3e*, are not expressed in LMPP cells. Using single-cell RT-PCR assays, it was found that nearly all LMPPs express granulocyte/monocyte specific genes while only roughly 30% expressed lymphoid specific genes. All cells that expressed a lymphoid program also expressed a granulocyte/monocyte program, highlighting the myeloid and lymphoid lineage potential and myeloid preference of these cells.

The next step in lymphoid development beyond LMPP cells is the production of B- and T-lineage specific progenitors. Early models of hematopoiesis focused upon Lin^{neg}IL-7R^{+}c-kit^{lo}sca-1^{lo} Common Lymphoid Progenitor (CLP) cells that were

hypothesized to precede both B and T-cell development[62]. CLP cells are capable of generating both B and T-cells *in vitro* and after transplant and have limited potential for other lineages[62]. More recent work has found that very few common lymphoid progenitors can be found circulating in the peripheral blood, decreasing the likelihood that these cells seed the thymus to generate T-cells[63]. Instead, LMPP cells are much more numerous in circulation and capable of generating T-cells *in vitro* and after transplant[51,52]. Therefore, they are thought to contain the thymus seeding population[63-65]. Newer models of hematopoiesis suggest that common lymphoid progenitors remain in the bone marrow and primarily give rise to B-cells[66,67].

Upregulation of the IL7 receptor (IL7R) is an important hallmark of lymphoid specific lineage programming and is a common component in both B- and T-cell development. IL7 signaling is crucial for all lymphoid development and in the absence of either *IL7* or its receptor, both B- and T-cell development are lost to varying levels[68,69]. Expression of the IL7R defines the CLP B-cell precursor population and IL7 supports the *in vivo* differentiation of CLP cells into the earliest B-cells, though $IL7R^{+}$ CLP production was not compromised in the absence of the *IL7* cytokine[70]. Additionally, $IL7R^{-/-}$ and $IL7^{-/-}$ B-cells arrested in the earliest stages of $B220^{+}$ B-cell development[68,69,71]. While the IL7R is not well expressed on the earliest cells of the thymus (Early thymocyte progenitor or ETP cells) its expression is upregulated with the transition to the next stage of thymocyte development and the initiation of T-cell commitment[66,72]. $IL7R^{-/-}$ thymocytes therefore arrest in the earliest stages of thymus development prior to T-Cell Receptor (TCR)β rearrangement[68]. Loss of *IL7* cytokine expression also leads to a sharp decrease in thymocyte number, though normal developmental stages exist[69]. In addition

to regulating the development of lymphocytes, IL-7 signaling also regulates the survival of T-cells, and the expression of a Bcl-2 transgene rescued T-cell development in *IL7R* deficient mice [73].

The important role for both Flt3 and IL7 in early lymphoid development is highlighted by the ability of IL7 and Flt3 to instruct *in vitro* lymphoid development[70,74]. Though T-cell development requires the addition of a strong Notch signal, IL7 and Flt3-ligand are sufficient to induce B- or T-cell development from uncommitted progenitors in OP9 culture systems[74] . Furthermore, loss of both *Flt3-ligand* and *IL7R* had an additive effect *in vivo*, and resulted in a more severe B-cell phenotype than either single deletion[75].

Lymphoid lineages are grouped together in part because of the common process of germ-line chromosomal rearrangements associated with V(D)J recombination that contribute to the development of mature, functional B and T cell receptors. V(D)J recombination is a unique feature of B and T-cells that, briefly, consists of Rag1 and Rag2 mediated rearrangement of either T-cell receptor or B-cell receptor/immunoglobulin loci[76,77]. Ultimately, T-cells must rearrange two T-cell receptor (TCR) chains, α and β, to produce a mature receptor, while B-cells rearrange two B-cell receptor chains, the immunoglobulin heavy chain (IgH) and the immunoglobulin light chain (IgL)[78]. V(D)J recombination facilitates the production of a diverse repertoire of these receptors, maximizing the capacity for the immune system to recognize foreign antigens. *Rag1* and *Rag2* expression can first be seen in the LSK compartment, where a small fraction of cells with lymphoid potential begin to express *Rag1* and *Rag2* at very low levels[79]. This expression leads to a small level of B-cell receptor V(D)J

recombination in cells prior to B-cell commitment. Rag levels increase throughout CLP and ETP populations and V(D)J recombination plays an important role in the maturation of lymphocytes, which will be discussed in more detail in later sections. While common processes such as V(D)J recombination and IL7R signaling contribute to the maturation of both B- and T-cells, B and T-cell development diverge beyond the LMPP population.

T-Cell Development

Once in the thymus, LMPP thymus seeding cells become early thymocyte progenitor (ETP) cells characterized by the expression of low levels of the progenitor cell marker c-kit and the lack of expression of maturing T-cell markers CD4 and CD8[66,80]. ETP cells sit in the first of four populations of $CD4^{-}CD8^{-}$, or double negative (DN) cells (Fig. 4). The thymic microenvironment is rich in Notch signaling activation, a necessary component for T-cell development, due to high levels of Notch ligand expression[81]. In this context, ETP cells then progress through distinct stages of T-cell development, first the four DN stages (DN1-DN4), followed by $CD4^{+}CD8^{+}$ double positive (DP) cells, to produce mature, functional $CD4^{+}CD8^{-}$ and $CD8^{+}CD4^{-}$ T-cells that exit the thymus to contribute to immune responses[80].

DN cells can be further subdivided based upon expression of CD44 and CD25 into four populations: DN1 $CD44^{+}CD25^{-}$, DN2 $CD44^{+}CD25^{+}$, DN3 $CD44^{-}CD25^{+}$, and DN4 $CD44^{-}CD25^{-}$[82]. ETP cells that seed the thymus are a small subset of the DN1 population[66,83]. These cells are not T-lineage committed, and retain the capacity to

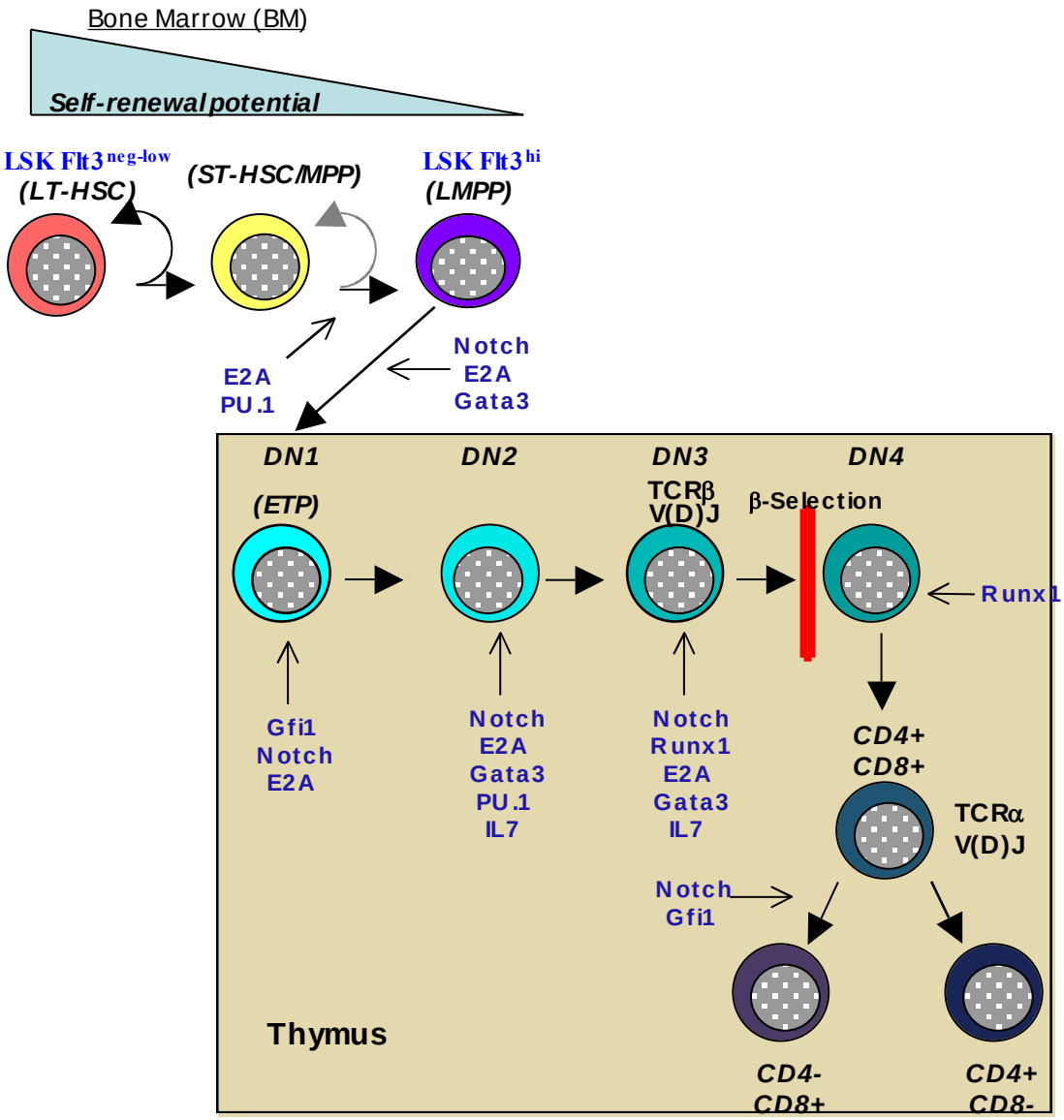

Figure 4. Transcription factor regulation of early T-cell development T-cells begin in the bone marrow as LT-HSCs and differentiate through the Lymphoid-primed multipotent progenitor (LMPP) population. The thymic seeding cells arise from the LMPP population and become Early thymocyte progenitor (ETP) cells. Thymocytes develop through four Double Negative (DN) stages, including the β-Selection checkpoint, to become Double Positive (DP) cells and $CD4^+$ and $CD8^+$ cells. Transcription factors and signaling molecules that regulate T-cell development are depicted in blue.

generate myeloid cells both *in vivo* and *in vitro* in addition to dendritic cell and natural killer cell capacity[84-87]. As cells travel into the DN2 subset, they begin the process of committing to the T-cell lineage and upregulating T-cell specific gene expression patterns[87-89]. Final T-cell commitment occurs in the DN3 stage as thymocytes undergo V(D)J rearrangement and produce a rearranged TCRβ; in the absence of successful TCRβ rearrangement and cell surface expression of TCRβ with a surrogate preT-α chain, cells are not able to move beyond this DN3 stage[76,77,90-93]. The process of stalling cells that do not express the TCRβ/preT-α complex is termed β-selection, and serves as a critical checkpoint in thymocyte development.

Once cells bypass β-selection, they traverse into the DN4 population and upregulate expression of CD4 and CD8, ultimately becoming $CD4^+CD8^+$ DP cells. From this point forward, they will undergo further V(D)J recombination to rearrange the α TCR chain, then positive and negative selection to identify T-cells with appropriate TCR expression for antigen identification and response[94,95]. Cells will then become either $CD4^+$ or $CD8^+$ and exit the thymus to play diverse roles in the immune response.

Transcriptional Regulation of Early T-cell Development

The process of early T-cell development is highly regulated by a number of different transcription factors, many which are Mtg16 interacting factors and contribute to the phenotypes described in Chapter III (Fig. 4). First and foremost on the list of T-cell regulatory factors is Notch signaling, though other critical factors include Gfi1, Gata3, Runx1, Sfpi/PU.1 and basic Helix-loop-helix (bHLH) E-protein transcription factors E2A and HEB[81,96-104]. These transcription factors work together to activate and

repress genes to form the T-cell lineage program. The gene targets of these transcription factors are varied, but some of the most important early targets in T-lineage specification and commitment include *Hes1*, *Ptcra*, *IL7Ra* and other T-cell transcription factors such as *Gata3*[9,89,105]. Given the importance of Notch and E-proteins in mediating the Mtg16 functions discussed in Chapter III, the biochemical properties and functions of Notch and E-proteins in T-lineage specification will be covered in more detail in subsequent sections. A general picture of other factors important in transcriptional control of early T-cell development follows.

Gfi1 is a zinc-finger transcriptional repressor that functions by recruiting corepressors such as MTGs and HDACs to repress downstream transcription[26]. Gfi1 regulates several steps in the process of maturing thymocytes including survival of DN1 and DN2 cells[98]. In fact, in the absence of *Gfi1*, mice have a severe reduction in thymocyte number to roughly 10% of their wild-type counterparts. This reduction in thymocyte number resulted from an increase in apoptosis of immature DN1 and DN2 cells, reducing the number of T-cell progenitors in the thymus capable of generating mature cells. Gfi1 also regulates the selection of CD4 or CD8 expression in favor of $CD8^+$ T-cells, though the mechanism remains unclear.

Gata3 is the essential GATA factor for T-cell development, and its expression is tightly controlled to the T-cell compartment within mature hematopoietic cells[106]. While an interaction between MTGs and Gata3 has not been previously shown, Mtg16 can interact with the GATA1 family member[32]. Furthermore, *Gata3* is a potentially important target of Mtg16, and deletion of Mtg16 leads to increased *Gata3* levels, as detailed in Chapter III. Gata3 is necessary for development of the earliest ETP cells of

the thymus, restriction of the T-cell fate in DN2 cells, and passage through the β-selection checkpoint, in part by regulating TCRβ expression. *Gata3* deletion is embryonic lethal, and therefore the effect in T-cell development was shown first by the absence of *Rag2*$^{-/-}$ thymocyte repopulation by *Gata3*$^{-/-}$ ES cells[100,107]. This finding was corroborated by the absence of even DN1 cells generated by *Gata3*$^{-/-}$ ES cells in chimeric mice[101]. Recent work using bone marrow transplant as well as *Mx-Cre* driven conditional deletion of *Gata3* showed that *Gata3* is necessary for the development of ETP cells, confirming the requirement for Gata3 in the earliest stages of T-cell development[108]. Additionally, mice with a conditional *Gata3* deletion driven by the *Lck* promoter (active in early DN3 stages of thymocytes and beyond) developed a strong decrease in total thymocyte number, largely due to a block in DN3 cells at the point of β-selection[109]. The appropriate amount of *Gata3* expression is critical for regulating T-cell development though: over-expression of *Gata3* was also deleterious to developing T-cells, and caused mast cell diversion of both hematopoietic progenitors and early DN1 and DN2 thymocytes in *in vitro* T-cell assays[99].

Runx1, also known as AML1, is a core-binding factor transcription factor and a critical mediator of definitive embryonic hematopoiesis[110,111]. Runx1 is also the translocation fusion partner for ETO in the t(8;21) and we have preliminary unpublished data that Runx1 is a direct target for Mtg16 regulation, suggesting misregulation of Runx1 may contribute to *Mtg16*$^{-/-}$ phenotypes[112]. Runx1 functions in T-cells to regulate CD4 expression and the generation of DN3 cells in part by regulating repression of the PU.1 transcription factor. Loss of Runx1 was embryonic lethal because of its crucial role in definitive hematopoiesis[110,111]. As a consequence, analysis of the role of Runx1 in

adult hematopoiesis relies upon conditional deletion models. When Runx1 was deleted in DN3 developing T-cells using the *Lck*-cre conditional knockout system, Runx1 mediated silencing of *CD4* expression was lost and *CD4* was aberrantly expressed in early double-negative thymocytes[113]. Furthermore, *Runx1*$^{-/-}$ thymocytes arrested in DN3 and insufficiently upregulated CD8 as they became DP cells, which collectively led to a reduction in total thymocyte levels[113]. Using the *Mx-Cre* inducible deletion mouse model to delete *Runx1* beginning in early hematopoietic stem cells and sustaining throughout hematopoiesis, *Runx1* was necessary for both megakaryocyte development and full lymphoid development, a phenotype that was exacerbated after competitive bone marrow transplant[102,103]. *Runx1*$^{-/-}$ developing thymocytes arrested at the DN2 population, which produced decreased DN3 and DN4 levels. One factor contributing to the mechanism of this phenotype was increased expression of PU.1, a critical regulator of cell fate decisions in hematopoiesis. The T-cell phenotype seen in these mice was reverted by deletion of one allele of PU.1, confirming that the enhanced PU.1 expression seen in the absence of *Runx1* contributed to the DN2 arrest[114].

PU.1 is another essential transcription factor for regulating cell fate decisions in hematopoiesis and T-cell development. PU.1 is necessary for initial T-cell development, though PU.1 expression is detrimental beyond the DN2 stage. Deletion of PU.1 was late embryonic/early neonatal lethal due to anemia and septicemia[115,116]. Deletion also caused a block in early lympho- and myelopoeisis, with no maturing B and T-cells or granulocytes and monocytes, though this disruption could be somewhat bypassed in the T-cell lineage by keeping the neonates alive with antibiotic treatment. Therefore, PU.1 contributes to lineage commitment and development of multiple hematopoietic lineages.

Given the partial rescue of T-cell development with survival, the role of PU.1 in later T-cell development was less clear from these early mouse models. Expression data showed that *PU.1* was repressed sharply in the thymus DN2 cells as they began commitment to the T-cell lineage[117]. Constitutive expression of *PU.1* in hematopoietic progenitors blocked T-cell development at the DN2/DN3 stage in fetal thymic organ cultures (FTOCs), and instead promoted macrophage development[104]. If *PU.1* expression was enforced in committed DN3 thymocytes, cells were reprogrammed to myeloid dendritic cells, an effect that was antagonized by the presence of a strong Notch signal or the expression of *Gata3*[118]. Therefore, downregulation of *PU.1* at the DN2 stage is a critical step in T-lineage cell fate specification.

In addition to DNA-binding transcription factors, transcriptional corepressors have also been shown to play an important role in regulating thymopoiesis. Conditional deletion of *Hdac3*, an MTG binding partner, had severe impacts on many different stages of T-cell development depending on the population where Cre is activated, including loss of early LMPP cells and impaired passage of cells from DP to single positive stages (Summers et al, in prep). Deletion of *NCoR*, another component of MTG repression complexes, also negatively effected T-cell development[119]. *NCoR*$^{-/-}$ mice have defects in fetal erythropoiesis, and therefore deletion was embryonic lethal. Using *in vitro* FTOC to allow for continued thymocyte development past the point of lethality showed a near complete block of *NCoR*$^{-/-}$ cells at the DN3 stage and an increase in apoptosis of developing thymocytes. Together, these results highlight the importance of transcriptional repression in T-cell fate specification and development.

Early B-Cell Development

In contrast to T-cell development, which occurs in the thymus, B-cells remain in the bone marrow and arise from CLP cells. Developing B-cells can be characterized according to Hardy Fraction subsets, based upon cell surface labeling of $B220^+$ cells developed by Dr. Hardy that use the cell surface markers CD43, CD24, BP-1, IgM, and IgD to characterize the different stages of B-cell development as Fractions A-F^{120} (Fig. 5). Fractions A through C' are $CD43^+B220^+$ early B-cells that are undergoing rearrangement of Ig heavy chain loci. Fraction A cells, or pre-pro B-cells, retain germ-line V(D)J loci, and are characterized as $CD24^-BP\text{-}1^-$. Fraction B cells, or early Pro-B cells, are $CD24^+BP\text{-}1^-$ and are the main location of D to J heavy chain rearrangement. Fraction C cells, or late Pro-B cells, are $CD24^+BP\text{-}1^+$ and are completing rearrangement of the Ig heavy chain. In the absence of functional heavy chain rearrangement on either chromosome, cells undergo apoptosis, leading to significant cell death in this population. In the event of a successful rearrangement, a pre-B cell receptor is expressed at the cell surface along with the λ5, VpreB1, Igα and Igβ accessory molecules. Pre-B cell receptor signaling leads to a halt in Ig heavy chain rearrangement and a drastic increase in proliferation. Fraction C' cells, or large Pre-B cells, are $CD24^-BP\text{-}1^+$ that have completed V(D)J rearrangement.

Fractions D through F are $CD43^-$ $B220^+$ and are undergoing Ig light-chain rearrangement. Fraction D cells, or pre-B cells, do not express surface Ig, and are undergoing rearrangement of one of two immunoglobulin light chains, κ or λ. Several attempts at light chain rearrangement are possible, and therefore, while non-productive rearrangements will result in cell death within this population, levels of apoptosis are

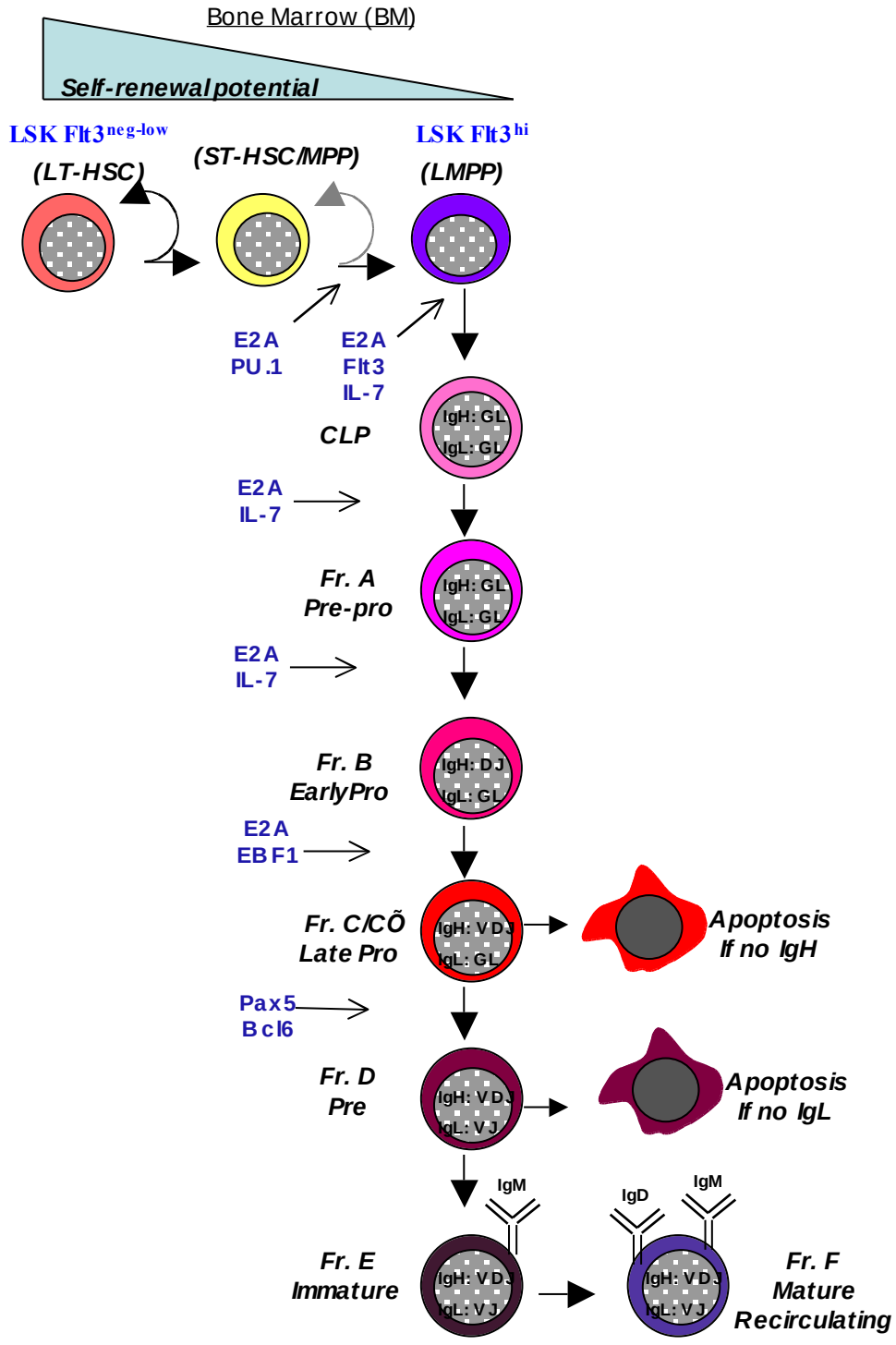

Figure 5. Transcriptional regulation of early B-cell development B-cells develop from LT-HSCs in the bone marrow, becoming LMPP cells, and then traveling through the Hardy Fractions A-F. Transcription factors and signaling molecules that facilitate B-cell development and commitment are noted in blue.

lower than in earlier fractions. With productive light chain rearrangement, a final IgM molecule is produced and expressed at the cell surface, producing Fraction E, or immature, B-cells. This population then undergoes negative selection for self-reactivity. Fraction E cells travel to the spleen to finish maturation, and become Fraction F cells that are recirculating naive B-cells expressing both surface IgM and IgD.

Transcriptional Regulation of Early B-cell Development

Much like T-cell development, B-cell development requires the coordinated action of transcription factors in a network of lineage commitment[121] (Fig. 5). The three primary effectors of the B-lineage program are E2A, Early B-cell Factor 1 (EBF1), and Pax5, of which only E2A is a known MTG interacting partner. All three factors work together to not only activate B-cell specific genes, but also repress alternate myeloid and T-cell fates[122-127]. While initial data suggested that these factors were activated in a linear fashion, with E2A expressed in stem and progenitor populations, which then activated EBF1 in early B-cells, followed by E2A and EBF1 concordantly activating Pax5 in later B-cells prior to lineage commitment, more recent evidence suggests that B-lineage priming is not as linear as originally thought, as EBF1 can regulate expression of E2A while Pax5 can regulate EBF1 expression[122,128-132]. Ultimately, it appears that these 3 transcription factors, together with IL7 and Flt3 signaling, regulate each other in a network of B-lineage priming and commitment.

As cells commit to the B-cell lineage, they upregulate the expression of B-cell specific genes such as EBF1 and Pax5. Gene expression data suggested that E2A, a critical transcription factor for all lymphoid development that is expressed in stem cell

populations, activates the expression of *EBF1* in the context of IL7R signaling[122,133,134]. Expression of *EBF1* was sufficient to rescue B-cell development from CLPs that were deficient in *IL7* or *E2A*, suggesting that *EBF1* expression is a crucial component of B-lineage commitment downstream of both IL7 signaling and *E2A*[133,135,136]. Furthermore, in the absence of *IL7* or the *IL7R*, *E2A* was expressed, but *EBF1* was not, suggesting that the action of both *E2A* and IL7 is necessary to activate *EBF1*[133].

EBF1 then, together with E2A, activates the expression of multiple B-lineage genes including Pax5[129]. In fact, EBF1 and E2A often bind in similar promoter/enhancer regions of genes that need to be activated or repressed to specify B-cell fate[121,128]. Finally, Pax5 facilitates finalization of B-cell commitment[125]. Expression of *Pax5* was sufficient to rescue $E2A^{-/-}$ B-cell development, further confirming its role downstream of E2A[136,137]. The biochemical properties of E2A and its role in early lymphocyte development will be discussed in more detail in subsequent sections, as it is a known Mtg16 interacting partner that contributes to the B- and T-cell phenotypes discussed in Chapters III and IV.

EBF1 is essential for B-cell development and mice lacking *EBF1* have early $B220^{+}CD43^{+}$ B-cells that express the IL7R, but no more mature B-cells that express surface immunoglobulins[138]. In addition to activating B-cell specific genes, EBF1 also represses targets necessary for B-lineage commitment. Downregulation of *Id2* and *Id3*, negative regulators of E-proteins, is an important function of EBF1 in specifying B-cell fate. Deletion of *EBF1* led to high levels of *Id2* and *Id3*, which prevented E-proteins from functioning[139]. As a consequence, *E2A* expression in *IL7R* deficient cells was not sufficient to upregulate *EBF1* and induce B-cell development due in part to impairment

of E2A function by Id2 and Id3. Overexpression of *Id2* or *Id3* was sufficient to impair B-cell development after transplant, highlighting the importance of EBF1, E2A, and Id proteins in a network that specifies B-cell fate.

Pax5 is a member of the paired box family if transcription factors and is critical for B-cell commitment. Pax5 functions as both a transcriptional activator and repressor, interacting with repressors such a Groucho to repress non-B-lineage gene expression and activators such as p300 to activate B-lineage specific genes in early B-cell populations[140]. Deletion of *Pax5* resulted in a block in B-cell development of uncommitted early B-cells that retain myeloid potential[125]. These *Pax5*$^{-/-}$ early B-cells began the process of B-lineage development and contained rearranged immunoglobulin loci, but were unable to complete B-cell development and therefore were capable of developing into myeloid cells. Furthermore, deletion of *Pax5* in later, committed B-cells reversed their commitment status and allowed them to revert to multilineage myeloid, erythroid, and T-cell potential[141].

Other factors that are capable of interacting with Mtg16 also regulate early B-cell development, including Bcl6[25,142]. Bcl6 is a BTB/POZ transcriptional repressor and MTG interacting protein. Through its N-terminal BTB/POZ domain, Bcl6 interacts with NCoR and SMRT, while its central repression domain facilitates interactions with other corepressors[142,143]. Bcl6 plays a role in maintaining the survival of early B-cells as they accumulate DNA damage due to V(D)J light chain recombination[142]. Bcl6 dampens the response to DNA damage by decreasing the expression of *CDKN2A/Arf*, *CDKN1A/p21*, and *CDKN1B/p27*, thus blocking the p53 response. This allows for cell survival in the presence of DNA damage, and in the absence of *Bcl6*, Pre-B cells could not repress these

genes and therefore could not grow, self-renew, or survive *in vitro*. Due to low levels of *Bcl6* expression in early cells undergoing heavy chain rearrangement, this phenomenon does not appear to be critical for repressing the DNA damage response in earlier populations, though it has not been specifically investigated.

Late B-cell Development

B-cell development is not confined to the early fractions of the bone marrow, and further maturation and lineage decisions occur in the spleen. Fraction E cells that have completed their BCR rearrangement and are ready to emigrate to the periphery, are known as transitional B-cells, or T_1 cells[144]. These cells do not have the capacity to re-circulate, but they do travel from the bone marrow to the spleen. T_1 cells enter splenic follicles and gain the cell-surface expression of IgD to become T_2 transitional cells. T_2 cells can enter circulation and travel to lymph nodes, but are not mature functional B-cells and cannot proliferate in response to B-cell receptor activation.

From the T_2 transitional population, B-cells can then become either marginal zone or follicular zone mature B-cells[145]. Follicular zone B-cells organize into lymphoid follicles surrounded by T-cell rich areas. These follicular zone B-cells are recirculating B-cells that participate in T-cell dependent immune responses in the spleen. Along the periphery of these lymphoid rich areas lies another B-cell rich region that contains marginal zone B-cells. These cells do not re-circulate, but instead stay localized to the marginal zone and self-renew with an unlimited life span and facilitate macrophage associated innate immunity. Marginal zone vs. follicular zone decisions rely upon several MTG interacting factors, including Notch signaling through the Notch2 receptor

and the Delta-like 1 ligand, which is expressed strongly in the marginal zone[146,147]. B-cell receptor signaling influences this cell fate decision as well, and a weak BCR signal and a strong Notch signal favors marginal zone development over follicular zone development. E-proteins also play a critical role in this decision: decreased *E2A* and increased *Id2* or *Id3* lead to increased marginal zone B-cells at the expense of follicular zone B-cells[148,149].

When foreign antigens enter the spleen, B-cells mount a germinal center response. This phenomenon is characterized by high rates of proliferation and rapid DNA changes in an attempt to improve the efficiency of the immune response, including variable region somatic hypermutation and class-switch recombination[150]. After the germinal center response has taken place, the high-affinity antibody producing B-cells become plasma cells, which are the immune effector cells, or memory cells, which retain the high-affinity antibody locus in their genomic DNA in preparation for the next immune challenge.

The process of germinal center maturation relies heavily upon the Bcl6 transcription factor, which represses the expression of genes that function in cell cycle arrest, including *p53*, *ataxia telangiectasia and Rad3 related1* (*ATR*), *Chek1*, and *Cyclin-dependent kinase inhibitor 1A* (*CDKN1A p21)*[151-156]. In addition, Bcl6 regulates the maturation of germinal center B-cells by directly repressing genes that lead to terminal differentiation, including *Prdm1*[156,157]. In the absence of Bcl6, these genes are not repressed and attempts at somatic hypermutation lead to DNA-damage induced cell cycle arrest and apoptosis and therefore loss of the germinal center response. Deletion of *Hdac3*, a corepressor that interacts with Bcl6 to facilitate transcriptional repression,

recapitulates these findings, with drastically decreased germinal center reactions in *Hdac3*$^{-/-}$ mice (Bhaskara et al, in prep).

Notch and E-Proteins

Mtg16 interacts with several transcription factors that regulate lymphoid development mentioned above, including Gfi1 and Bcl6. The two most prominent regulators of lymphoid development that bind to Mtg16 are E-protein transcription factors and components of the Notch signaling cascade, specifically CSL and the intracellular domain of the Notch receptor[31,43]. Notch signaling and E-protein mediated transcription are important facilitators of Mtg16 function referenced in Chapters III and IV; therefore, these topics and their relationship to Mtg16 and hematopoiesis will be covered in more detail.

Notch Signaling, Mtg16, and Hematopoiesis

The Notch signaling family consists of four different transmembrane receptors, titled Notch 1 through 4, that interact with ligands of the Delta-Serrate-Lag2 (DSL) and Jagged family of cell surface proteins. In mammalian cells, five ligands exist: Delta-like 1, 3, and 4 and Jagged 1 and 2[158]. Notch receptors are proteolytically cleaved in the first of three cleavage-processing steps for activation by the furin protease as they are trafficked to the cell surface. Receptors exist at the cell surface with these two resulting parts non-covalently linked together and heavily modified with N- and O-linked glycosylation of the extracellular portion. Upon ligand binding, the second proteolytic

cleavage site is exposed. Cleavage then occurs extracellularly by the ADAM protease, and the membrane bound remainder of the receptor is cleaved by γ-secretase to release the functional Notch Intracellular Domain (NICD). The NICD subsequently translocates to the nucleus to activate Notch-driven transcription.

Once in the nucleus, the NICD binds to the transcription factor of the Notch signaling cascade, CBF-1/Su(H)/Lag-1 (CSL), and recruits the transcriptional coactivator mastermind (MAM) to activate downstream transcription. This completed complex recruits general transcriptional activators such as p300 to regulate chromatin acetylation and transcription[159]. This complex can bind to promoters as either a monomer or a dimer, a phenomenon that appears to be promoter specific[160]. The Notch signal is terminated by ubiquination of the NICD by Fbw7 and subsequent proteosomal degradation[161]. This degradation process involves phosphorylation of the NICD on its C-terminal PEST domain by cyclin-dependent kinase 8 (Cdk8)[162]. The strength and duration of the Notch signal is also regulated by acetylation, and loss of the deacetylation molecule *SIRT1* led to increased Notch signaling[163].

In the absence of a Notch signal, CSL functions as a transcriptional repressor by binding corepressors such as NCoR/SMRT, SMRT-HDAC Associated Repressor Protein (SHARP), Groucho, and/or MTGs[164-166] (Fig. 6). A number of different CSL repressor complexes have been identified and appear to be target specific in their formation[167]. The first evidence suggesting MTGs regulate Notch signaling identified an indirect interaction between MTG family members and CSL, facilitated by SHARP[29]. This interaction was identified through a yeast two hybrid screen and confirmed by coimmunoprecipitation and *in vitro* binding assays. The interaction between MTG8 and SHARP localized

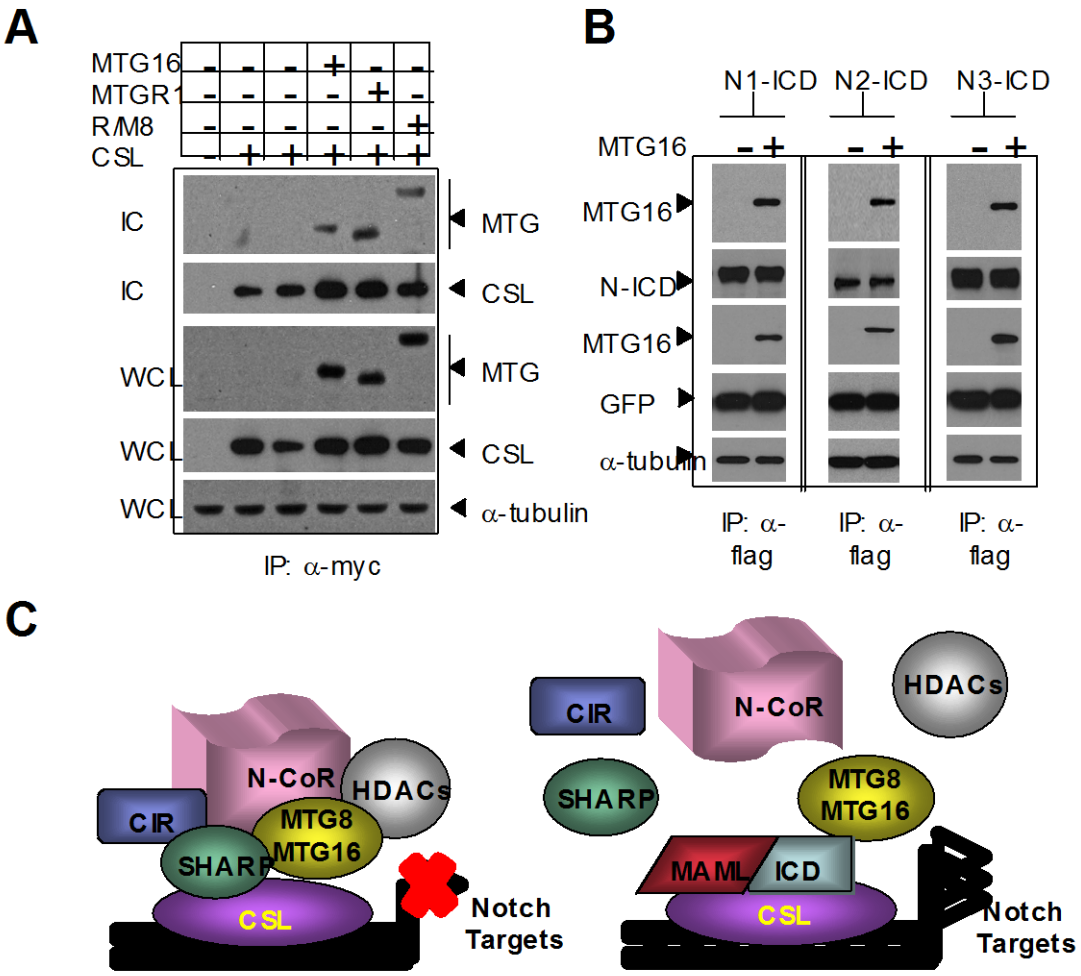

Figure 6. Myeloid Translocation Gene 16 interacts with components of the Notch signaling cascade (A) Mtg16, Mtgr1, and Runx1-Mtg8 (AML1-ETO) all interact with CSL, the transcription factor of the Notch signaling cascade. (B) Mtg16 interacts with the intracellular domain of all four Notch receptors (N4-ICD not shown). (C) Schematic for proposed MTG function in the context of Notch signaling. In the absence of an activated Notch receptor, CSL represses downstream transcription by binding corepressors such as SHARP, NCoR, HDACs, and Mtg16. In the presence of an activated Notch receptor, the Notch ICD translocates to the nucleus, disrupts the MTG-CSL interaction, and liberates the repressor complexes, allowing the NICD to bind CSL and recruit activators such as Mastermind (MAML). Adapted from Engel et al 2008[43]

broadly to the N-terminal portion of MTG8 and MTG8 bound to the promoters of the Notch target genes *Hes1* and *Nrarp* by Chromatin Immunoprecipitation (ChIP). In addition to an indirect interaction through SHARP, MTG16 also interacts directly with CSL through the NHR3 region, further confirming the importance of MTGs in CSL repression complexes[43] (Fig. 6A). Interestingly, MTG8 increased the repression of Notch target genes by luciferase assay, while the AML1-ETO fusion protein, which was also capable of interacting with SHARP as part of the CSL complex, actually had the opposite effect and augmented expression of Notch targets when overexpressed. Activation of Notch target genes by the AML1-ETO fusion proteins has previously been reported, though initial analysis suggested this increased expression of Notch targets was due to regulation of the expression of the *Jagged2* Notch ligand by AML1-ETO[168].

More recently, an interaction between MTGs and the NICD was identified[43]. This interaction occurred between Mtg16 and all four Notch receptors and localized to the very N-terminal portion of Mtg16, upstream of the conserved NHR1 region (Fig. 6B). Overexpression of the NICD disrupted the interaction between Mtg16 and CSL, suggesting a mechanism for active de-repression of CSL targets by the NICD (Fig. 6C). Loss of Mtg16 led to misregulation of some, but not all, Notch targets in hematopoietic stem and progenitor cells, including upregulation of the important Notch targets *Hes1* and *Nrarp*. Of note, these targets are also regulated by other transcription factors that interact with MTGs, including E2A, and changes to expression may not be attributed solely to disruption of Notch signaling[9].

Notch signaling is a key regulator of hematopoiesis, most specifically T-cell development. Expression of Notch ligands is an important component of the thymic

niche, and a strong Notch signal through ectopic expression of a constitutively active Notch1 is sufficient to drive T-cell development in the bone marrow[169,170]. Conversely, absence of Notch signaling through deletion of either *Notch1* or *CSL* led to a block to early T-cell development and ectopic B-cell development in the thymus[81,170,171]. ETP formation from LMPP cells also required the strong Notch signal of the thymic microenvironment[80]. Notch signaling is critical for the earliest stages of V(D)J recombination, and Notch-deficient cells were arrested at the DN3 stage due to lack of αβ T-cell receptor formation[172,173]. This was partially due to the necessary function of Notch in activating the expression of *Ptcra,* a surrogate receptor chain that pairs with a rearranged TCRβ in immature T-cells[174]. Enforced expression of *Ptcra* was not sufficient to drive *Notch1*-deficient cells through the DN3 checkpoint, confirming that additional targets must also be activated to fully restore the Notch signal necessary for T-cell development. Beyond the DN3 stage, Notch signaling is attenuated, at least in part by downregulation of *Notch1* expression[175,176].

Deletion of a transcriptional corepressor that modulates Notch signaling highlights the importance of appropriate regulation of the Notch signal in T-cell development[177]. Msx2-interacting nuclear target protein (Mint) is a CSL binding partner that competes with the NICD for binding and suppresses Notch-mediated transcriptional activation. Deletion of *Mint* led to an increase in DN1 fetal thymocytes, as expected given the role for Notch in specifying ETP generation. Surprisingly, this did not correspond to an overall increase in thymocytes, and instead coexisted with a relative decrease in DN2 cells, suggesting that an excess of Notch signal impairs the DN1 to DN2 transition. This impaired transition led instead to an overall decrease in developing

thymocyte cell number, supporting the idea that appropriate dosage of Notch signaling is critical for T-cell development.

Overactive Notch signaling plays a significant role in most T-cell neoplasms[178]. In fact, mutations in the Notch receptor that lead to ligand-independent activation or mutations in the C-terminal PEST domain that produce a more stable Notch-ICD contribute to greater than 50% of human T-cell acute lymphoblastic leukemia (T-ALL)[179]. Overexpression of constitutively active N1, N2, and N3-ICDs was sufficient to induce T-ALL after bone marrow transplant in mouse models[180-182]. More commonly, T-ALL associated mutations in NOTCH1 activate Notch signaling less aggressively than constitutive NICD expression, and produced leukemia in mouse models only in the presence of a K-Ras oncogene[183]. The resulting tumors were still addicted to the Notch signal and responsive to Notch inhibitors, though, further supporting the importance of Notch signaling in T-cell leukemia. Targeting of the Notch transcription complexes is a current goal for T-ALL therapeutics, and a better understanding of the components and dynamics of activation complexes will be useful for future therapy design. Therefore, the functional characteristics and consequences of Mtg16 interaction with Notch mediated transcription may help the targeting of Notch in T-ALL.

Notch signaling plays a controversial role in hematopoietic stem cell maintenance which is of particular interest given that *Mtg16*$^{-/-}$ stem cells have increased activation of Notch target genes[43]. Deletion of *Notch1* in mice had no effect on the long-term repopulating potential of hematopoietic stem cells, as *Notch1*$^{-/-}$ marrow contributed normally to all lineages, with the exception of T-cells, 6 months after competitive bone marrow transplant[81]. Alternate experiments suggested that Notch signaling expands

hematopoietic stem cells. More specifically, retroviral overexpression of *Hes1*, a critical downstream mediator of Notch signaling, in mouse LSK cells led to increased long term repopulating capacity after transplant[184]. Additionally, overexpression of the *Notch1*-ICD in *Rag1*$^{-/-}$ Lin^{neg}sca-1^{+} cells led to an increase in hematopoietic stem cells, shown both by an increase in stem cell number in *in vitro* long-term culture initiating cell (LTC-IC) assays and an increase in stem/progenitor pools (Lin^{neg}sca-1^{+}) *in vivo* after both primary and secondary bone marrow transplants[185]. More recently, the effect of loss of Notch signaling in hematopoietic stem cells has been examined with alternate mouse models that used overexpression of a dominant negative mastermind protein (DNMAML) or deletion of CSL[186]. Using the *Mx-cre* conditional activation system, this group showed that expression of *DNMAML*, and thus disruption of Notch signaling by all four Notch receptors, did not impair the ability of hematopoietic stem cells to maintain and self-renew long-term stem cells after transplant. Similar results were obtained after deletion of CSL, further confirming that loss of Notch signaling has little effect on hematopoietic stem cells.

While the role of Notch signaling in hematopoietic stem cells has been controversial, the impact of Notch on mature lineages other than T-cells is becoming more well defined. Megakaryopoiesis is positively regulated by Notch signaling and expression of DNMAML leads to reduced megakaryocyte numbers after transplant[187]. Notch also plays a significant role in regulating mature B-cell development in the spleen. Immature circulating B-cells that that home to the spleen can develop into either marginal zone or follicular zone B-cells. In the absence of *CSL*, there was a complete loss of

marginal zone B-cells with a corresponding increase in follicular zone cells and deletion of *Notch2* or *Delta-like 1* also led to reduced numbers of marginal zone B-cells[146,147,188].

E-proteins, Mtg16, and Hematopoiesis

While Notch signaling is critical for T-cell development, it cooperates with another Mtg16 interacting protein in specifying T-cell fate, namely the E-protein E2A[9,97]. E-proteins are also critical for B-cell development and likely contribute to Mtg16 functions in both contexts[189]. The E-protein family is a family of basic helix-loop-helix transcription factors that includes E2-2 (*Tcf4*), HeLa E-Box binding protein (HEB) (*Tcf12*), and E2A (*Tcf3*). E2A consists of dimers of two alternative splice forms, E12 and E47, encoded by the *Tcfe2a* or *Tcf3* gene. These proteins function in transcriptional regulation by binding to consensus CANNTG E-box motifs (Fig. 7). They bind DNA as homo- or heterodimers with other E-proteins and can also bind as a heterodimer with other classes of bHLH proteins, including SCL/Tal-1 and Lyl1[190,191].

E-proteins have three conserved regions: N-terminal Activation Domain 1 (AD1) and Activation Domain 2 (AD2) and the C-terminal basic-Helix-Loop-Helix (bHLH) motif that facilitates DNA binding and dimerization with other HLH proteins[192]. All three family members are highly homologous in their bHLH domains, with decreased homology in the AD1 and AD2 regions[193,194]. E-proteins can be negatively regulated by four different Inhibitor of Differentiation (ID1-4) proteins, which consist of a bHLH domain alone and dimerize with E-proteins to impair their ability to bind DNA[195,196].

Traditionally thought of as transcriptional activators, E-proteins bind p300 and histone acetyl transferases (HATs) through both their AD1 and AD2 domains[31]. Both

individual AD1 and AD2 domains activated expression of a luciferase construct in the context of gal4 fusion proteins[193,194]. In the context of full-length E12, removal of each AD domain impaired the ability of E12 to activate an E-box luciferase construct, while removal of both AD domains had an additive effect[123]. For full termination of E-box luciferase activation, though, the entire N-terminal region of E12 must be deleted.

While E-proteins function as transcriptional activators in luciferase assays, they are also capable of interacting with transcriptional corepressors, namely MTG family members (Fig. 7). Using immunoprecipitation followed by Mass-Spectrometry analysis, HEB was identified as one of two predominant ETO interacting proteins in HeLa cell lysates, with the other being Mtgr1[31]. This interaction was unusually robust and could withstand high NaCl and detergent levels. Overexpression of ETO family members converted HEB to a transcriptional repressor by reporter assay, suggesting a dual function for E-proteins in regulating transcription. E-protein repression targets are under current investigation, and to date include genes such as *Bcl2*, *Id2*, *Cebpb*, *Gata3*, and *Notch1* in early B-cells, though these genes have yet to be identified as direct MTG targets[121].

E2A is the primary family member implicated in regulating lymphoid development, playing a variety of roles throughout both B and T-cell development that coincide with the functions of Mtg16 identified in Chapters III and IV. Knockout mouse models of *E2A* led to decreased thymocyte number, due to a dose-dependent decrease in the production of LMPP cells and ETP cells and a partial arrest *in vivo* at the DN1 to DN2 transition[197-199]. E2A also regulates the DN3 β-selection checkpoint, and, in the

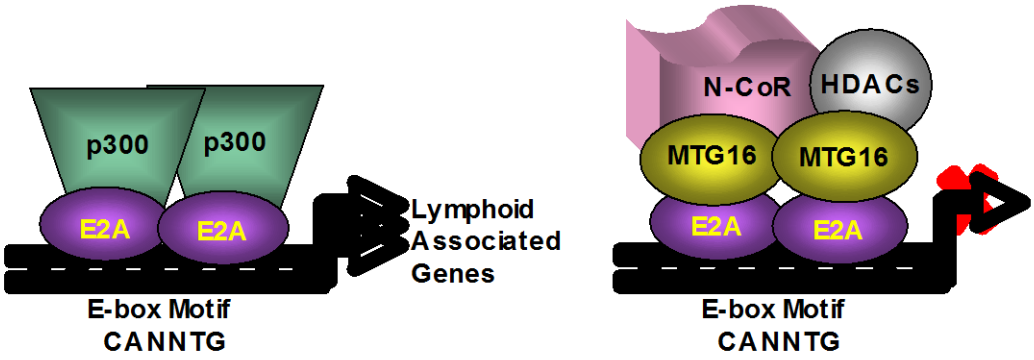

Figure 7. Mtg16 and E-protein mediated transcription bHLH E-proteins such as E2A bind promoters as dimers, recruit transcriptional activators such as p300, and activate lymphoid associated genes. E-proteins can also interact with transcriptional repressors such as Mtg16, which inhibit E-protein mediated transcription.

absence of *E47*, thymocytes escaped to the DP and $CD8^+$ stages of development even in the absence of *Rag1* expression and V(D)J recombination[200]. As part of this DN3 β-selection checkpoint, E2A negatively regulated the ability of non-TCRβ DN3 expressing cells to cycle[201].

Using *in vitro* assays that present a strong Notch signal from the Delta-like1(DL1) ligand engineered on OP9 stromal cells (OP9-DL1 cells), in concert with the lymphoid cytokine IL7, $E2A^{-/-}$ progenitors were unable to produce T-cells at all, magnifying *in vivo* phenotypes[9,74]. E2A functions in T-cell specification in part by cooperating with activated Notch signaling. Notch and E2A share common activation targets in early T-cells, including the critical T-cell modulators *Hes1* and *Ptcra*[9]. E2A also activates expression of *Notch1* itself, and defects in *in vitro* T-cell specification from $E2A^{-/-}$ progenitors were bypassed by expression of the NICD[9,202].

As previously mentioned, E2A is one of the initiating factors in specifying B-cell fate, in large part due to induction of B-cell specific genes including *EBF1* and *Pax5*[97,189]. In the absence of *E2A* virtually no mature B-cells developed, though some early Hardy Fraction A B-cells were produced[189,203]. Concurrent with the absolute arrest in Fraction A in $E2A^{-/-}$ mice were decreases in the common lymphoid progenitor cells and LMPP cells that precede B-cell commitment[198,203].

In addition to regulating expression of the B-cell lineage program, E2A regulates several parts of V(D)J recombination, including, but not limited to, expression of *Rag1* and *Rag2*, D to J rearrangement of the Ig Heavy chain locus, and Igκ light chain rearrangement. In fact, E-proteins were first identified due to their ability to bind an Igκ enhancer element[204]. In the absence of E2A, *Rag* expression was decreased relative to

wild-type controls as early as the CLP population, and no D to J rearrangement occurred in either these early cells or later Fraction A B-cells[189,203]. Ectopic expression of *Rag1* and *Rag2* in concert with *E2A* was sufficient to induce Igκ and D to J IgH rearrangements in non-lymphoid cells, further suggesting E2A controls access to and rearrangements of Ig germline DNA[205].

As E2A is necessary for B-cells to develop *in vivo*, *in vitro* assays to assess B-cell development and survival are not possible from *E2A*$^{-/-}$ mice. Therefore, primary pre-B cell cultures can only be generated using transformation methods such as the expression of Abelson Murine Leukemia Virus[206]. These *E2A*$^{-/-}$ pre-B cultures exhibited a slight G_0/G_1 arrest by Propidium iodide staining[207]. More strikingly, treatment with STI-571, which inhibits the v-Abl transforming oncogene and induces cell cycle arrest and differentiation, caused a strong increase in apoptosis. Therefore, E2A is also necessary for the *in vitro* growth and survival of developing B-cells.

E2A plays minor roles in mature B-cells of the spleen that have been discovered using conditional deletion models. E2A regulates the marginal zone vs. follicular zone cell fate decision, and deletion of *E2A* favored marginal zone development[137,148]. Germinal center development was also perturbed in the absence of *E2A*, though germinal centers could still form[137]. These germinal centers were smaller and fewer in number, and while decreased proliferation could be ruled out, the mechanism for E2A function in germinal centers is unknown.

In both B- and T-cell *in vitro* assays, E2A regulates myeloid versus lymphoid cell fate decisions. In OP9-DL1 T-cell development assays, *E2A*$^{-/-}$ progenitors failed to give rise to T-cells and instead develop into Natural Killer (NK) and granulocyte/monocyte

cells[9]. In B-cell development assays, *E2A* was necessary to suppress $Mac1^+$ macrophage development from MPP cells, and this function localized to the MTG interacting AD1 domain[123]. $E2A^{-/-}$ LMPP cells also preferentially developed along granulocyte/monocyte lineages in cultures that support multilineage myeloid potential, further supporting the hypothesis that E2A functions in part to restrict granulocyte/monocyte potential[198]. In *in vivo* competitive transplant assays, $E2A^{-/-}$ hematopoietic progenitors gave rise to a slightly increased proportion of $Gr1^+$ granulocytes, with little to no contribution to lymphocyte lineages[208].

In addition to the well-characterized roles in lymphoid development, it is becoming increasingly apparent that, like Mtg16, E2A also functions to regulate stem cell populations[208,209]. Long-term reconstitution after competitive transplant was defective in the absence of *E2A*, a phenotype that was exacerbated after secondary transplant[208]. Stem cell exhaustion in the $E2A^{-/-}$ mice was associated with an increase in cell cycling in LT-HSCs[198,208]. $E2A^{-/-}$ mice were sensitive to treatment with 5-Fluorouracil (5-FU), a cytotoxic drug that kills rapidly cycling cells. It is possible that normally quiescent LT-HSCs were also susceptible to 5-FU treatment due to an increase in active cell cycling. Additionally, the LT-HSCs may have been susceptible to stem cell exhaustion due to aberrantly increased cycling of HSCs as they repopulated hematopoietic cells[209]. The cell cycle regulator *CDKN1A (p21)* is a potential target of E2A in regulating stem cell cycling, and loss of *E2A* led to a 50% reduction in *p21* transcript levels, a phenomenon that could be reverted by re-expression of *E47* [209].

HEB is the second E-protein family member to play a role in T-cell development. Deletion of *HEB* led to a five-to-ten fold reduction in total thymocytes due to an

accumulation of both DN3 cells and immature single positive cells that exist between the DN4 and DP populations[210]. HEB and E2A form heterodimers in developing thymocytes and together regulate a number of genes including the *CD4* locus and *Ptcra*[211,212]. Conditional double deletion of both *HEB* and *E2A* resulted in a more severe thymocyte phenotype than individual *HEB* and *E2A* deletions, with a complete block to T-cell development in the DN population[213]. This block could not be localized to one particular subset, but nonetheless very few DP cells developed.

E2-2 is perhaps the least studied family member, and its best understood function is as a determinant of plasmacytoid dendritic cell development[214]. While E2A is the family member most commonly implicated in regulating B-cell development, E2-2 also appears to play a role. Mice double heterozygous for *E2A* and *E2-2* or *HEB* were deficient in B-cell development, with reduced early B-cell number[215]. Adoptive transfer of *E2-2*$^{-/-}$ fetal liver cells into *Rag2*$^{-/-}$ mice exposed a defect in early B-cell development in the absence of *E2-2*, with a two-fold reduction in both B220^{+}CD43^{-} early B-cells and B220^{+}CD43^{+} late B-cells[216]. This relatively minor defect was much more severe in the context of a competitive transplant and *in vitro* differentiation assays. Furthermore, these mice had altered marginal zone vs. follicular zone cell fate choice, with a relative increase in marginal zone mature B-cells. The role of E2-2 in thymocyte development was also subtle, with a slight DN3 block and decreased *Ptcra* expression in *E2-2*$^{-/-}$ thymocytes, though expression profiles suggest the HEB and E2A are the critical E-proteins in the thymus[217] .

Increased expression of ID family members also has deleterious effects on E-protein function and lymphocyte development. Overexpression of *Id1* led to an increase

in myelopoiesis at the expense of lymphopoiesis, increased apoptosis in early DN thymocytes, and decreased V(D)J recombination in developing B-cells, which impairs the number of mature B-cells[218-221]. Overexpression of *Id2* impaired T-cell development both *in vivo* and *in vitro*, with a block in early thymopoiesis and diversion from the T-cell lineage towards Natural Killer cells[222,223]. Deletion of *Id2* led to an increase in B-cell development and increased expression of *Id2* impaired B-cell development, confirming a negative regulatory role for Id2 in B-cell development[224]. This defect localized to the pro-B or fraction C stage. Id3 also plays a role in lymphocyte development, and overexpression of *Id3* impaired B-cell development by inducing apoptosis[225]. Therefore, E-proteins and their negative regulator Id proteins regulate a variety of stages in lymphocyte development.

MTG16 and Hematopoiesis

As detailed in the previous section, Mtg16 interacts with transcription factors that regulate a variety of hematopoietic stages. Subsequently, deletion of *Mtg16* has a significant impact on multiple facets of hematopoiesis (Fig. 8). While the transcription factors disrupted by loss of *Mtg16* vary according to the lineage, common targets exist and some of the effects are consistent across lineages. Therefore, an understanding of the consequences of *Mtg16* deletion on other hematopoietic lineages informed and contributed to the analysis in Chapters III and IV.

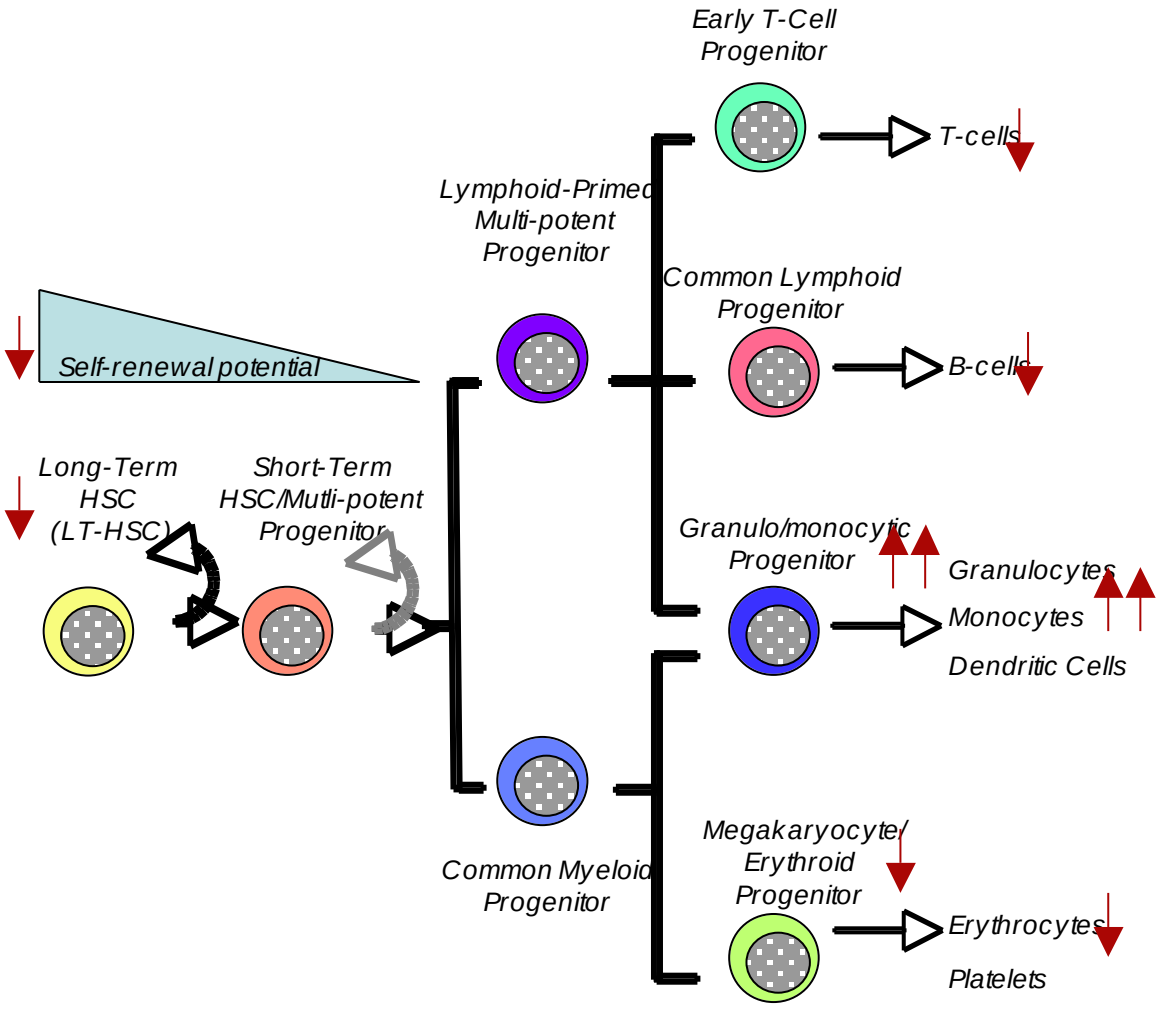

Figure 8. Effect of deletion of *Mtg16* on hematopoiesis Deletion of *Mtg16* leads to changes in several different hematopoietic populations, depicted in red.

Mtg16 and Erythroid and Myeloid Development

Mtg16 interacts with critical regulators of erythrocyte and megakaryoctye differentiation, including Stem Cell Leukemia (SCL) and GATA1[30,32,226]. In both Murine Erythroid Leukemia (MEL) cells and L0857 (Megakaryoblastic) cells, Mtg16 could be found in a complex with LMO2 and LDB1 that was nucleated by SCL, a critical regulator of both erythropoiesis and megakaryopoiesis[227,228]. This complex, which also includes GATA1 and Gfi1b in MEL cells, was readily found in immature erythrocytes but dissociated with erythroid differentiation[30]. Over-expression of Mtg16 impaired the activation of *α-Globin* and *band 4.2* as a part of erythroid differentiation and *band 4.2* is a direct repression target of Mtg16 in early erythrocytes[30,226].

Mtg16 exhibited similar functions in L0857 megakaryoblastic cells where SCL/Mtg16 complexes repressed expression of megakaryocyte differentiation genes[32]. As a consequence, short-hairpin RNA (shRNA) knockdown of *Mtg16* levels in L0857 cells increased the production of mature megakaryocytes after 12-0 tetradecanoylphorbol-13-acetate (TPA) induced differentiation. This increase in differentiation was associated with increased expression of megakaryocyte specific genes such as acetycholine esterase. Together, this over-expression and knockdown data created a strong precedence for Mtg16 to regulate erythroid and megakaryocyte differentiation through SCL complexes.

At four weeks of age, *Mtg16*$^{-/-}$ mice suffer from mild anemia and therefore exhibited an accompanying extramedullary hematopoiesis consistent with the increased need for red blood cell formation in maturing young mice[19]. In addition, there was an increase in circulating reticulocytes and Howell-Jolly bodies, immature red blood cells

that carry nuclear remnants. The anemia, increased reticulocyte count and extramedullary hematopoiesis defects corrected by 8 weeks of age, or the onset of adulthood, suggesting that after the stress period of early growth, *Mtg16*$^{-/-}$ mice were capable of reaching a homeostatic condition of sufficient red blood cell production. Despite the correction of anemia, *Mtg16*$^{-/-}$ mice still showed decreased erythroid lineage commitment by flow cytometry, as confirmed by decreased Ter119 and CD71 labeling of total bone marrow. While overall decreases in Ter119 labeling persisted, cells that did commit to the erythroid lineage were capable of differentiating normally, suggesting that the major defect in erythropoiesis in the absence of *Mtg16* is not in erythrocyte lineage development, but rather in lineage commitment.

Consistent with the finding of decreased erythrocyte commitment *in vivo*, *Mtg16*$^{-/-}$ bone marrow had an absolute inability to produce erythrocyte colonies in *in vitro* methylcellulose assays supplemented with erythropoietin[19]. This result suggests two things: one, commitment to the erythroid lineage is impaired in the absence of *Mtg16* and two, a subtle phenotype under homeostatic conditions of the *Mtg16*$^{-/-}$ mouse can become much more dramatic in response to stress. This second suggestion is a common theme in the *Mtg16*$^{-/-}$ mouse, as many of the phenotypes that occur under homeostasis, including those identified in Chapters III and IV, are magnified in response to stress.

As a further example of the impact of stress on erythropoiesis in the absence of *Mtg16*, these mice rapidly succumbed to treatment with the erythro-lytic drug phenlyhydrazine[19]. This drug lyses red blood cells and is well tolerated by wild-type mice that are capable of activating their stem and progenitor cells to proliferate and differentiate to repopulate the lost erythrocytes. In fact, five days after the first drug

administration wild-type mice had a 2-fold decrease in red blood cell number and hematocrit and a corresponding four-fold increase in the weight of the spleen as the hematopoetic system responded with extramedullary hematopoiesis. This extramedullary response rapidly repopulated the missing erythrocytes in wild-type mice. In contrast, *Mtg16*$^{-/-}$ mice were significantly more sensitive, with a near 10-fold decrease in red blood cell number and hematocrit. These mice were not capable of mounting a hematopoietic response, bone marrow or extramedullarly, as evidenced by a lack of increase in spleen size and absence of BFU-E colonies from both the bone marrow and spleen of treated mice. They could not survive the significant loss of red blood cells.

In addition to the defects in erythropoiesis, *Mtg16*$^{-/-}$ mice have changes to lineage allocation (Fig. 8)[19]. Adult null mice under homeostatic conditions have increases in Gr1^{+}/Mac1^{+} myeloid cells; these increases were further confirmed by methylcellulose assay, as *Mtg16*$^{-/-}$ marrow produced increased granulocyte and granulocyte/monocyte colonies in both complete methylcellulose supplemented with stem cell factor, IL3, IL6, and erythropoietin, and myeloid specific methylcellulose supplemented with stem cell factor, IL3, and IL6. While there were not increased monocyte colonies, normal numbers of this colony type formed. Likewise, normal megakaryocyte colonies formed in a megakaryocyte specific assay. This result was in contrast to previous reports of increases in megakaryopoiesis in the absence of *Mtg16* by shRNA knockdown[32]. Overall decreases to B220^{+} B-cell number were also observed; this phenotype will be explored in more detail in Chapter III. Collectively, initial analysis of the *Mtg16*$^{-/-}$ mouse suggested commitment to erythroid and lymphoid lineages were decreased in favor of an increase in the default myeloid pathway.

One potential contributor to the increase in myeloid $Gr1^+/Mac1^+$ cells was the aberrant production of a $CD34^{hi}FC\gamma R^{lo}$ myeloid progenitor population[19]. This c-kit^+ population rarely occurs in wild-type mice, but accounts for roughly 20% of myeloid progenitors in *Mtg16*$^{-/-}$ mice. Methylcellulose analysis of sorted populations of these abnormal cells revealed granulocyte and monocyte potential. In addition, *Mtg16*$^{-/-}$ mice have increases in common myeloid progenitors (CMPs) and granulocyte/monocyte progenitors (GMPs) but decreases in megakaryocyte/erythrocyte progenitors (MEPs) that reflect the decreased erythroid but increased granulocyte/monocyte production under homeostasis. Changes within the myeloid progenitor populations therefore contributed to the increase in $Gr1^+/Mac1^+$ cells and decreased erythroid cells.

Progenitor cell function was also altered in the absence of *Mtg16* in the setting of the colony-forming unit spleen (CFU-S) assay[19]. This assay determines the function of hematopoietic stem and progenitor cells in repopulating a lethally irradiated recipient mouse by the expansion of colonies in the spleen. At day 8 after transplant, these colonies are derived from MEP cells, while at day 12 they are derived from ST-HSCs and MPP cells. While 50,000 wild-type cells leads to the development of robust colonies both 8 and 12 days after transplant, *Mtg16*$^{-/-}$ bone marrow produced virtually no colonies at either time point. This deficit in colony formation can be rescued by re-introduction of *Mtg16* through retroviral infection. Furthermore, overexpression of the cell-cycle regulator c-Myc also rescued colony formation from *Mtg16*$^{-/-}$ bone marrow, suggesting that reduced cell cycling is the cause of absence of colonies. This data provides the first example of Mtg16 as important for cell cycling.

Gene expression profiling of both myeloid progenitor populations and overall immature hematopoietic precursors, or lineage negative cells, provided many clues to the important targets and transcription factor binding partners for Mtg16. Consistent with the function of MTGs as transcriptional corepressors, many interesting genes were upregulated in Lin^{neg} cells in the absence of *Mtg16*, though a similar number were downregulated, perhaps through off-target effects. Some of the most interesting upregulated genes were also upregulated in myeloid progenitor populations, suggesting these are common and important targets of Mtg16. Among these are cell cycle regulators such as *cyclin D1* and hematopoietic differentiation factors like *Id1, Gfi1, and Cebpb*. This gene expression data further confirms Mtg16 as an important regulator of hematopoietic development and the cell cycle.

Mtg16 and Hematopoietic Stem Cell Function

Loss of *Mtg16* also has severe effects on stem cell function (Fischer et al, in prep). In the absence of *Mtg16* long-term hematopoietic stem cells are decreased in both relative percentage and absolute number, a phenotype that becomes more pronounced with age. Stem cell function is also compromised, as assessed by bone marrow transplant. Due to the defects in erythropoiesis seen in the absence of *Mtg16*, recipient mice transplanted with $Mtg16^{-/-}$ marrow fail the transplant and die within 30 days; increasing the amount of marrow transplanted five-fold extends life to 50 days post-transplant, but is not sufficient to overcome the defect in stress erythropoiesis (Fig. 9A).

To bypass this defect and assess stem cell function, competitive bone marrow transplants were used. In this assay, 90% $CD45.2^{+}$ test marrow is supplemented with

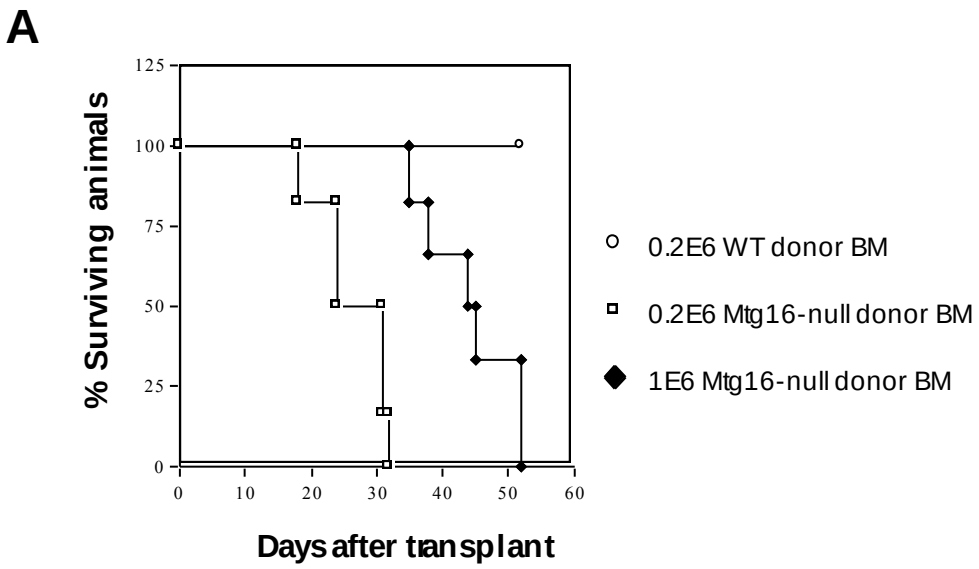

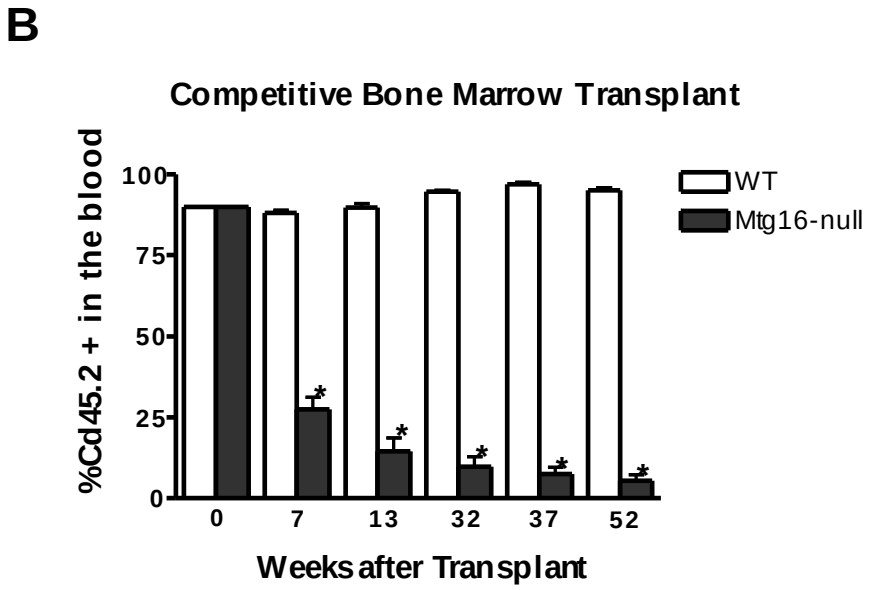

Figure 9. Defects in stem cell function in *Mtg16*$^{-/-}$ mice (A) *Mtg16*$^{-/-}$bone marrow fails to reconstitute a lethally irradiated recipient mouse, even with a five-fold increase in donor cells injected. Survival curves shown. (B) Wild-type CD45.2^{+} bone marrow contributes to peripheral blood at a consistent 90% level up to a year after transplant. CD45.2^{+}*Mtg16*$^{-/-}$bone marrow cannot compete with CD45.1^{+} wild-type bone marrow in a competitive transplant. Adapted with permission from Melissa Fischer and Scott Hiebert.

10% CD45.1^{+} wild-type marrow that is capable of providing all the necessary mature hematopoietic cells for survival. This system also allows for a baseline level of hematopoiesis and therefore removes the stress on stem cells that causes extra cycling and differentiation of hematopoietic stem cells. Instead, CD45.2^{+} test stem cells are allowed to self-renew and repopulate the stem cell compartment. In these assays, CD45.2^{+} *Mtg16*$^{-/-}$ bone marrow contributed at a much lower level to hematopoiesis than CD45.2^{+} wild-type marrow, as assessed by the percent of CD45.2^{+} cells contributing to both the peripheral blood and the bone marrow (Fig. 9B). This defect was more pronounced in the peripheral blood than associated bone marrow, due in part to decreased contribution to lymphoid lineages. Nonetheless, the contribution of *Mtg16*$^{-/-}$ stem cells to long-term hematopoietic stem cells after transplant was decreased which suggests a defect in self-renewal.

This hypothesis is further confirmed using serial replating and long-term colony-initiating cell (LT-CIC) *in vitro* stem cell assays. In both of these assays, *Mtg16*$^{-/-}$ hematopoietic stem cells exhausted much sooner than their wild-type counterparts, potentially due to either decreased self-renewal or decreased growth and survival. Other assays to directly test self-renewal were therefore performed. The most specific stem cell self-renewal assay is the secondary bone marrow transplant that assesses the repopulation capacity of stem cells after a primary transplant. Bone marrow was harvested from primary competitive transplant recipients and re-transplanted into new recipient mice. Wild-type marrow repopulated the hematopoietic system of recipients, including the production of more long-term hematopoietic stem cells after self-renewal. In contrast, *Mtg16*$^{-/-}$ marrow, regardless of the initial amount transplanted, did not contribute to

hematopoiesis in secondary recipients at all, particularly to the maintenance and expansion of LT-HSCs. Even a short time after secondary transplant, no CD45.2^{+} *Mtg16*$^{-/-}$ LT-HSCs existed, suggesting that any LT-HSCs transplanted differentiated instead of self-renewing. These phenotypes could be accounted for, at least in part, by an increase in cell-cycle entry of *Mtg16*$^{-/-}$ HSCs that leads to stem cell exhaustion and precocious differentiation *in vitro.* Mtg16 regulates a number of important cell cycle genes, including *E2F2*, and increased expression of *E2F2* can lead to increased cell cycle entry. Mtg16 was localized by chromatin immunoprecipitation to a regulatory region in intron 1 of *E2F2* that is bound by E2A, implicating *E2F2* as a direct repression target for Mtg16.

Collectively, this data highlights the importance of Mtg16 in regulating hematopoietic differentiation and the cell cycle of hematopoietic cells, particularly after stress. Given that most of the transcription factor interacting partners for Mtg16 act in multiple stages of hematopoiesis, we hypothesized that defects in hematopoiesis in the absence of *Mtg16* would extend beyond erythropoiesis and stem cell function. In particular, we were interested in how the interaction with important regulators of lymphoid development such as Notch signaling and E2A affected *Mtg16*$^{-/-}$ phenotypes. Combined with preliminary data on lineage allocation, this question led directly to the work presented in Chapters III and IV.

AML1-ETO Fusion Protein Leukemogenesis

The ultimate goals for studying Mtg16 function are twofold: one, to provide an increased understanding of basic hematopoiesis and the role of Mtg16 transcriptional

regulation in this process and two, to inform the understanding of how AML1-ETO and AML1-ETO2 fusion proteins function in cancer. While the work presented here focuses on the first aim, knowledge of AML1-ETO function informed our understanding of how endogenous MTGs function. Additionally, we hope to extend the new information generated by this dissertation to new theories on AML1-ETO function, and my hypotheses on the potential implications for fusion protein understanding will be a topic covered in Chapter V.

The AML1-ETO fusion protein results from a t(8;21) that fuses the DNA-binding Runt-homology domain (RHD) of the Runx1/AML1 transcription factor to nearly all of ETO[4]. Runx1 is a component of the Core-binding factor (CBF) complex as a heterodimer with CBFβ and binds DNA through the RHD at conserved (TGT/cGGT) sites found in many hematopoietic genes[229,230]. Runx1 binds transcriptional activators such a p300 through its C-terminus to activate transcription[14,229]. On its own, Runx1 is a weak activator of transcription, but Runx1 also facilitates the formation of much stronger transcriptional activation complexes with other transcription factors, including CEBPα and the ETS family member PU.1[231,232]. Runx1 also represses transcription through interactions with mSin3a and HDACs, and this was the dominant function of Runx1 by transcriptional reporter assay when Runx1 was expressed by itself[233,234]. The fusion protein replaces the C-terminal activation domain with the vast majority of the ETO protein. AML1-ETO recruits ETO-bound corepressors to Runx1 target sites in place of coactivators, ultimately both repressing Runx1 downstream transcription and disrupting ETO function[23,235].

It is notable that the t(8;21) fusion protein forms stable hetero-tetramers with native MTG family members[14,31]. This raises the possibility that the fusion protein recruits endogenous MTG proteins or impairs the function of endogenous MTG family members via the NHR2 domain. The NHR2 domain is the only domain of ETO within the context of the AML1-ETO fusion protein that is necessary for leukemogenesis, highlighting the importance of MTG dimerization, potentially with endogenous wild-type MTGs, to fusion protein function[236]. Given that Mtg16 is the dominant member of the MTG family expressed in hematopoietic stem cells and Mtg16 is the only family member with a knock-out hematopoietic phenotype, we are particularly interested in how disruption of Mtg16 may contribute to AML1-ETO mediated leukemia[19,48]. Furthermore, overexpression of the AML1-ETO fusion protein impaired the ability of Mtg16 to interact with NCoR, disrupting the endogenous functions of Mtg16[237]. Restoring an excess of Mtg16 by overexpression in concert with AML1-ETO overexpression disrupted the ability of the fusion protein to impair granulocyte differentiation, returning cells to normal and suggesting that the effects of AML1-ETO on hematopoietic differentiation are due, at least in part, to disruption of Mtg16 function. Therefore, understanding the normal function of Mtg16 is critical for fully understanding how the t(8;21) and t(16;21) cause AML.

AML1-ETO Fusion Protein Targets

Overexpression of AML1-ETO leads to immortalization of hematopoietic precursors, with increased self-renewal and a block to terminal granulocyte differentiation. In addition, the fusion protein causes an increase in DNA damage and

alters cellular growth and survival with increases in apoptosis and a G_0/G_1 arrest[20,238-241]. One hypothesis for the mechanism of AML1-ETO fusion protein function is disruption of Runx1 function by AML1-ETO repression of Runx1 targets. Contributing to this hypothesis is the fact that *Runx1*$^{-/-}$ mice develop a mild myelo-proliferative disorder[103]. Evidence also exists that AML1-ETO has a variety of activation targets that result from disruption of both Runx1 binding partners and ETO binding partners.

One important target for AML1-ETO mediated repression is the *p14(ARF)* tumor suppressor, which is otherwise activated by Runx1[242]. Repression of *p14(ARF)* facilitates loss of the p53 checkpoint and therefore allows immortalization of hematopoietic precursors. *Neurofibromatosis type 1 (NF-1)* is another such target activated by Runx1 and repressed by AML1-ETO, and NF-1 serves as a negative regulator of proliferation of myeloid progenitors in response to Granulocyte-Macrophage Colony Stimulating Factor (GM-CSF)[243]. Loss of NF-1 sensitizes cells to GM-CSF, leading to a myeloproliferative disorder even in *NF-1*$^{+/-}$ mice. Repression of *NF-1* levels by AML1-ETO may contribute to leukemogenesis by increasing proliferation in response to cytokines.

In addition to direct repression of Runx1 targets, the AML1-ETO fusion protein also interacts with other transcription factors and interferes with their ability to function. CEBPα is one such target, as it interacts directly with both Runx1 and the AML1-ETO fusion protein through the RHD domain[240,244]. While Runx1 and CEBPα act synergistically at promoters to enhance transcription, the AML1-ETO fusion protein impaired the ability of CEBPα to activate downstream transcription. CEBPα plays a critical role in terminal myeloid differentiation and overexpression of the fusion protein impaired the ability of granulocytes to differentiate, likely by impairing CEBPα

function[245]. One direct genetic target for CEBPα activation that is repressed by the expression of AML1-ETO is CEBPα itself, and AML1-ETO patient samples had reduced levels of CEBPα when compared to other types of AML[246]. Overexpression of CEBPα rescued differentiation of Kasumi-1 cells, a cell line that carries the t(8;21). Similarly, AML1-ETO interacted with PU.1, another AML1 binding partner and a critical transcription factor for hematopoiesis, and disrupted its functions as a transcriptional activator[247]. PU.1 exerts many of the same functions as CEBPα in hematopoiesis, and restoration of PU.1 function through overexpression also restored differentiation of Kasumi-1 cells.

Runx1 targets are not the only casualties of AML1-ETO expression; the fusion protein also interacts with many of the ETO-directed transcription factors and disrupts their function. AML1-ETO exerted inhibitory effects on PLZF, an ETO interacting factor and BTB/POZ transcriptional repressor that negatively regulates proliferation and differentiation of myeloid cells[248]. AML1-ETO blocked the function of this transcriptional repressor, partially through its ability to cause PLZF mislocalization and inhibit PLZF DNA binding, potentially leading to increased proliferation[27]. Additionally, AML1-ETO interacts with the E-protein HEB through the NHR1 domain of ETO, which led to repression of E-protein mediated transcription in luciferase assays[31]. Expression of the fusion protein caused mislocalization of HEB at new promoter targets and an overall increase in HEB protein levels[249]. This interaction had varied effects on AML1-ETO mediated leukemogenesis, as point-mutants that decrease the ability of AML1-ETO to repress E-protein mediated transcription had little impact on the ability of AML1-ETO to

repress terminal granulocyte differentiation, but did impair the ability of AML1-ETO to increase self-renewal[250].

AML1-ETO also induces upregulation of some targets indirectly, including *CDKN1A (p21)*[251]. Expression of AML1-ETO in human $CD34^+$ cord blood cells led to the accumulation of DNA damage foci (γH2Ax foci), an effect that can cause upregulation of *p21*[241,252]. This increase in *p21* has controversial effects. It may have deleterious effects for the ability of the fusion protein to induce leukemia: expression of AML1-ETO in mouse models does not induce leukemia, but, in the absence of *p21*, the fusion protein was sufficient to produce disease[251]. This data suggests that the cell cycle arrest induced by increased *p21* expression inhibited leukemia progression. Alternatively, expression of *p21* may have protective effects in stem cell populations, with p21-mediated cell cycle arrest protecting against accumulation of excessive DNA damage and preventing exhaustion of leukemia stem cells[252]. The DNA damage that accumulates in AML1-ETO expressing cells accumulates gradually, and is hypothesized to result from defects in DNA damage repair that occur as a result of repression of repair genes, such as *OGG1* and *POLE*. Alternative hypotheses driven by a potential direct role for MTG family members in DNA damage and repair are currently under investigation.

Finally, AML1-ETO can activate some target genes indirectly by disrupting the ability of transcription factors to interact with NCoR and other corepressors (Moore et al in revision). Over-expression of AML1-ETO activates a Tcf4 dependent transcription assay (TOP-FLASH) and does so by impairing the ability of Tcf4 to interact with co-repressors. Similar interaction data is obtained with Gfi-1, as expression of AML1-ETO impairs its ability to bind NCoR as well. AML1-ETO blocks the ability of Mtg16 to

interact with NCoR, a function that affects AML1-ETO's ability to repress granulocyte differentiation.

Effect of AML1-ETO Expression on Hematopoiesis and Leukemogenesis

To better understand how AML1-ETO expression leads to leukemia, several groups have developed knock-in mouse models for AML1-ETO expression. Knock-in of AML1-ETO in the Runx1 locus produced a phenotype much like Runx1 knockout mice with embryonic lethality from lack of definitive hematopoiesis[253,254]. Given the absolute requirement for Runx1 in definitive hematopoiesis, this phenotype is likely just an alternate form of a *Runx1*$^{-/-}$ mouse. Using an alternative locus for knock-in shows that expression of AML1-ETO alone is not sufficient to induce leukemia. A tetracycline-off system driving AML1-ETO expression in mice shows no formation of leukemia as a result of the expression of AML1-ETO[239]. AML1-ETO expressing bone marrow cells were grossly normal, with normal hematopoietic lineage allocation by both flow-cytometry and methylcellulose colony assays. However, AML1-ETO bone marrow cells had increased replating efficiency by methylcellulose serial replating assays, producing colonies through at least 13 rounds of replating, compared to 3 for wild-type controls. The colonies were composed of immature myeloid cells, and showed a delay in myeloid maturation that could be reverted by loss of AML1-ETO expression, which caused differentiation of the immature myeloid cells and loss of replating ability. Collectively, this data indicates an effect on general hematopoiesis short of leukemia by the presence of AML1-ETO.

Mice that express the fusion-protein under the direction of the human MRP8 promoter, and therefore in myeloid (neutrophil and monocyte) lineages, also do not develop leukemia as a result of AML1-ETO expression[255]. When these mice were treated with the DNA-alkylating agent N-ethyl-N-nitrosourea (ENU) to provide second-hit mutagenesis, though, both transgenic and wild-type controls developed leukemia and were sacrificed within seven months after initiating ENU treatment. However, wild-type mice and half of the AML1-ETO transgenic mice developed acute lymphocytic leukemia (ALL) while only AML1-ETO transgenic mice developed acute myeloid leukemia. These leukemias were comprised of immature myeloid cells and had an increased latency when compared to ALL disease. With lower doses of ENU, transgenic mice developed an accumulation of immature myeloid progenitors skewed away from the Megakaryocyte/Erythrocyte Progenitor (MEP) population, suggesting an expanding precursor cell population with granulocyte/monocyte skewing prior to the development of full-blown myeloid leukemia. Similar results were obtained with a different AML1-ETO expression model[256].

Retroviral overexpression of the AML1-ETO fusion protein in bone marrow cells prior to transplant likewise does not lead to leukemia, but does have a strong effect on lineage allocation and differentiation[257,258]. The presence of the fusion protein reduced development of transduced B and T lymphocytes to 13% and 3% of control cells, respectively, in one model[257]. Contributing to this phenotype was a block of B-cell development from immature to mature recirculating B-cells (Fractions E to F). AML1-ETO expressing cells also showed defects in erythropoiesis and increases in granulopoiesis, a phenotype similar to the loss of *Mtg16*. The increased granulocytes

were of an immature type, lacking terminal differentiation[258] . Finally, overexpression of AML1-ETO affected the self-renewal potential of hematopoietic stem cells, as AML1-ETO expressing marrow showed a strong increase in HSC number, but a decrease in contribution to mature cells after transplant[258].

Perhaps the most faithful model of AML1-ETO mediated leukemogenesis is one where AML1-ETO expression is targeted to hematopoietic stem cells using the Sca-1 promoter for knock-in[259]. Studies of samples from patients who were in remission confirmed that the fusion protein is present in hematopoietic stem cells that can give rise to multiple lineages, suggesting that the stem cell compartment is the place of origin for t(8;21) mediated leukemia[260]. Like similar overexpression models, lymphopoesis was affected by the presence of AML1-ETO expression in stem cells from the Sca-1 promoter; in this model, though, surviving developing lymphocytes reduced expression of AML1-ETO significantly to bypass the deleterious effects of AML1-ETO of B and T-cell development. Granulocyte skewing was also seen with AML1-ETO expression. Ultimately this increase in granulopoiesis led to a myeloproliferative disorder, highlighting the importance of cell-type specific expression in recapitulating *in vivo* models.

Structure/Function Analysis of AML1-ETO

Structure function analysis of AML1-ETO has identified important functions for many conserved regions of the protein in inducing leukemogenesis. C-terminal NHR3 and NHR4 are not only dispensable for leukemogenesis, but may also be inhibitory, as AML1-ETO truncation mutants that removed these regions were capable of inducing

leukemia in the absence of a second hit[261]. C-terminal deletion of AML1-ETO negatively affected the ability of the fusion protein to induce cell-cycle arrest in G_0/G_1, suggesting that NHR3 and/or NHR4 play a role in cell cycle regulation. *Cyclin D3*, *Cyclin A*, and *Cyclin Dependent Kinase 4* levels were decreased by the presence of full-length AML1-ETO but not by the c-terminal truncation form, providing possible targets for differential regulation that contribute to the different phenotypes seen by the two isoforms of AML1-ETO.

Further deletion analysis showed that removal of NHR4 alone was sufficient to increase the leukemogenic potential of AML1-ETO and in fact mutation of a single residue in NHR4 (C663S) that abrogates the Zn-chelating structure of NHR4 conferred the same enhanced potential on AML1-ETO[262]. This region and, specifically, this mutated residue facilitate interaction with SON, a protein that facilitates RNA splicing[263]. SON is nuclear protein that is necessary for cell cycle progression, as knockdown of SON led to cell cycle arrest in mitosis due to spindle defects. Therefore, the full-length AML1-ETO isoform may interact with SON and block it's ability to enhance cell cycle progression, leading to the cell cycle arrest seen in the presence of the fusion protein. Deletion of this interacting domain reversed this phenomenon, restoring cell growth even in the presence of the rest of AML1-ETO.

An alternative splice isoform of AML1-ETO was identified in 2006 that removes the 9th through 11th exons of Mtg8 by introducing a stop codon after the 8^{th} exon[264]. The alternative fusion protein, termed AML1-ETO9a, is 575 amino acids, as opposed to the 752 amino acids of the full-length fusion protein, and no longer contains NHR3 or NHR4. Found in patient samples alongside full-length AML1-ETO at varying ratios,

AML1-ETO9a induced acute myeloid leukemia in mice within 16 weeks post-transplant. This is particularly interesting given that expression of full-length AML1-ETO was not capable of inducing leukemia in the absence of a secondary mutation and corresponds with reports that a C-terminal truncation mutant of AML1-ETO that artificially removes the NHR3 and NHR4 regions also induced leukemia without a secondary hit [255,261]. Co-expression of both full length and 9a isoforms, mimicking the physiologic conditions found in most patient samples, was strongly leukemogenic, and even more effective in inducing leukemia than expression of each construct alone. Co-expression shortened the leukemia latency from 16 weeks for AML1-ETO9a alone to just five weeks. The cell types comprising the leukemia differed according to the isoforms of AML1-ETO expressed. AML1-ETO9a alone leukemias were 30% myeloid progenitor cells, or $Lin^{neg}sca1^{-}c\text{-}kit^{+}$, and fell within an abnormal $FC\gamma RII/III^{med}CD34^{-}$ population. AML1-ETO9a and AML1-ETO co-expressing leukemias were more like patient samples, with over 60% myeloid progenitor cells contained diffusely across normal myeloid progenitor populations ($Fc\gamma RII/III^{lo\text{-}high}CD34^{+}$) and also contained a higher amount of hematopoietic stem/progenitor cells (20% $Lin^{neg}sca\text{-}1^{+}c\text{-}kit^{+}$). While deletion of NHR3 and NHR4 is known to delete interaction with SON and corepressors such as NCoR, other regions of MTGs can also recruit NCoR, and therefore corepressor function is retained. Alternative binding partners for the C-terminal NHR3 and NHR4 regions that may contribute to this phenotype are under current investigation.

In the context of the AML1-ETO9a isoform that produces leukemia *in vivo* the contribution of other conserved regions to leukemia initiation and progression can be assessed. DNA binding by the AML RHD domain and oligomerization by the NHR2

dimerization domain were both necessary for AML1-ETO9a to induce leukemia while the presence of NHR1 was dispensable for leukemia formation[236]. Furthermore, CBFβ binding and DNA binding are critical for AML1-ETO to function in disrupting hematopoiesis and inducing leukemia in concert with the TEL-PDGFβR fusion protein as a second hit[265]. Therefore, NHR3 and 4 contribute to the function of AML1-ETO in a negative regulatory role, while NHR2 and the RHD are indispensable for AML1-ETO leukemia. The contribution of NHR1 has yet to be determined.

Associated Mutations in AML1-ETO Leukemia

Mouse models of AML1-ETO leukemia show that AML1-ETO expression alone is not sufficient to induce leukemia. Furthermore, second-hit mutations generated by ENU treatment in the presence of AML1-ETO can help induce myeloid leukemia. Therefore, several groups have investigated the nature of cooperating mutations in AML1-ETO driven AML. The second-hit necessary *in vivo* to produce AML in the presence of the fusion protein is not p53 mutation, as p53 was not found to be mutated in primary t(8;21) AML samples[266]. This result is surprising given that deletion of *p21* allowed AML1-ETO to induce leukemia in mouse models[251]. The most common type of second-hit mutation occurs in signal transduction pathways, including receptor tyrosine kinases Flt3 and Kit[267]. In a study of 135 patients with AML1-ETO translocation associated AML, 18.5% carried activating mutations in Flt3 or Kit. Another 9.6% had activating mutations in NRAS. Mouse bone marrow transplant models expressing AML1-ETO or mutant Flt3 alone did not develop leukemia, while all recipients who received AML1-ETO^{+}/Activated-Flt3^{+} bone marrow developed an acute leukemia,

confirming that AML1-ETO and Flt3 activating mutations can cooperate in the pathogenesis of AML. This leukemia was not a 100% faithful recapitulation of AML, though, as half of the recipient mice developed ALL instead of AML. Further analysis of patient samples with the AML1-ETO fusion protein showed expression of some lymphocyte markers, though, suggesting that immature AML cells from AML1-ETO patients may be a mixed myeloid/lymphoid lineage. Recent evidence shows that classic Ras mutations (NRasG12D) can enhance transformation of AML1-ETO expressing cells, as evidenced by increased self-renewal and cytokine independent growth, though no evidence of leukemia in mouse engraftment models was shown[268]. Activating C-kit mutations, which are frequently seen in AML1-ETO driven AML, can cooperate with AML1-ETO to induce myeloid leukemia in mouse models[269]. Importantly, these myeloid leukemias were responsive to tyrosine kinase inhibitors, suggesting a potential therapeutic avenue for AML1-ETO AML with cooperating c-Kit mutations.

Conclusions

Mtg16 is a transcriptional corepressor that does not bind DNA directly, but instead binds DNA-binding transcription factors, many of which are important for hematopoiesis. Among the list of transcription factor binding partners for Mtg16 are many that are involved in B- and T-cell development, including CSL and the NICD of the Notch signaling cascade, E-proteins such as E2A, HEB, and E2-2, and Bcl6. Disruption of Mtg16 in knockout mouse models led to altered lineage allocation with increased granulopoiesis, decreased lymphopoiesis, and impaired erythropoiesis. Mtg16 also

regulates hematopoietic stem cell function, and loss of *Mtg16* impaired the ability of LT-HSC cells to self-renew. These *Mtg16*$^{-/-}$ phenotypes are more severe after stress and are often associated with alterations to cell growth and survival.

Disruption of MTG family members by chromosomal translocations leads to AML1-ETO fusion proteins and leukemia. The function of the fusion protein requires the ability to dimerize with other MTG family members. Furthermore, over-expression of AML1-ETO impairs lymphoid development and causes skewing towards immature granulocyte/monocyte lineages with increased self-renewal capacity. Therefore, in an attempt to better understand Mtg16 contribution to AML1-ETO and AML1-ETO2 fusion protein mediated leukemia, we study *Mtg16*$^{-/-}$ mouse models. Given the number of transcription factors Mtg16 binds, particularly those that are involved in lymphoid development, and the precedence for targets of chromosomal translocations in leukemia to be involved with several different facets of hematopoiesis, we hypothesized that Mtg16 would play a role in regulating lymphoid development. In Chapter III, the role of Mtg16 in T-cell development is explored: ultimately, *Mtg16* is required for efficient murine T-cell development and it functions in part to regulate both Notch and E2A expression functions. In Chapter IV, this analysis is extended to murine B-cell development, with the surprising finding that Mtg16 contributes to not only early B-lineage fate decisions, but also mature immune function. Hypotheses of the impact of these novel findings on understanding AML1-ETO function will be presented in Chapter V.

CHAPTER II

MATERIALS AND METHODS

Mice

Generation of *Mtg16*-null mice was previously described [19]. For studies shown here, *Mtg16*-null mice were backcrossed into the C57Bl/6 background for ten generations. Mouse genotyping was performed as follows: anesthetized mice were labeled by ear punch and the distal portion of the tail was removed. The tail portion was placed in 500μl of Jeffers Tail Mix (0.1M Tris, pH 8.0; 5mM EDTA, 0.2% SDS, and 0.2M NaCl) supplemented with 250μg Proteinase K over night at 55^{o}C. The digested tail remnants were collected by centrifugation and the supernatant was transferred to a new tube. 800μl of ice cold isopropanol were added to the tail DNA solution and this suspension was placed on ice for 30 minutes. The DNA was pelleted by a 10 minute centrifugation at maximum speed, followed by two 100% EtOH washes. The pelleted DNA was allowed to air dry, then resuspended in 100μl of TE.

Genotyping Polymerase Chain Reactions (PCRs) were performed with two PCRs, one that identified a wild-type band between exons 8 and 9 of 704 base pairs (primer pair 129T forward and 130B reverse) and one that identified a wild-type band spanning exon 7 to 9 of 1.4kb and a null band of 280 base pairs that no longer contains exon 8 (primer pair 135T forward and 130B reverse). The primer sequences are as follows:

130B 5'-GTCCATGATGCAGTTCAGAAG-3';

129T 5'-CTGGGTCTCGACAAGAAGAAGTG-3';

135T 5’-GATGCAAGAACTAGGCAGGGTT-3’.

PCRs were performed with GoTaq Flexi Taq polymerase and the following cycle parameters: 1 Cycle 94^{o}C 5 minutes, 55^{o}C 1 minute, 72^{o}C 1.5 minutes; 30 cycles 94^{o}C 1 minute, 55^{o}C 45 seconds, 72^{o}C 1.5 minutes; and 1 cycle 72^{o}C 10 minutes. PCR products were visualized on 1-2% agarose gels. Sex and age matched wild-type and *Mtg16*$^{-/-}$ mice were used between 6 and 8 weeks of age unless otherwise noted.

Plasmids

The E-protein point mutant plasmids were generated using QuickChange II XL Site Directed Mutagenesis Kit (Agilent Technologies). Primers were designed based upon the structure of the Eto-HEB interaction [270] to mimic the following mutations: F210A-F154A and R220A-R164A.

F210A:

Forward: 5’ CACTGAGGCCGTTTGTTATCCCTGCTCTGAAGGCTAATCTT 3’

Reverse: 5’ AAGATTAGCCTTCAGAGCAGGGATAACAAACGGCCTCAGTG 3’

R220A:

Forward: 5’ CTTCCACTGCTGCAGGCTGAGCTCCTGCACTG 3’

Reverse: 5’ CAGTGCAGGAGCTCAGCCTGCAGCAGTGGAAG 3’

MSCV-Id1 and *MSCV-Id2* were generous gifts of Dr. Jonathan Keller. Fragments of Mtg16 deleted from the 5’- or 3’- ends were generated by PCR amplification and assembled in appropriate combinations to create interstitial deletion mutants ΔNHR1, ΔNHR2, ΔNHR3, ΔNHR4, ΔPST2, and ΔNHR1-PST2. Fragments were subcloned into *EcoR1/XhoI* restricted *MSCV* or *pCMV5* for use in terminal experiments. The regions

deleted in each mutant were as follows: ΔNICD deleted amino acids 1-85, ΔNHR1 deleted amino acids 145 to 242, ΔNHR2 deleted amino acids 365 to 402, ΔNHR3 deleted amino acids 460 to 510, ΔNHR4 deleted amino acids 532 to 567, ΔPST2 deleted amino acids 242 to 364, and ΔNHR1-PST2 deleted amino acids 145 to 364.

Cell Culture and Expression Analysis

Bosc23, Cos7, and 293T cells were cultured in Dulbecco's modified Eagle Medium (DMEM) supplemented with 10% fetal bovine serum (FBS), 50 U/ml Penicillin, 50 μg/ml streptomycin, and 2mM L-glutamine. MEL cells are grown in DMEM supplemented with 10% FBS, 50 U/ml Penicillin, 50 μg/ml streptomycin. Plating densities for MEL cells ranged between $1x\ 10^5$ and $2\ x\ 10^5$ and cells should not become more confluent than $2\ x\ 10^6$. OP9 and OP9-DL1 stromal cells were cultured in α-MEM (GIBCO) supplemented with 20% heat-inactivated FBS, 50 U/ml Penicillin, 50 μg/ml Streptomycin. OP9 cells were passaged at less than 80% confluency to preserve expression of the DL1 ligand. Expression from *MSCV-IRES-GFP* plasmids was confirmed after transfection of 3 μg of plasmid into Bosc23 viral producing cells with Polyfect (Qiagen). 48 hours post-transfection, cells were harvested into Radio-immune precipitation assay (RIPA) buffer (50mM Tris, 150mM NaCl, 1% NP-40, 0.25% Na-deoxycholate, 1mM EDTA, pH 7.4) containing protease inhibitor cocktail (Roche) and diluted 1:2 in Laemmli's Sample Buffer (Bio-Rad), sonicated, and subjected to 10% sodium dodecyl sulfate polyacrylamide gel electrophoresis. Immunoblots were performed using anti-Myc 9E10 antibody (1:2000), with GAPDH expression (AbCam) as

a loading control. Expressed proteins were visualized using fluorophore-conjugated secondary antibodies (1:3000) and the Odyssey system (LiCor).

Flow Cytometry and Cell Sorting

Single cell suspensions were formed after flushing the tibia and/or femur with PBS to collect bone marrow cells or mincing the spleen or thymus and passing the fragments through a 70 μM filter. Erythrocytes were lysed with 1mL Buffer EL (Qiagen) for five to ten minutes on ice. Antibody staining for flow cytometry was carried out on 1 x 10^6 cells in single wells of a round-bottom 96-well plate for 15 minutes at 4^0C in the dark. For lineage labeling, cells were stained with biotinylated antibodies directed toward lineage-specific cell surface markers (CD3, B220, Gr1, Mac1, and Ter119 eBioscience), followed by fluorochrome-conjugated streptavidin. For all other flow cytometry, cells were labeled with the appropriate combination of fluorochrome – conjugated anti-c-Kit, anti-Sca-1, anti-FLT3, anti-IL7R, anti-CD44, anti-CD25, anti-CD4, anti-CD8, anti-GR-1, anti-Mac-1, anti-B220, anti-CD43, anti-IgM, anti-BP-1, anti-CD24, anti-CD21, and anti-CD23 (eBioscience). Biotinylated anti-IgD, anti-AA4.1, and anti-γδ T-cell Receptor were used followed by fluorochrome conjugated streptavidin (eBioscience). Analysis was performed on a 3-Laser BD LSR II using FACSDiva software. For rare populations of cells, bone marrow samples were first lineage-depleted using a lineage depletion kit and magnetic cell sorting (Miltenyi Biotec). For rare thymocyte populations, thymi were lineage depleted using a biotinylated lineage panel as above supplemented with biotinylated anti-CD4 and anti-CD8 (eBioscience), followed by

anti-Biotin microbeads and magnetic cell sorting (Miltenyi Biotec). Sorting of hematopoietic cell populations was performed on the BD FACSAria.

Murine MTG Family Member Expression Analysis

Expression of individual genes was measured using reverse transcriptase PCR, with total RNA isolated using the 5Prime PerfectPure RNA extraction kit from sorted populations of cells. The Reverse Transcriptase step was carried out using 100-200ng total RNA per 20μl iScript (BioRad) cDNA synthesis reaction; ¼ of the reaction was used for PCR using the iQ Sybr Green SuperMix (BioRad) with GAPDH as an internal control. PCR reactions were performed in duplicate.

mMtg8F: 5'-ATTTACGCCAACGACATTAACGA-3';

mMtg8R: 5'-CTGAGTTGCCTAGCACCACA-3';

mMtgr1F: 5'-ACCTGGCCCAGCATGAGC-3';

mMtgr1R: 5'-AATGTCTTCTAGTGTATAGTGC-3';

mMtg16F: 5'-CCACGGCTGCTTAAAGTGGT-3';

mMtg16R: 5'-GTCATTGCCAAATTGCTGTAGG-3'

GAPDHF: 5'-GCCTTCCGTGTTCCTACCC-3';

GAPDHR: 5'-TGCCTGCTTCACCACCTTC-3'.

In vitro Differentiation Assays

The indicated sorted populations of cells were plated on irradiated (20gy), confluent OP9-DL1 stromal cells in Alpha-MEM (GIBCO) supplemented with 20% FBS, 50 U/ml Penicillin, 50 μg/ml Streptomycin, 5 ng/ml IL-7 (Peprotech) and 5ng/ml Flt3L

(Peprotech.) Initial plating densities ranged from 500-4000 cells per well of a 24-well plate. The hematopoietic cells were collected by manual dissociation, counted, and passaged every 4-7 days onto a fresh stromal layer at concentrations less than 5×10^5 cells per well. T-cell differentiation was assessed every 7 days for 4 weeks by flow cytometry.

Cell Cycle Analysis

Cell cycle analysis of hematopoietic cells co-cultured with OP9-DL1 cells or in M3630 methylcellulose was performed using propidium iodide staining of genomic DNA. Cells were collected from culture, washed with PBS, and counted. Collected cells were fixed in 70% EtOH overnight at -20^{o} C. The following day, samples were spun to collect and the EtOH was removed; a PBS wash was performed to remove residual ethanol. Washed, fixed cells were treated with 0.1% Triton-X100, 20 µg/ml Propidium Iodide (Sigma), 0.1mg/ml RNase A (USB) in 500µl Phosphate Buffered Saline (PBS) for 30 minutes at room temperature prior to FACS analysis.

Annexin V Staining

Annexin V analysis on hematopoietic cells co-cultured with OP9-DL1 stromal cells or M3630 methylcellulose was performed using the Annexin V-FITC Apoptosis Detection Kit I (BD Pharmingen) per the manufacturer's instructions. Briefly, *in vitro* cells were collected from day 7 OP9-DL1 or methylcellulose cultures, washed in PBS, and counted. Cells were resuspended in Annexin V Binding Buffer at a concentration of 1×10^6/mL and labeled with Annexin V FITC (5µl per 100µl sample) for 15 minutes at

room temperature in the dark then filtered through a filter cap tube and analyzed by flow cytometry. Where possible, PI stain (5μl per 100μl sample) was added immediately prior to flow cytometry.

Retroviral expression

MSCV-myc-Eto2-GFP and variants, *MSCV-Id1-GFP*, and *MSCV-Id2-GFP* were transfected into Bosc23 viral producing cells at a concentration of 3μg per 60mm plate and supplemented with 1μg of pCL to facilitate viral packaging. Viral supernatant was collected 48 hours post-transfection and filtered through a 45 μm syringe filter (Nalgene). Sorted LSK cells were centrifuged at 1500rpm for 1 hour at room temperature with viral supernatant prior to co-culture with OP9 or OP9-DL1 stromal cells. Infection was monitored using flow cytometry to detect GFP expression.

Transcription Assays

Luciferase reporter assays were performed in 293T cells transfected with the indicated plasmids. Luciferase values were assessed from an E-box reporter plasmid, a generous gift of Dr. Robert Roeder. For each transfection, equivalent amounts of E-box luciferase and Renilla luciferase and the appropriate combinations of test plasmids or empty vector plasmids were mixed to achieve the same amount of total DNA transfected. Transfections were carried out using Polyfect (Qiagen). 48 hours post transfection, cells were lysed with Passive Lysis Buffer from the Promega Dual-Luciferase Reporter Assay System and luciferase activity was measured on a BD Pharmingen Monolight 3010 luminometer using 10 second exposures for both the first reading (Firefly luciferase) and

the second reading (Renilla luciferase). All values were performed in triplicate and normalized to a Renilla Luciferase internal control.

Co-immunoprecipitation assays

Cos7 cells were transfected with the indicated combinations of plasmids and 40 hr later the cells were washed with PBS and harvested into HERR buffer (100mM KCl, 0.02M Hepes pH7.9, 0.002M EDTA, 0.1% NP-40, 10% Glycerol) supplemented with a Protease Inhibitor Cocktail (Roche). For Mtg16-E47 interactions, 600mM KCl HERR was used. For Mtg16-NICD interactions, 100mM KCl HERR was used. Lysates were sonicated with three short pulses at 4.5 watts and cleared by centrifugation for 10 minutes at 4^0C at maximum speed. Immunoprecipitation of lysates was performed for 2-3 hours nutating at room temperature using anti-Myc 9E10 for Mtg16-E47 interactions and the Flag M2 antibody (Sigma) for Mtg16-NICD interactions. Immune complexes were collected using 30μl of a 50% slurry of protein G sepharose 4B (Sigma). Co-precipitating proteins and whole cell lysates were subjected to 10% sodium dodecyl sulfate polyacrylamide gel electrophoresis and identified by immunoblot analysis of immune complexes using anti-Myc 9E10 (1:2000), anti-Flag M2 (1:3000), and anti-E47 sc-763 (1:400) (Santa Cruz).

Bone marrow transplant-CFU-S

Bone marrow was harvested from two hind legs from wild-type and *Mtg16*$^{-/-}$ mice and a sterile single cell suspension was created. Red blood cells were lysed and total bone marrow cells were plated in DMEM supplemented with heat-inactivated ES-cell

FBS, 50 U/ml Penicillin, 50 μg/ml streptomycin, and 2mM L-glutamine, 50ng/ml stem cell factor (SCF), 5ng/ml IL-6, and 10^3U/ml leukemia inhibitory factor (LIF). To ensure all conditions received the same *Mtg16*$^{-/-}$ donor cells, multiple mice were pooled and equivalent numbers of cells were used for each condition. The next day, cells were transferred onto irradiated (30gy) Bosc23 cells transfected with the appropriate MSCV reconstitution plasmids or MSCV empty vector and incubated for 48 hours to allow for infection. Bone marrow cells were collected, counted, and resuspended in PBS to allow for injection of 300μl total volume by tail vein injection into lethally irradiated recipients (900 rads). For wild-type controls, 5 x 10^4 cells were injected. For *Mtg16*$^{-/-}$ cells of the various conditions, 4 to 5 x 10^5 cells were injected, depending on the experiment. Mice were placed on acidified water and monitored for twelve days. On day 12, spleens were harvested and fixed in Tellesniczky's's Fixative (75% EtOH, 3.75% Acetic acid, and 7.5% Formalin) to allow for visualization of spleen colonies.

Competitive Bone Marrow Transplants

For competitive reconstitution assays, a sterile single cell suspension of bone marrow cells was obtained from the tibia and femur, and the red blood cells were lysed with erythrocyte lysis buffer (Buffer EL, Qiagen). Bone marrow cells were injected via the tail vein into lethally irradiated (900 rads) recipient C57Bl/6 CD45.1 congenic mice. The *Mtg16*$^{+/+}$ or *Mtg16*$^{-/-}$ donor cells were mixed with C57Bl/6 CD45.1 wild-type bone marrow cells (9:1) in PBS, with a final total of 1.8 x 10^6 CD45.2$^+$ test cells and 2 x 10^5 CD45.1$^+$ competitive cells. Reconstitution potential of the donor (CD45.2) cells was

monitored by flow cytometry of the peripheral blood every two to four weeks and analysis of the bone marrow, thymus, and spleen at the end of the experiment.

Chromatin Immunoprecipitation Assays.

Chromatin Immunoprecipitation (ChIP) assays were performed using Murine Erythroleukemia (MEL) cells. 1 x 10^7 cells per condition were crosslinked with 1% Formaldehyde (Sigma) for 20 minutes and the crosslinking reaction was quenched by the addition of glycine to a final concentration of 125mM for 5 minutes. Cells were collected, washed, and resuspended in a low salt ChIP buffer (50mM HEPES KOH, ph7.5, 140mM NaCl, 1mM EDTA pH8.0, 1% Triton X-100, and 0.1% Sodium Deoxycholate). Samples were sonicated and cleared by centrifugation for 15 minutes at maximum speed at 4^0C. Protein estimations were performed using the DC Protein Assay (BioRad) per the manufactures instructions and equivalent amounts of protein were allocated to each antibody conditions. 5% of each sample was saved overnight at -20^0C for input controls, then subjected to reverse crosslinking and all subsequent steps. Samples were then precleared with the addition of Protein G Sepharose 4B (Sigma). Samples were incubated over-night with 6μg either Goat IgG (Santa Cruz) or anti-Eto2 G20 (Santa Cruz). Immune complexes were collected by incubation with a 50% slurry of Protein G Sepharose 4B (Sigma) then washed with a low salt ChIP buffer, a high salt ChIP buffer (50mM HEPES KOH pH7.5, 500mM NaCl, 1mM EDTA pH8.0, 1% Triton X-100, and 0.1% Sodium Deoxycholate) and Lithium Chloride/NP40 buffer (10mM TrisCl, pH8.0, 250mM LiCl, 0.5% NP-40, 0.5% Sodium Deoxycholate). DNA-antibody complexes were eluted with elution buffer (1% SDS and 100mM Sodium Bicarbonate)

and the crosslink was reversed with 200 µM NaCl at 65^{o}C for 5 hours. DNA was precipitated with the addition of 100% EtOH and incubation over-night at -20^{0}, RNase treated (Macherey-Nagel), Proteinase K (Sigma) treated, and isolated using the Qiagen PCR Purification kit. RT-PCR was performed with 2 µl of each sample in duplicate using SybrGreen (BioRad) and the BioRad ICycler and normalized to input. Primer sequences are as follows:

E2F2 Intron 1: F- 5'-GGACTCTGGAGGGCTAATGTTG-3'

R-5'-GCAATGTCTTCACTCGGCTCGG-3'

E2F2 Intron 2: F-5'TCAGACAGATGAGCGGGGAGGTG-3'

R-5'-GCCTCTGCCAGCCGCTTGAAA-3'

E2F2 3' UTR F-5'-TGGTTTCCCCTCCCTGTGAGGC-3'

R-5'-AGACCTGTAGCCACCACGGTCC-3'

CCND1 TCF F-5'-CTGCCCGGCTTTGATCTCT-3'

R-5'-AGGACTTTGCAACTTCAACAAAACT-3'

CCND1 EBox/CSL F-5'-CTGGTCTGGCATCTTCGG-3'

R-5'-GAGAATGGGTGCGTTTCCG-3'

NMyc F-5'-CCCGAATGCCTACATAATTCT-3'

R-5'CCTTGGAAGGGTGGCTCA-3'

Mtg16 F-5'-AATATTCACAGGGCCTGACCAA-3'

R-5'-AAATGCCTGCAAGCGGATTA-3'

LPS Stimulation

$B220^+$ populations were created by labeling total spleen suspensions with B220-biotin (eBioscience) followed by anti-Biotin magnetic microbeads and magnetic cell separation (Miltenyi Biotec). Total splenic cell populations or $B220^+$ positively-selected populations were cultured in 96-well round bottom dishes at 100,000 cells/well in a total volume of 200μl in Roswell Park Memorial Institute (RPMI) media, 10% FBS, 50 U/ml Penicillin, 50 μg/ml streptomycin, and 2mM L-glutamine. Wells were supplemented with LPS (Sigma) at 20μg/mL for three days. At 24 hour intervals, alamar blue (Invitrogen) was added to the wells at 10% of total well volume, incubated for 4-6 hours, and read using a Biotek plate reader and the Gen5 program (Biotek) to assess cell viability.

V(D)J Recombination PCR

V(D)J recombination was assessed by PCR in total bone marrow $B220^+$ cells collected by magnetic cell sorting. Total genomic DNA was collected using the DNeasy Blood and Tissue Kit (Qiagen) per the manufacturer's instructions and equivalent amounts of DNA (500ng) were used for each of 4 PCRs: D_H to J_H, V_{H558} to J_H , V_{H7183} to J_H, and C_{Mu} heavy chain loading control. PCR primers are as follows:

D_H Forward: 5'-TTCAAAGCACAATGCCTGGCT-3'

V_{H558} Forward: 5'-CGAGCTCTCCARCACAGCCTWCATG-3'

V_{H7183} Forward: 5'-CGGTACCAAGAASAMCCTGTWCCTG-3'

J_H Reverse: 5'-GTCTAGATTCTCACAAGAGTCCGATA-3'

C_{mu} Forward: 5'-TGGCCATGGGCTGCCTAGCCCGGGA-3'

C_{mu} Reverse: 5'-GCCTGACTGAGCTCACACAGGGAGG-3'

Where R= A,G; W=A,T; S=C,G; and M=A,C. PCRs were performed with GoTaq Flexi Taq polymerase and the following cycle parameters: 1 Cycle 95^{o}C 5 minutes; 30 cycles 95^{o}C 30 seconds, 60^{o}C 1 minute, 72^{o}C 2.25 minutes; and 1 cycle 72^{o}C 10 minutes. PCR products were visualized on 1-2% agarose gels.

Peripheral Blood Analysis

Complete Blood Counts were performed after tail-vein bleeds on the Hemavet HV950FS blood analyzer (Drew Scientific, Inc.)

Methylcellulose Assays

Total bone marrow was harvested into a single-cell suspension in Iscove's Modified Dulbecco's Medium (IMDM) from one femur of either Wild-type or *Mtg16*$^{-/-}$ mice. Red blood cells were lysed with Erythrocyte Lysis Buffer (EL Buffer; Qiagen) and cells were counted. 7.5 x 10^4 total bone marrow cells were plated in methylcellulose supplemented with 10ng/ml IL-7 (M3630 methylcellulose; Stem Cell Technologies) in 1.1mL per plate on methylcellulose specific plates (Stem Cell Technologies). Colonies were allowed to grow for 14 days and were counted manually at day 7 and 14. A positive colony was judged as containing greater than 30 cells. A Nikon Eclipse T5100 inverted scope was used and pictures of colonies were taken at day 7 and day 14 using a Nikon Coolpix P5100 camera. To trace total cell counts and for flow cytometric analysis, methylcellulose plates were harvested by washing plates three times with Phosphate Buffered Saline (PBS) then collected by centrifugation and counted using a 1:2 dilution with trypan blue (Cellgro). IL-7 titration in methylcellulose was performed using varying

degrees of IL-7 (Peprotech) and M3234 methylcellulose without cytokines (Stem Cell Technologies.)

Germinal Center Assay

Wild-type and *Mtg16*$^{-/-}$ mice were injected with phosphate buffered saline (PBS), Alum, or Alum + NP-CGG intraperitoneally. NP(59)-CGG (Biosearch Technologies) was dissolved at 1mg/mL in sterile PBS then mixed in a 1:2 solution with Alum (Thermofisher) and 200μl total solution was injected. 7 days later, spleens were harvested, weighed, and frozen in Optimal Cutting Temperature (OCT) Compound (Tissue-Tek). 5μm sections were cut and frozen sections were warmed to room temperature and fixed in ice-cold acetone for 10 minutes. Slides were dried and endogenous peroxidases were blocked with 3% H_2O_2 (Sigma) in MeOH for 30 minutes. Slides were washed in TBS-T and blocked with normal horse serum from the RTU vectastain kit (Vector), followed by Avidin-Biotin blocking (Vector). Slides were incubated in biotinylated peanut agglutinin (PNA) (Vector) at a concentration of 8μg/mL for 5 hours at room temperature, washed with TBS-T, and incubated with biotinylated anti-PNA (EyLab) for 45 minutes at room temperature at a concentration of 8μg/mL. Slides were washed and incubated with streptavidin-Horseradish peroxidase (HRP) (Dako) for 30 minutes at room temperature using a 1:300 dilution, washed, and developed using SIGMA *FAST* 3,3'-Diaminobenzidine tablets dissolved immediately before use per the manufacturer's instructions and applied for 90 seconds, followed by washing with tap water. Slides were mounted with cytoseal (Richard-Allan Scientific) and imaged using a Nikon Eclipse T5100 microscope and pictures were taken with a

Nikon Coolpix P5100. Germinal centers positive follicles were counted manually and depicted as the percent of total follicles.

Microarray Analysis

Fraction A B-cells were sorted from pooled wild-type and *Mtg16*$^{-/-}$ mice per cell sorting procedures detailed above. RNA was collected using the 5'-Prime PerfectPure RNA Kit. RNA was amplified using the NuGen WT Pico RNA Amplification Kit and hybridized to Affymetrix Exon/Gene (WT) arrays.

Intracellular γH2aX Flow Cytometry

Methylcellulose plates were collected and cells were resuspended in PBS and counted. Equivalent numbers of cells were fixed and permeablized using the BrdU intracellular staining kit (BD Pharmingen). Briefly, cells were fixed with for 15 minutes at room temperature with Cytofix/Cytoperm buffer, washed, and permeablized with Cytoperm Plus. After permeablization, cells were re-fixed with Cytofix/Cytoperm then labeled with 1:1500 dilution of anti-γH2aX (Milipore) for one hour at room temperature in the dark. Secondary antibody labeling was performed for 30 minutes at room temperature in the dark using an anti-mouse conjugated to AlexaFluor488 (Invitrogen) and analyzed by flow cytometry.

CHAPTER III

MYELOID TRANSLOCATION GENE 16 (MTG16) CONTRIBUTES TO MURINE T-CELL DEVELOPMENT

Abstract

Mtg16/Eto2 is a transcriptional co-repressor that is disrupted by the t(16;21) in acute myeloid leukemia. Using mice lacking *Mtg16,* we find that Mtg16 is a critical regulator of T-cell development. Deletion of *Mtg16* led to reduced thymocyte development *in vivo* and after competitive bone marrow transplantation there was a nearly complete failure of *Mtg16*$^{-/-}$ cells to contribute to thymocyte development. This defect was recapitulated *in vitro* as *Mtg16*$^{-/-}$ Lineage^{-}/Sca1^{+}/c-Kit^{+} (LSK) cells of the bone marrow or DN1 cells of the thymus failed to produce CD4^{+}/CD8^{+} cells in response to a Notch signal. Complementation of these defects by re-expressing *Mtg16* showed that 3 highly conserved domains were somewhat dispensable for T cell development, but required the capacity of Mtg16 to suppress E2A-dependent transcriptional activation and to bind to the Notch intracellular domain. Thus, Mtg16 integrates the activities of signaling pathways and nuclear factors in the establishment of T-cell fate specification.

Introduction

The progeny of hematopoietic stem cells receive external signals and integrate them into altered transcriptional programs that direct multi-potent progenitor cells to become lineage committed and generate all the mature cell types found in the peripheral blood[53,271]. Development along these distinct lineages requires that the external cues be faithfully interpreted at the transcriptional level to activate and repress lineage-specific gene expression programs[59,96]. Transcriptional co-activators and co-repressors are ideally situated to integrate the activities of multiple DNA binding transcription factors and signaling pathways to alter gene expression programs and regulate lineage allocation [119,272].

Myeloid translocation gene (*MTG*) *16* is disrupted by the t(16;21) in acute myeloid leukemia (AML)[12]. MTG16 (gene name *CBFA2T3*; also known as *ETO2*) is a member of a family of transcriptional co-repressors that also includes MTGR1 and MTG8 (also known as ETO), which is targeted by the t(8;21)[4,11,14]. These translocations fuse the DNA-binding domain of RUNX1 to nearly all of either MTG16 or MTG8 to repress the transcription of RUNX1-regulated genes[4,11,12,21]. As expected for co-repressors, MTG16 binds to both DNA binding proteins and chromatin modifying factors[20,28,30,43,226,273]. Four highly homologous domains within MTGs are evolutionarily conserved in the *Drosophila* factor Nervy and mediate some of these contacts.

The action of E proteins and Notch signaling are critical to T-cell development and a potential role for Mtg16 in lymphopoiesis was further suggested by the

identification of an association between MTGs and these pathways[29-31,43,226,273]. Upon ligand binding, the Notch receptor is cleaved and the intracellular domain of Notch (ICD) moves to the nucleus and binds the transcription factor CBF1-Suppressor of Hairless-Lag1 (CSL) to activate transcription[274]. MTGs appear to act as co-repressors for CSL, and independent of CSL, Mtg16 also associates with the Notch ICD, suggesting that Mtg16 mediates some aspects of Notch functions[29,43].

Likewise, Mtg16 associates with transcriptional activation domain-1 (AD1) in E-proteins to impair E-protein-dependent transcription, and E2A instructs lymphoid development while inhibiting myelopoiesis[31,97,123,189,198,270]. *E2A*-null mice have decreased numbers of thymocytes due to reduced lymphoid-primed multi-potent progenitor (LMPP) and early thymocyte progenitor (ETP) production and impaired progression from the earliest $CD4^-CD8^-CD44^+CD25^-$ Double Negative (DN) 1 thymocytes to the subsequent $CD4^-CD8^-CD44^+CD25^+$ DN2 thymocytes[97,197-199]. Furthermore, *E2A*-null progenitor cells fail to produce T-cells in *in vitro* cell fate specification assays initiated by Notch signaling[9,74]. Here, we show that inactivation of *Mtg16* impairs the development of T-lineage thymocytes, indicating that Mtg16 has the capacity to interact with key factors that specify the T-lineage, potentially serving as a master regulator of this cell fate decision.

Results

Mtg16 is required for thymopoiesis after bone marrow transplantation

Mtg16-null mice are able to produce all of the hematopoietic lineages, though myeloid development is enhanced with increased numbers of $Gr1^+/Mac1^+$ myeloid cells in the spleen and bone marrow (Fig. 10). However, there was a two-fold decrease in total thymocyte number that was visible upon gross dissection (Fig. 11A), which caused us to examine T-cell development in more detail. Using flow cytometry, all populations were decreased in absolute number in the absence of *Mtg16* (Fig. 11B) with a small relative decrease in $CD4^+CD8^+$ cells and a slight relative increase in $CD4^-CD8^-$ cells and both $CD4^+$ and $CD8^+$ mature thymocytes as a percent of total thymocytes. When the earliest thymocytes of the $CD4^-CD8^-$ DN population were further subdivided using CD44 and CD25, there was a substantial decrease in both $CD25^-CD44^+$ DN1 cells and $CD25^+CD44^+$ DN2 cells in the absence of *Mtg16* (Fig. 11C). Consistent with the lower level of thymocytes, there were somewhat fewer γδ T cells (Fig. 12).

Our interest in the role of Mtg16 in T-cell development was heightened when we noted that after competitive bone marrow transplantation using 90% $Mtg16^{-/-}$ $CD45.2^+$ bone marrow cells and 10% control CD45.1-expressing cells, there was a dramatic loss of T-cell production from the null bone marrow (Fig. 13A). As measured by flow cytometry, control $CD45.2^+$ bone marrow showed robust reconstitution, which was similar to the percentage of $CD45.2^+$ WT marrow transplanted. By contrast, only 2-3% of the thymocytes were derived from the $Mtg16^{-/-}$ bone marrow (Fig. 13B). Thus, when

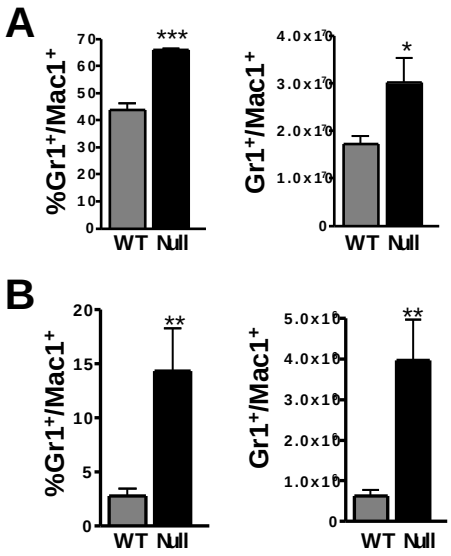

Figure 10. Increased development of myeloid lineages in the *Mtg16*$^{-/-}$ mouse. (A) Increased production of Gr1^{+}/Mac1^{+} cells in *Mtg16*$^{-/-}$ bone marrow, both as a percentage of total cells and as an absolute number in 2 hind limbs (both femur and tibia). An unpaired, two-tailed t-test shows * $p<0.05$, *** $p<0.001$. Shown are data from a representative experiment from one of two independent experiments performed with 3 mice of each genotype, for a total N=7 mice. (B) Increased population of Gr1^{+}/Mac1^{+} cells in *Mtg16*$^{-/-}$ spleens shown both as a percentage of total cells and as an absolute number per spleen. An unpaired, two-tailed t-test shows ** $p<0.01$. N=3. Shown are data from a representative experiment from one of two independent experiments, for a total N=7 mice.

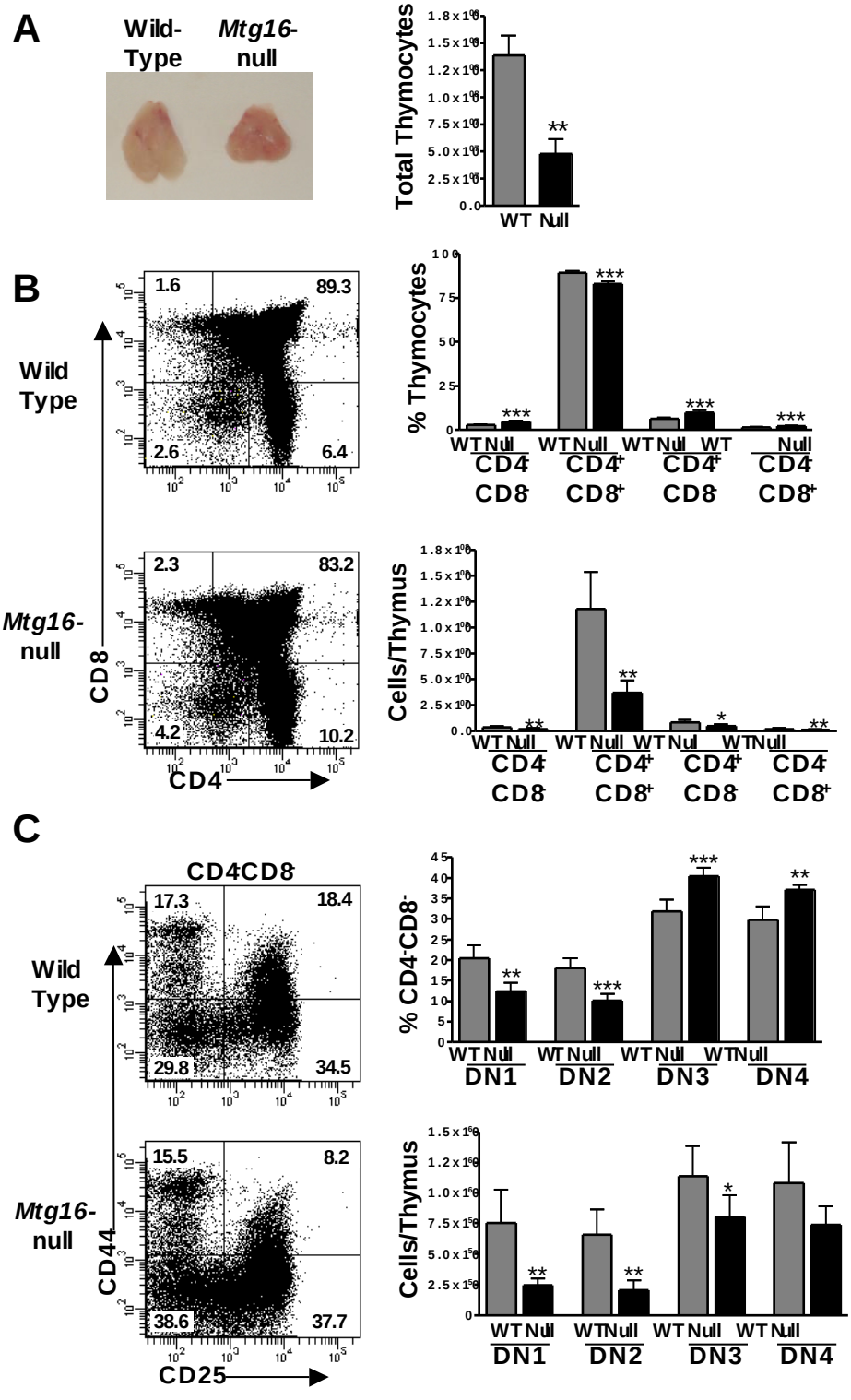
A
Wild-Type
Mtg16-null
Total Thymocytes
WT Null
B
Wild Type
Mtg16-null
CD8
CD4
1.6
89.3
2.6
6.4
2.3
83.2
4.2
10.2
% Thymocytes
Cells/Thymus
CD4- CD8-
CD4+ CD8+
CD4+ CD8-
CD4- CD8+
C
CD4CD8
17.3
18.4
29.8
34.5
15.5
8.2
38.6
37.7
CD44
CD25
% CD4-CD8-
DN1
DN2
DN3
DN4

Figure 11. Analysis of the *Mtg16*-null thymus. (A) Left panel shows a photo of a representative thymus from a 6-8 week old wild type and *Mtg16*-null mouse. The right panel shows a graph of the average of the total numbers of WT and *Mtg16*-null thymocytes, +/- standard deviation (SD). An unpaired, two-tailed t-test shows ** $p<0.01$. Shown are data from a representative experiment with 5 mice of each genotype, with a total N= 17. (B) Left panels show flow cytometric plots of CD4 and CD8 expression in the WT and *Mtg16*-null thymus. Graphs in the right panels depict both the average percentage of total thymocyte number (top) and the average absolute cell number (bottom) in each population, +/- SD. Shown are data from a representative experiment with 5 mice of each genotype, with a total N=17. An unpaired, two-tailed t-test shows * $p<0.05$, ** $p<0.01$, ***$p<0.001$ (C) Flow cytometric analysis of $CD4^-CD8^-$ thymocytes for expression of CD44 and CD25 of the double negative population shown in B. Graphs depict both the average of the percentage of total $CD4^-CD8^-$ number (top) and the absolute cell number (bottom) in each population, +/- SD. Shown are data from a representative experiment with 5 mice of each genotype, with a total N= 17. An unpaired, two-tailed t-test shows * $p<0.05$, ** $p<0.01$, ***$p<0.001$. For (A-C) a minimum of three independent experiments were performed with at least three pairs of age-matched WT and Null mice.

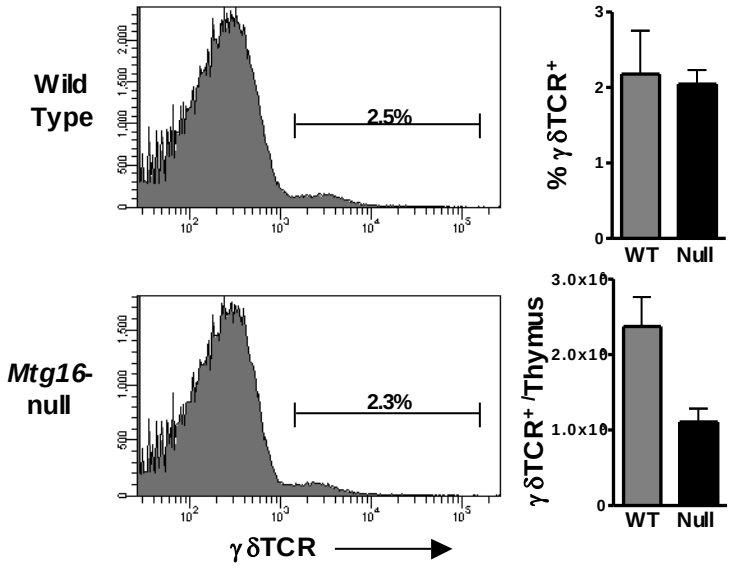

Figure 12. γδ T-cell development occurs normally in the absence of *Mtg16.* Representative plots show labeling of total thymocytes with anti- γδ T-cell Receptor. Graphs depict relative percentage of total thymocytes and absolute number of γδ TCR^+ cells per thymus from one of three experiments. The two fold reduction corresponds to a two fold reduction in total thymocytes. Mean ± SD. Total N=9.

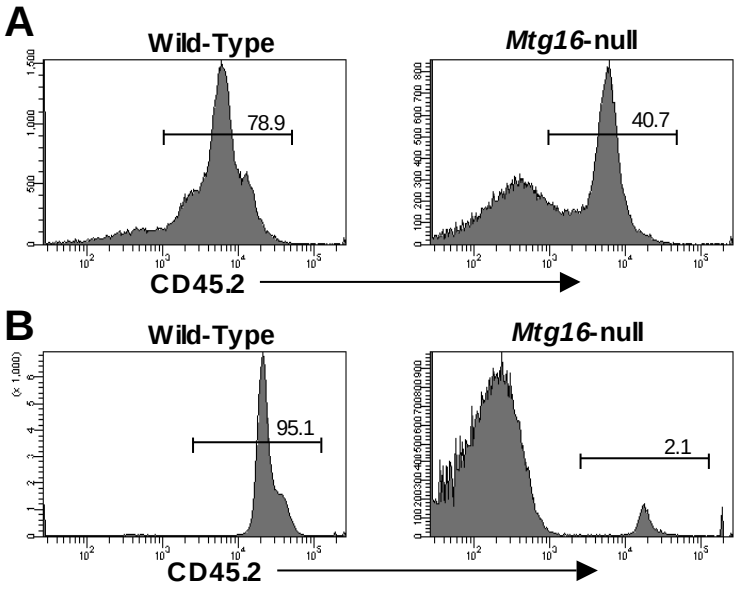

Figure 13. Mtg16 is required for thymopoiesis after bone marrow transplantation. *Mtg16*$^{-/-}$ cells fail to repopulate the thymus in competitive transplant. Shown are representative CD45.2 FACS plots six weeks after bone marrow transplantation using 10% wild type CD45.1 cells and 90% control or *Mtg16*$^{-/-}$ CD45.2 cells. Representative FACS plots of cells harvested from the bone marrow (A) and thymus (B). These data are from one of two experiments with total N = 5 WT recipients and N=9 *Mtg16*-null recipients.

homeostasis was disrupted and the null cells placed in a competitive environment, *Mtg16* was required for T-cell formation *in vivo*.

To better interpret the defects in *Mtg16*-null early T-lineage progenitor cells, we measured the expression of *Mtg16* and the other MTG family members, *Mtg8* and *Mtgr1*, by quantitative RT-PCR in wild-type mice across several hematopoietic populations. The highest levels of *Mtg16* expression were seen in early stem/progenitor cell populations (LSK cells), common myeloid progenitors (CMPs), and bone marrow $B220^+$ cells (Fig. 14), whereas *Mtgr1* was widely expressed and *Mtg8* was poorly expressed, with undetectable expression in some populations. In the thymus, *Mtg16* expression was generally lower, with the highest levels in the $CD4^+CD8^+$ cells and lower levels of *Mtg16* expression in the early T-cell progenitor cells. These data suggested that the defect in T-cell development might lie in the earliest T-cell progenitor cells of the bone marrow. Flow cytometric analysis supported this hypothesis, and indicated that the "lymphoid-primed multi-potent progenitor" cells (LMPP) of the bone marrow and the $CD4^-/CD8^-/CD25^-/c\text{-}Kit^+$ "early thymocyte progenitor" cells (ETP) that seed the thymus were reduced in the absence of *Mtg16* (Fig. 15A, B). The two-fold reduction in progenitors observed was consistent with the two fold-reduction in thymocytes (Fig. 11).

Mtg16 is required for T-cell commitment *in vitro*

To directly assess the T-cell potential of *Mtg16*-null bone marrow progenitor cells and early thymocytes, we cultured wild type and *Mtg16*-null bone marrow stem cells and thymus double negative cells in the presence of Flt3 ligand and IL-7 on OP9 stromal cells expressing the Delta-like 1 Notch ligand, which triggers T-cell development[74]. We

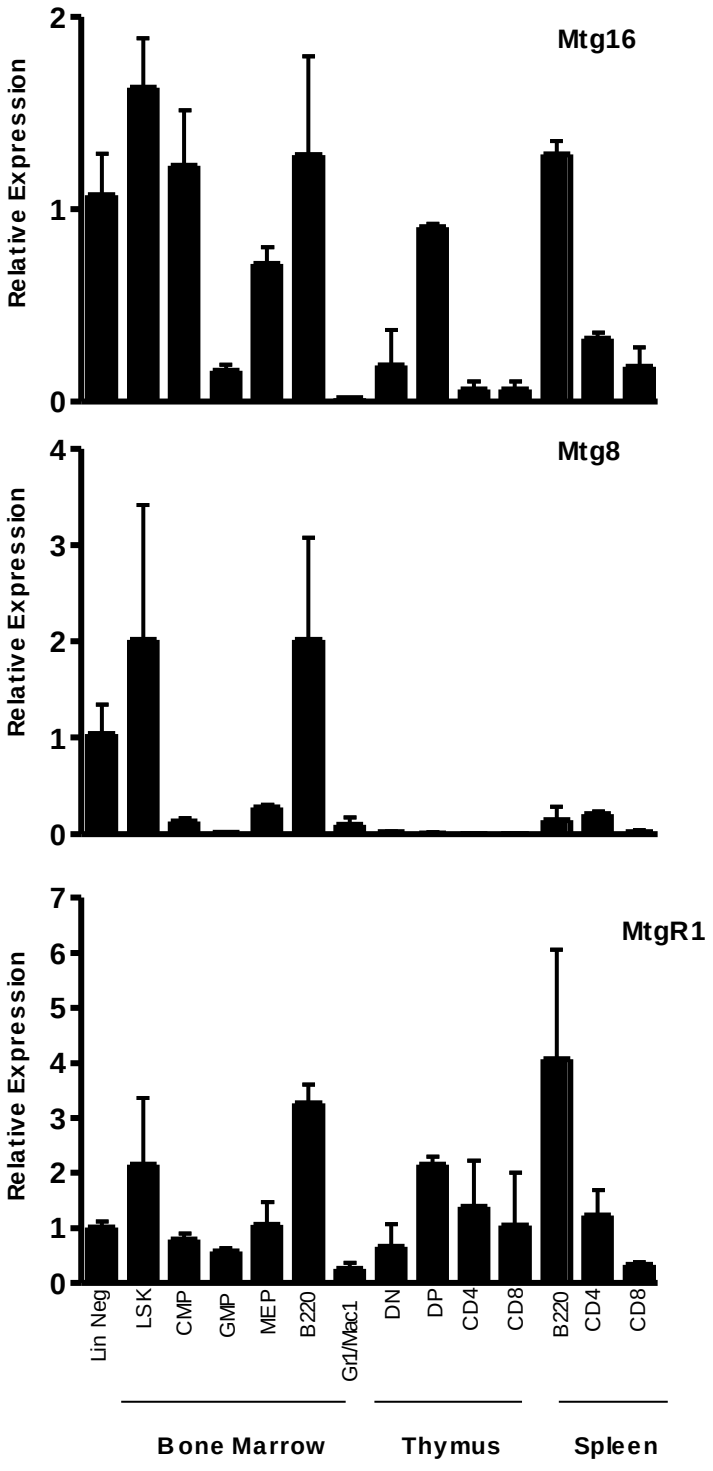

Figure 14. Relative expression of *Mtg* family members across murine hematopoiesis. The indicated populations were isolated by flow cytometry and the mRNA levels determined using qRT-PCR. For each population, at least two independent samples were collected and analyzed in duplicate. The average relative expression is shown +/- SD.

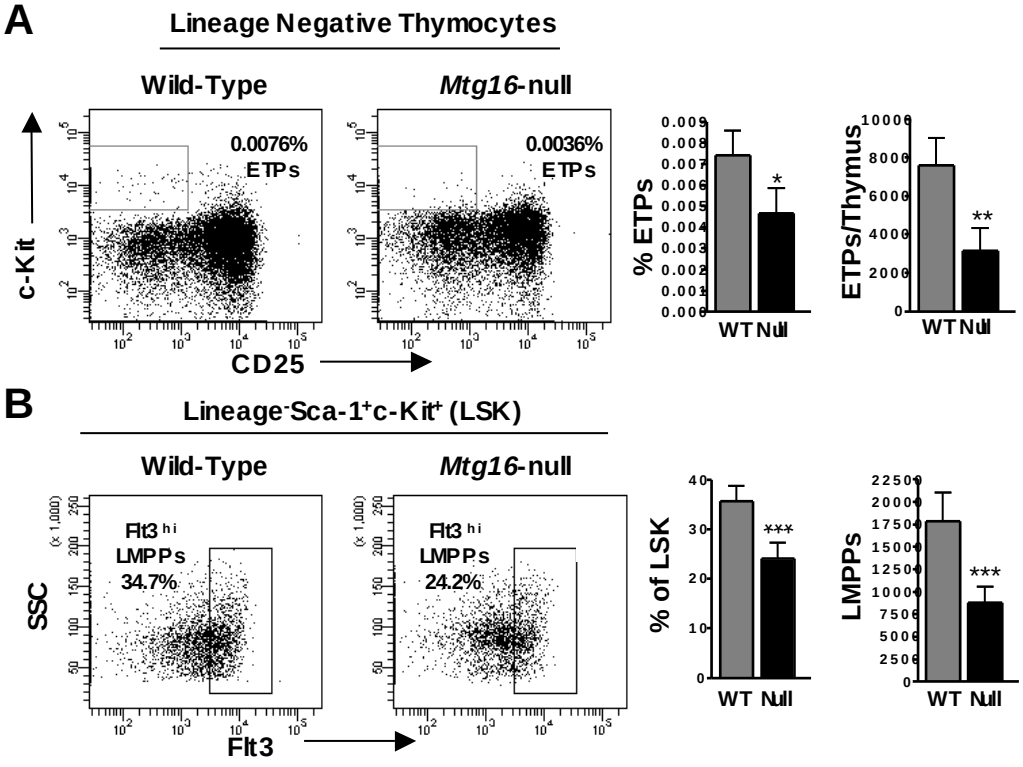

Figure 15. Loss of *Mtg16* leads to decreased early thymocyte progenitor cells in the thymus and lymphoid primed progenitor cells in the bone marrow. (A) Decreased presence of Lin$^-$CD25$^-$c-Kit$^+$ ETPs in the *Mtg16*-null thymus shown both as percentage of total thymocytes and absolute number per thymus +/- SD. Representative FACS plots are shown from one of three independent experiments with 4 mice of each genotype, with a total N=12. An unpaired, two-tailed t-test yielded * $p<0.05$, ** $p<0.01$. (B) Decreased Lin$^-$ Sca-1$^+$c-Kit$^+$Flt3^{hi} LMPPs in *Mtg16*$^{-/-}$ bone marrow shown both as percentage of LSKs and absolute number per hind limb (both femur and tibia), +/- SD. Shown are data from a representative experiment with 5 mice of each genotype, with a total N=15. An unpaired, two-tailed t-test shows ***$p<0.001$.

the thymus and assessed their ability to develop into $CD4^+CD8^+$ T-cells using flow cytometry[74]. Between day 21 and 28, wild-type LSK and DN1 cells produced $CD4^+CD8^+$ T-cells. As DN2 cells have already begun the process of committing to the T-lineage, $CD4^+CD8^+$ T-cells developed between day 7 and 14 (Fig. 16A). By contrast, *Mtg16*-null LSK and DN1 cells failed to develop into $CD4^+CD8^+$ T-cells (Fig. 16A). However, *Mtg16*-null DN2 cells developed into $CD4^+CD8^+$ T-cells within 7 to 14 days of culture on OP9-DL1 stroma, albeit at a reduced rate (Fig. 16A, right panels). The reduced numbers of T-cells could reflect reduced proliferative capacity or increased cell death, as the null cells failed to expand to the levels of wild type DN2 cells (Fig. 17). Together, these data indicate that Mtg16 is required for efficient T-cell development *in vivo* and *in vitro* and that this defect precedes lineage commitment into DN2 T-cells of the thymus (Fig. 16A).

Given that the *Mtg16*-null LSK cells failed to develop into T-cells, we determined their lineage fate in this *in vitro* system. Seven days after the initiation of the cultures, there was an exaggerated production of $Gr1^+/Mac1^+$ myeloid cells in the absence of *Mtg16* (Fig. 16B). These data suggest that *Mtg16*-null stem cells are incapable of developing along T-cell lineages *in vitro* and prefer to develop along the myeloid lineages, even in conditions favorable for lymphoid development.

Ex vivo complementation of the *Mtg16*$^{-/-}$ defect in T-cell Development

To begin to define how Mtg16 functions in regulating T-cell development, we sought to complement the *Mtg16*-deficient T-cells by exogenous expression of *Mtg16*. Recombinant *Murine Stem Cell Virus* (*MSCV*) expressing *Mtg16* and *GFP* was used to

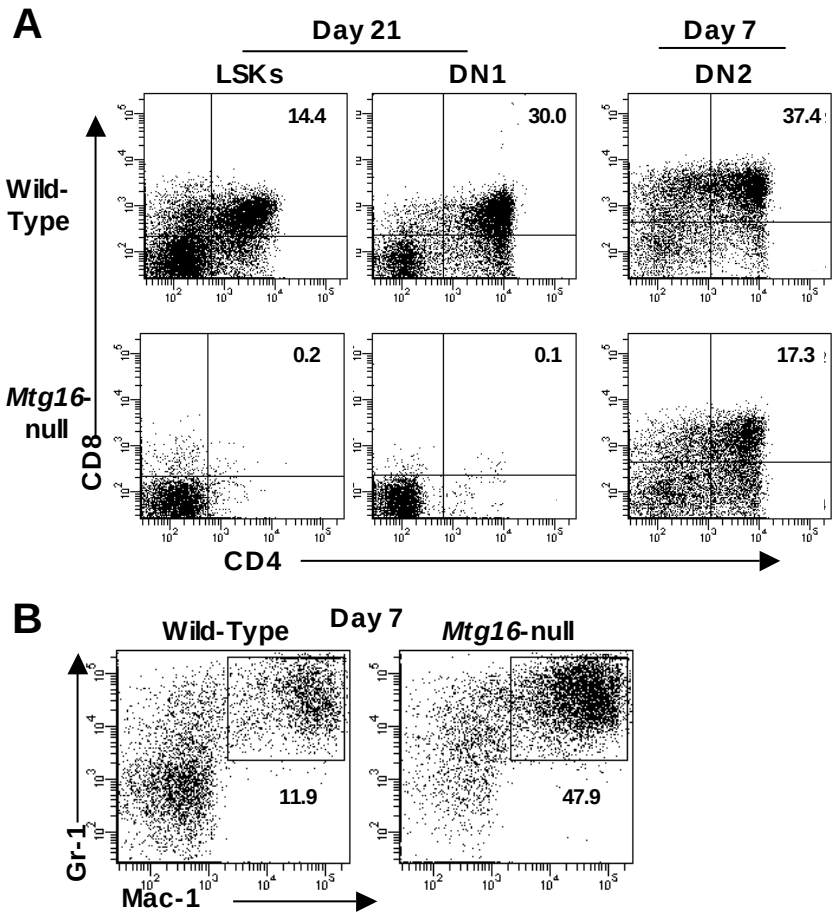

Figure 16. *Mtg16*-null LSK and DN1 progenitor cells fail to develop into T-cells *in vitro*. (A) FACS sorted LSK, DN1, and DN2 populations were plated on OP9-DL1 cells and $CD4^{+}CD8^{+}$ T-cell development was assessed at day 21 for LSK and DN1 cells and day 7 for DN2 cells. Representative FACS plots are shown from one of at least two experiments. Shown are data from a representative experiment with 2-3 mice of each genotype, with a total N=5 (LSK) N=7 (DN1) and N=4 (DN2). (B) *Mtg16*-null LSK cells display enhanced myelopoiesis. FACS plots for Gr1 and Mac1 7 days after culturing LSK cells with OP9/DL1 stromal cells. Shown are data from a representative experiment from one of five independent experiments performed with 2 mice of each genotype, for a total N=10 mice.

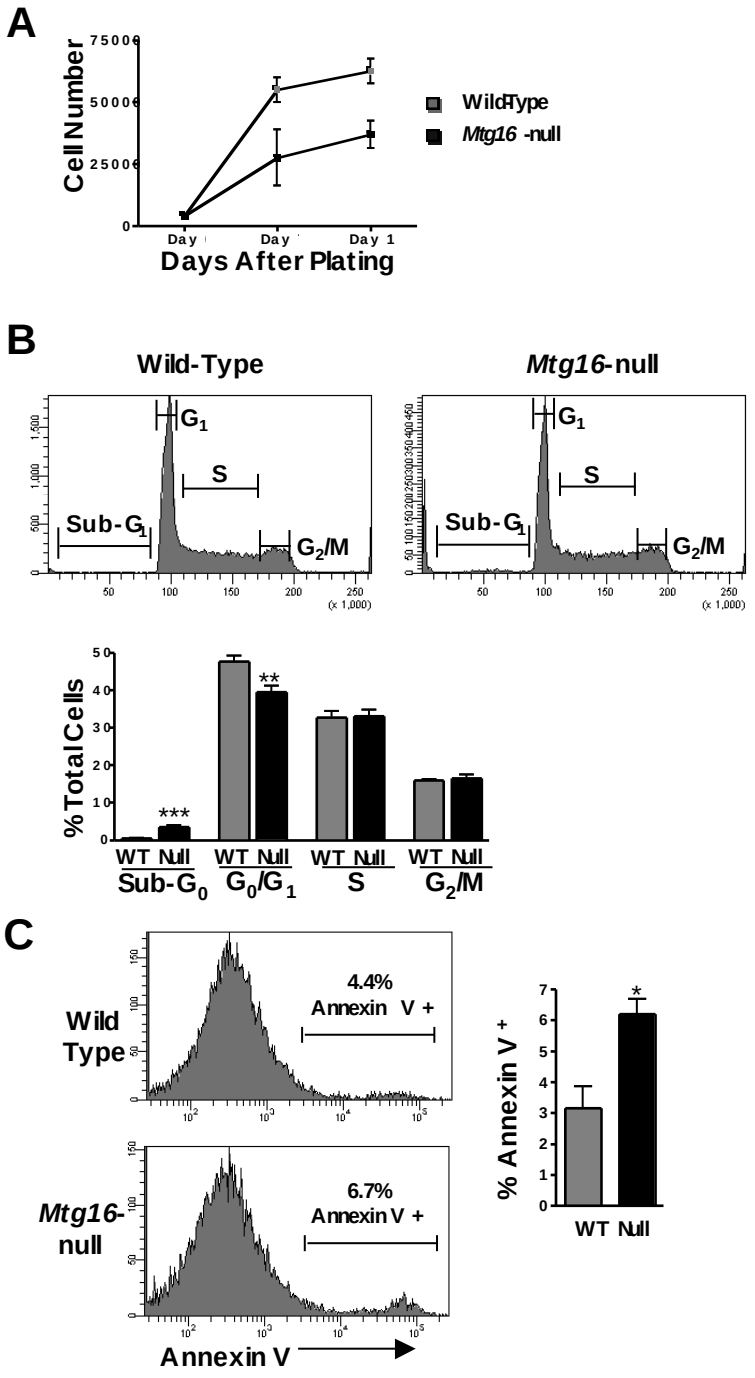

Figure 17. ***Mtg16*$^{-/-}$ DN2 thymocytes cultured on OP9-DL1 stroma exhibit growth defects**. (A) Growth curves for DN2 cells cultured on OP9-DL1 stroma as assessed by cell counts. Shown are data from a representative experiment from one of three independent experiments performed with 2-3 mice of each genotype, for a total N= 7 mice. (B) Representative flow cytometry plots of DN2 cells assessed for DNA content using propidium iodide staining of day 7 OP9-DL1 cultures. Lower panel shows a quantitative assessment of this analysis. Shown are data from a representative experiment from one of two independent experiments performed with 3 mice of each genotype, for a total N=6 mice. (C) Annexin V staining of Day 7 OP9-DL1 cultures from DN2 cells. Shown are data from a representative experiment from one of two independent experiments performed with 3 mice of each genotype, for a total N= 6 mice.

infect FACS purified LSK cells followed by culture with OP9-DL1 cells. Re-expression of *Mtg16* yielded T-cell differentiation typically producing from 7-30% $CD4^+CD8^+$ cells in numerous biological replicates when compared to the *Mtg16*-null cells infected with control *MSCV* (e.g., Fig. 18A, 18B). Therefore, the failure to differentiate into T-cells was dependent on Mtg16 rather than an off target effect of the deletion.

Next, we utilized a panel of deletion mutants that removed each of the Nervy Homology Regions (NHRs) in Mtg16. Each of these domains is highly conserved between MTG family members and facilitates interaction with different proteins, thereby allowing the identification of the crucial interactions that contribute to Mtg16 functions. *Mtg16*-null LSK cells were infected with *MSCV-IRES-GFP, MSCV-Mtg16-IRES-GFP*, or deletion mutants of the conserved domains and the cells were cultured on OP9-DL1 stroma in the presence of IL-7 and Flt3L (see Fig. 19 for the levels of expression). The *Mtg16* deletion mutant lacking NHR1 failed to complement the null phenotypes, whereas deletion of NHR2, NHR3 and NHR4 allowed reconstitution of T-cell development (Fig. 18B), but with somewhat lower efficiencies. Like the ΔNHR1, deletion of a domain just upstream of NHR1, which mediates association with the Notch intracellular domain, ΔNICD, also failed to restore T-cell development. These results suggest that Mtg16 must be able to associate with the NICD and specific transcription factors via NHR1 to fully regulate cell-fate decisions.

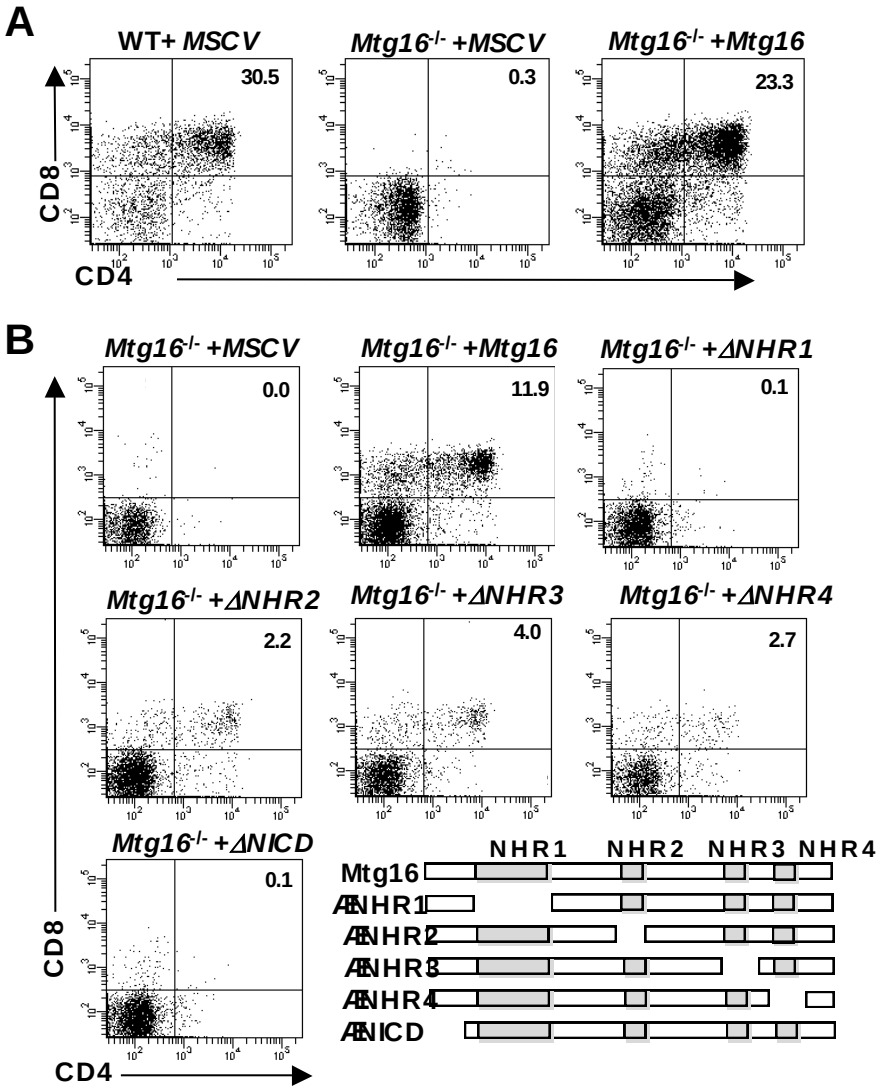

Figure 18. Reconstitution of *Mtg16*$^{-/-}$ LSK cells with *Mtg16* and *Mtg16* deletion mutants. (A) Representative FACS plots from day 21 cultures of LSK cells infected with *MSCV* or *MSCV-myc-Mtg16-GFP* co-cultured with OP9-DL1 stroma to assess T-cell development using cell surface expression of both CD4 and CD8. GFP^{+} events are shown. Shown are data from a representative experiment from one of four independent experiments performed with 2 mice of each genotype, for a total N=8 mice. (B) Mutant analysis of Mtg16 and contribution to T-cell development. Representative plots from day 21 cultures of LSK cells expressing MSCV or *MSCV-myc-Mtg16-GFP* on OP9-DL1 stroma assessing T-cell development by the cell surface expression of both CD4 and CD8. GFP^{+} events are shown. Shown are data from a representative experiment from one of two independent experiments performed with 2 control Wild-Type mice and 4 *Mtg16*$^{-/-}$ mice pooled into two samples, for a total N=8 mice. A schematic diagram of the deletion mutants is shown in the lower right hand portion. ΔNH1=Δ145-242; ΔNH2=Δ365-402; ΔNH3=Δ460-510; ΔNHR4=Δ532-567; ΔNICD=Δ1-85.

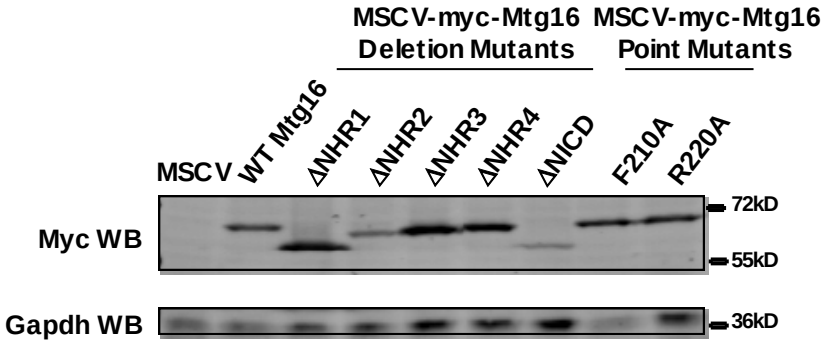

Figure 19. Expression of MSCV-*myc-Mtg16*-GFP mutant proteins. Immunoblot analysis is shown of cell lysates expressing the indicated proteins using anti-c-Myc.

The defect in *Mtg16*$^{-/-}$ T-cell development cannot be overcome by ectopic NICD expression

Given that deletion of the NICD interacting domain removed the ability of *Mtg16* to rescue *in vitro* T-cell development, we asked whether overexpression of the activated form of the Notch1 receptor, the NICD, could rescue T-cell development from *Mtg16*$^{-/-}$ LSK cells in the OP9-DL1 assay. This approach has the added benefit of bypassing the cell-to-cell contacts and the cytoplasmic events required to propagate a Notch signal. LSK cells from wild type or *Mtg16*-null mice were isolated by flow cytometry and infected with *MSCV-NICD-GFP* and plated on OP9-DL1 stromal cells. In control LSK cells, the Notch ICD enhanced the formation of T-cells on OP9-DL1 stroma (Fig. 20A, B). *Mtg16*$^{-/-}$ LSK cells did not respond fully to the strong Notch signal, though a minor increase in T-cell development occurred in some samples (Fig. 20B). Furthermore, overexpression of the NICD had a strong growth advantage in wild-type cells, as evidenced by expansion of the GFP^{+} population that did not occur in *Mtg16*$^{-/-}$ cells (Fig. 20C). These results suggest that the NICD is not capable of exerting its full potential in instructing T-cell development in the absence of *Mtg16*. This could be due to either defects in other pathways that prevent T-cell development even in the presence of NICD overexpression or direct impairment of NICD function in the absence of *Mtg16.* Given that Mtg16 interacts with both CSL and the NICD, it is possible that it facilitates removal of repression complexes and activation of Notch-mediated transcription, though this hypothesis is still under investigation.

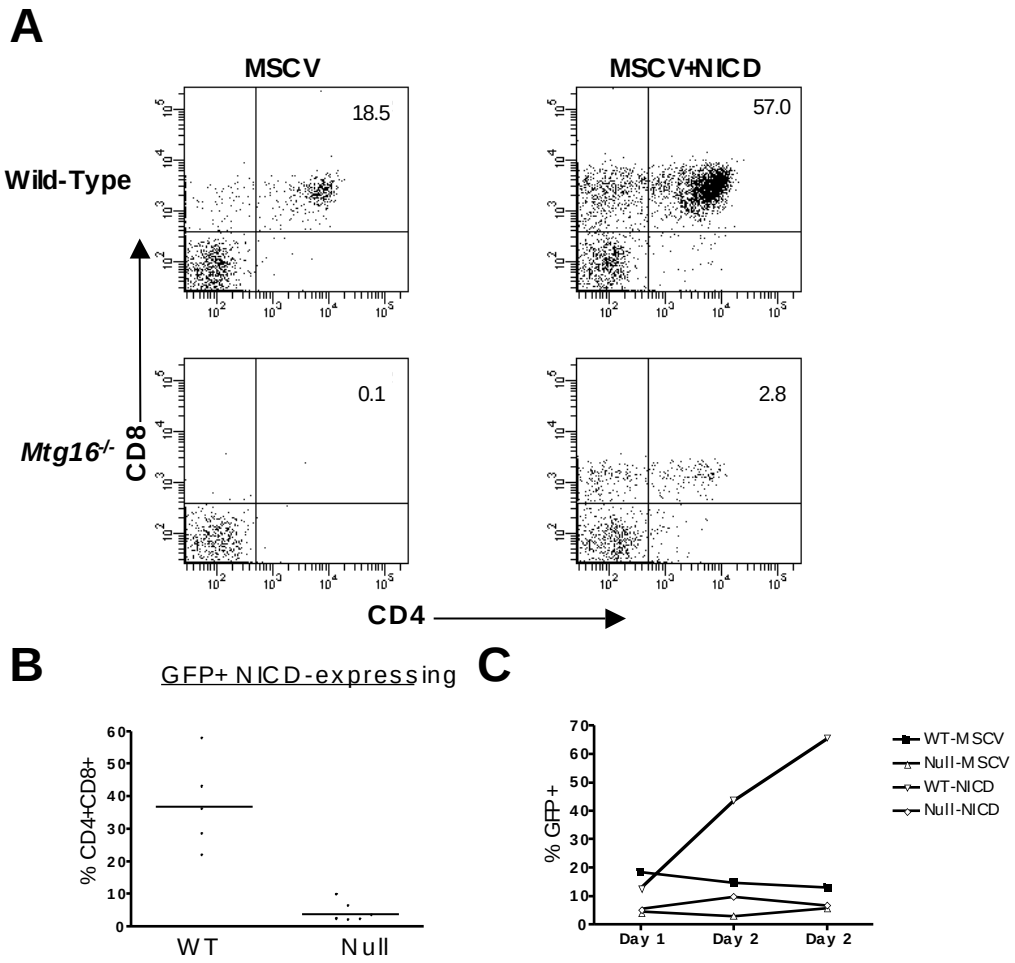

Figure 20. Expression of the Notch Intracellular Domain cannot rescue *Mtg16*$^{-/-}$ T-cell development *in vitro* (A) Representative plots show CD4/CD8 labeling of wild-type and *Mtg16*$^{-/-}$LSK cells infected with *MSCV-IRES-GFP* or *MSCV-IRES-GFP-NICD* and cultured in the OP9-DL1 system. (B) A small level of T-cell development occurs from *Mtg16*$^{-/-}$ LSK cells expressing the NICD. Graphical depiction of $CD4^{+}CD8^{+}$ percentage from all replicates. Data from three independent experiments (C) Expression of the NICD confers a growth advantage on wild-type cells as shown by GFP^{+} expansion that does not occur in *Mtg16*$^{-/-}$ cells. Representative data from one of three independent experiments.

Structure/Function analysis of Mtg16 in alternate progenitor cell assays

To assess whether defects seen in Mtg16 deletion mutants were specific to T-cell development, we utilized the same panel of mutants in another Mtg16 reconstitution assay, namely the Colony-Forming Unit Spleen (CFU-S) assay. In this context, the impaired ability of *Mtg16*$^{-/-}$ progenitors to proliferate leads to a loss of spleen colony formation after bone marrow transplant. Retroviral expression of wild-type *Mtg16* rescues colony formation and the NICD interacting domain is dispensable in this assay, confirming that this portion of Mtg16 contributes specifically to T-cell development (Fig. 21). The NHR panel of deletion mutants shows that NHR3 is dispensable for CFU-S reconstitution, a similar result to that seen in the OP9-DL1 T-cell assay (Fig. 22). Deletion of NHR1, 2, and 4 impairs the ability of Mtg16 to rescue colony formation, though the quanitative effect of this impairment is difficult to determine.

E-protein regulation is necessary for the function of Mtg16 in T-cell development

One of the interactions disrupted by the deletion of NHR1 is the interaction between this portion of Mtg16 and activation domain 1 (AD1) of HEB[31]. Given that the *Mtg16*-null phenotype is similar to that of *E2A*-deficient mice [97,197,198,275], we mined gene expression data from *Mtg16*$^{-/-}$ LSK cells (Fischer et al., in preparation) and found that *E2A* expression was slightly decreased, while *Id1* and *Id2*, negative regulators of E-protein DNA binding and T-cell development[195,196,218-221,223], were increased 4-8 fold. Expression of *Id1* in *in vitro* culture systems designed to permit B-cell development favored myeloid development over B-cell commitment and similar results were seen *in vivo*[218,220]. Because double shRNA-mediated knockdown of *Id1* and *Id2* was inefficient

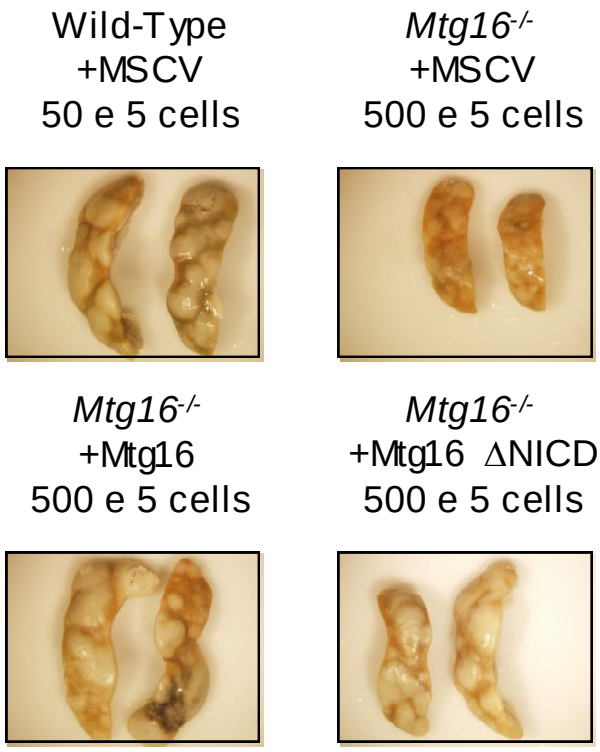

Figure 21. NICD binding is dispensable for Mtg16 function in the CFU-S assay Wild-type and *Mtg16*$^{-/-}$ total bone marrow were infected with *MSCV-IRES-GFP, MSCV-IRES-GFP-myc-Mtg16,* or *MSCV-IRES-GFP-myc-Mtg16* Δ NICD and transplanted into lethally irradiated mice. Day 12 colonies shown from one of two experiments for a total N=4-5 recipients.

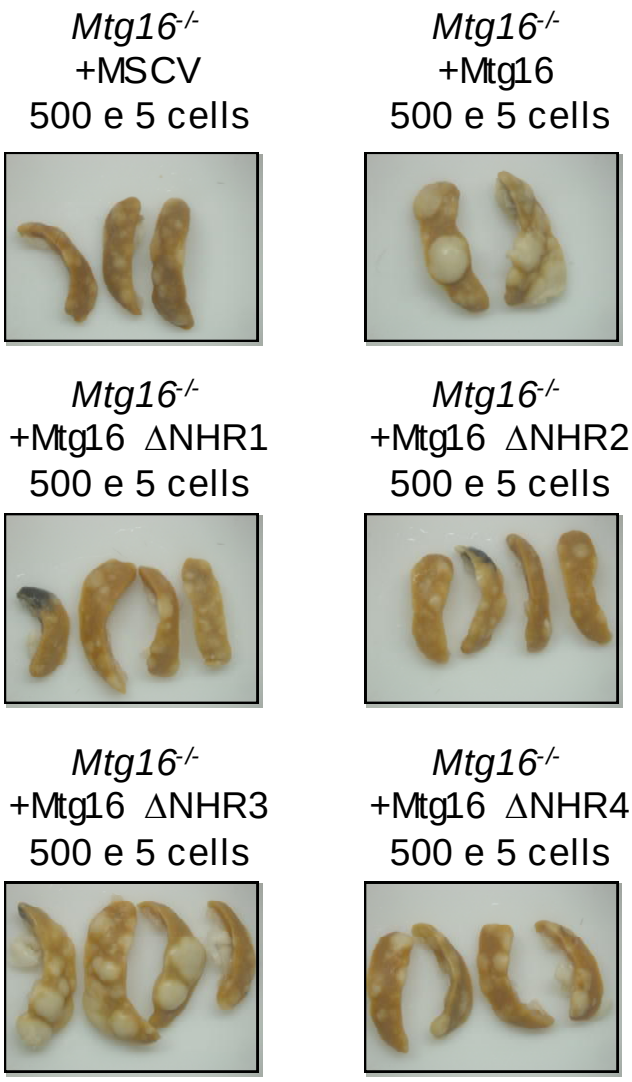

Figure 22. Contribution of Nervy Homology Regions to Mtg16 function in the CFU-S assay. Day 12 spleen colony formation from wild-type or *Mtg16*$^{-/-}$ total bone marrow infected with *MSCV-IRES-GFP* or *MSCV-IRES-Myc-Mtg16* and associated deletion mutants. Data from one of two experiments for a total N=8 recipients per condition.

(data not shown), we asked whether expression of *Id1* or *Id2* was sufficient to enhance myelopoiesis and block T-cell development in the OP9-DL1 system. *MSCV-Id1-GFP* and *MSCV-Id2-GFP* infected wild-type LSK cells were plated on OP9-DL1 stroma and FACS analyzed at day 7 to test for increased $Gr1^{+}Mac1^{+}$ production, which was seen in the absence of *Mtg16*. Both *Id1* and *Id2* over expression led to increased myeloid production at day 7, suggesting that the increased expression of *Id1* and *Id2* in *Mtg16*-null LSK cells contributes to this phenotype (Fig. 23A). Over-expression of *Id2* inhibited, but did not completely abolish, $CD4^{+}CD8^{+}$ T-cell development in the OP9-DL1 assay [222]. Similarly, we noted that *Id1*-expressing LSK cells also yielded some T-cell differentiation (Fig. 23B). Therefore, increases in *Id1* and *Id2* expression likely contribute to the enhanced myelopoiesis observed in the absence of *Mtg16* (Fig. 16B), but are unlikely to completely explain the block in T-cell differentiation.

The E proteins E2A and HEB are critical for T-cell development[97,210]. The structure of the NHR1 domain of MTG8 in association with the HEB AD1 domain identified residues that mediate this contact[270]. While HEB binds to MTG8 through 2 sites, mutations within the NHR1 domain of MTG8 were sufficient to disrupt repression of E-protein-mediated transcriptional activation[270,276]. Therefore, to define the contributions of E-protein functions to the role of Mtg16 in T-cell development, we engineered a point mutation in *Mtg16* that is homologous to changes that abrogated the binding of the MTG8 NHR1 domain to HEB AD1. F210A in Mtg16 mimics the F154A MTG8 mutant to eliminate E-protein AD1 binding, whereas a control R220A mutation mimics the R164A mutant that retained the ability to bind to HEB AD1[270]. The F210A and R220A mutants were reintroduced into *Mtg16*-null LSK cells using

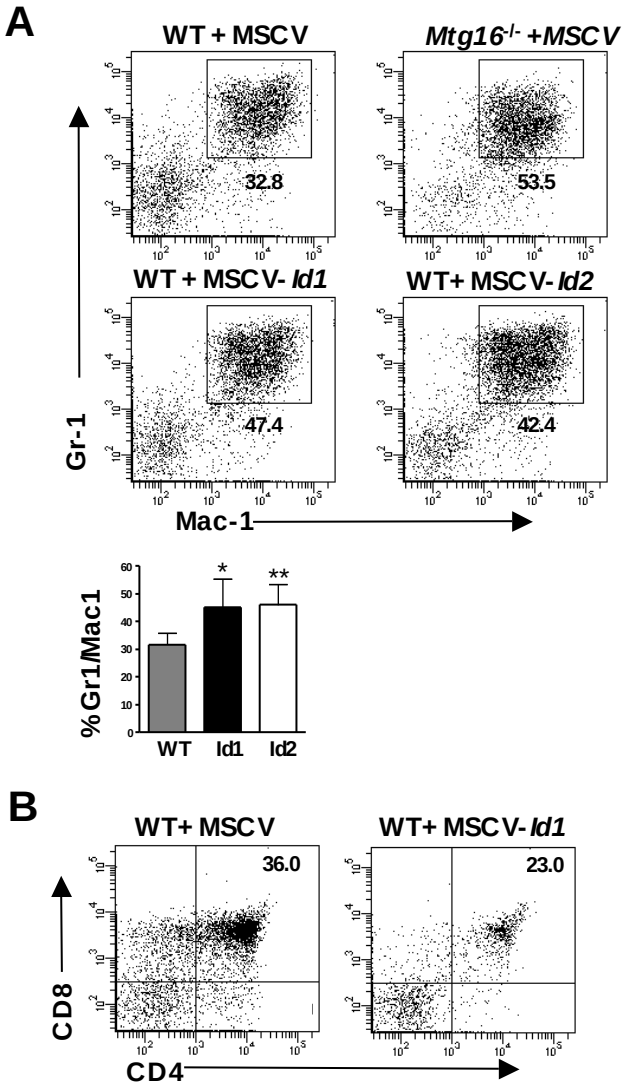

Figure 23. Over expression of *Id1* and *Id2* enhanced myelopoiesis. (A) LSK cells infected with *MSCV-Id1-GFP* or *MSCV-Id2-GFP* phenocopy *Mtg16*$^{-/-}$ LSK cells with increased production of Gr1^{+}/Mac1^{+} cells. Representative FACS plots of GFP^{+} populations 7 days after co-culture on OP9/DL1 stromal cells. Shown are GFP+ data from a representative experiment from one of two independent experiments performed with 2-3 mice of each genotype, for a total N=5 mice. The average of the percentage of the cells that were Gr1^{+}Mac1^{+} that were obtained from 2 experiments are shown graphically in the panel below. An unpaired, two-tailed t-test shows * $p<0.05$, ** $p<0.01$. (B) WT LSK cells infected with *MSCV-Id1-GFP* retain the capacity to generate CD4^{+}CD8^{+} T-cells after co-culture on OP9/DL1 cells. Shown is GFP+ representative data from one of three experiments.

MSCV-IRES-GFP, and both Mtg16 and the R220A mutant were capable of rescuing T-cell development (Fig. 24A). However, the F210A point mutant failed to rescue T-cell development (Fig. 24A). Therefore, the appropriate regulation of E-protein activity is a necessary function of Mtg16 in T-cell development.

As E-proteins also function in regulating hematopoetic stem and progenitor cell populations, we included these mutants in the CFU-S assay as well. The R220A mutant functioned like wild-type *Mtg16* (Fig. 25). F210A *Mtg16* was impaired in this assay as well, suggesting that the Mtg16-E-protein interaction also contributes to $Mtg16^{-/-}$ stem cell phenotypes, a hypothesis that is under current investigation.

Given that deletion of the Notch ICD contact site and mutation of the E protein binding motif both impaired T-cell production, we probed the molecular contacts that these mutants retain. We confirmed that the point mutants in NHR1 did not disrupt E-protein binding and found that further deletion of a region between NHR1 and NHR2 (the PST2 domain) was necessary to completely abrogate E-protein binding (Fig. 24A, B). The NHR1 domain of MTGs also contacts NCoR[277], but we found normal levels of repression by mutant GAL4-Mtg16 fusion proteins using a Gal-reporter assay (Fig. 24D). In addition, the F210A mutant retained the ability to bind to the Notch ICD (Fig. 24C), yet failed to properly respond to a Notch signal. Finally, we used a luciferase construct carrying E-box binding sites in the promoter to show that *Mtg16* and *Mtg16(R220A)* suppressed E47-dependent transcriptional activation, while the F210A mutant was deficient in repression (Fig. 24B). Importantly, deletion of the N-terminal NICD binding region did not affect the ability of Mtg16 to repress E47-mediated transcriptional activation (Fig. 24B), indicating that suppression of E protein-dependent transcription

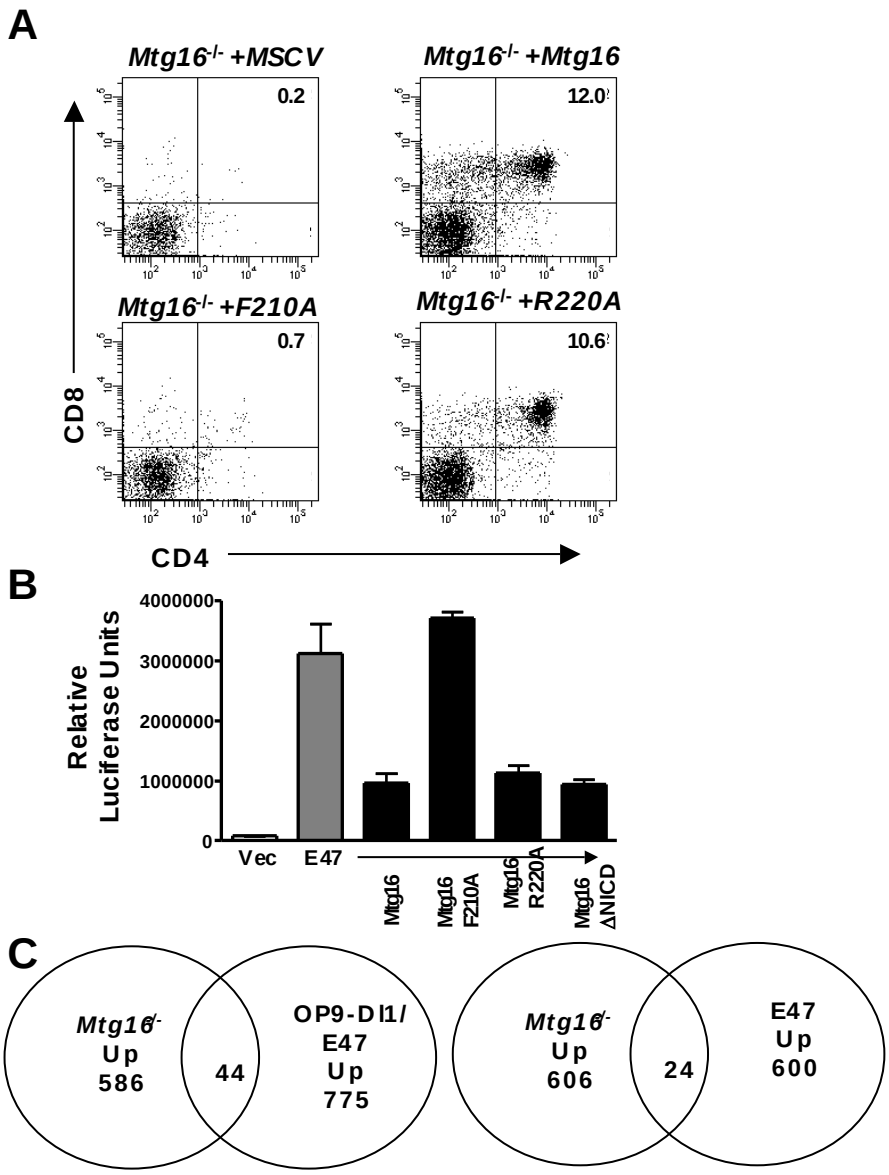

Figure 24. Suppression of E-protein mediated transcriptional activation is necessary for Mtg16 to reconstitute T-cell development. (A) Retroviral introduction of wild-type MSCV-*myc-Mtg16-GFP* and the R220A mutant rescues $CD4^+/CD8^+$ T-cell development, but F210A does not. Representative day 21 FACS plots using anti-CD4 and anti-CD8 are shown, with GFP^+ cells shown and GFP percentage at day 21 listed under each plot. Shown are data from a representative experiment from one of three independent experiments performed with 2 mice of each genotype, for a total N=6 mice. (B) An F210A point mutant in *Mtg16* abrogates the ability of Mtg16 to repress transcription from an E-box promoter activated by the expression of E47, while the NICD deletion mutant suppresses E-protein functions. Graph shows the average relative luciferase values +/- SD from an E-box reporter plasmid co-transfected with vector control or vector expressing E47 and the indicated Mtg16 or mutant thereof. The values were normalized to a renilla-luciferase plasmid to control for specificity and transfection efficiency. The experiment was performed twice in triplicate. (C) Venn diagrams are shown that display the intersection between genes up-regulated in *Mtg16*$^{-/-}$ LSK cells relative to wild-type controls and genes up-regulated by activated Notch signaling in OP9-DL1 co-culture and E47 expression left panel or E2A-deficient thymic lymphoma cells that were complemented by re-expressing E2A.

was not sufficient to trigger T-cell development (Fig. 16) and that Mtg16 must associate with the Notch ICD to restore function.

MTG family members function in transcriptional repression, and therefore these results implied that E-protein-mediated repression contributes to T-cell development. By comparing gene expression profiles from *Mtg16*$^{-/-}$ LSK cells (Fischer et al., submitted) to genes that were repressed by over-expression of E47 [9,278], we identified 19 genes that were repressed by E47 in hematopoietic progenitor cells, but up regulated upon *Mtg16* inactivation in LSK cells (Fig. 26C and Table 1). In addition, we compared the changes in *Mtg16*$^{-/-}$ gene expression profiles to genes regulated by over-expressed E47 in the context of Notch signaling from OP9-DL1 cells (Table 2). 44 genes that were up regulated by loss of *Mtg16* were also co-activated by Notch signaling and E47 expression. Most importantly, key regulatory genes were found within this group including *Gata3, Id2, Socs3, Hes1,* and *Tle6,* which were also regulated by E47 in thymic lymphoma cells[278] (Tables 3, 4). Of note, the expression of *Mtg16,* but not *Mtg8* or *Mtgr1,* was activated by E47[9], suggesting a possible regulatory loop between these proteins. Collectively, these data indicate that Mtg16 plays a key role in integrating Notch signals and E protein actions to suppress myelopoiesis and direct T-cell differentiation.

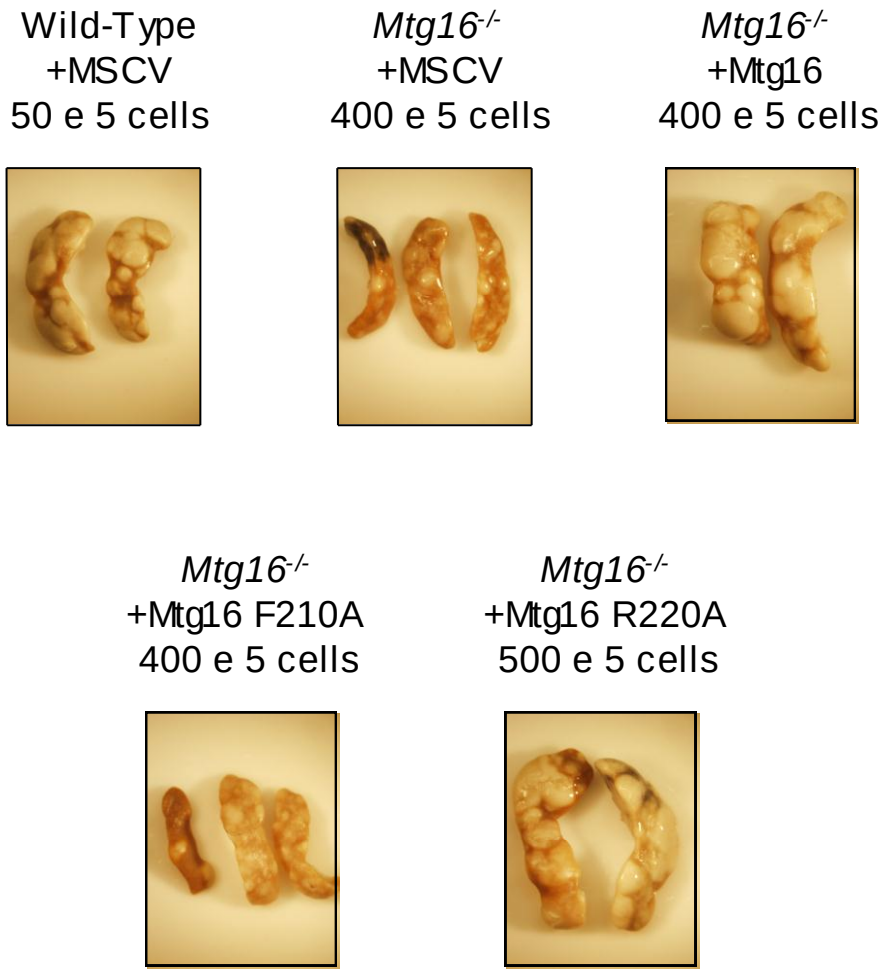

Figure 25. E-protein regulation is necessary for Mtg16 function in the CFU-S assay Wild-type and *Mtg16*$^{-/-}$ total bone marrow were infected with *MSCV-IRES-GFP, MSCV-IRES-GFP-myc-Mtg16, MSCV-IRES-GFP-myc-Mtg16* R220A or *MSCV-IRES-GFP-myc-Mtg16* F210A and transplanted into lethally irradiated mice. Day 12 colonies shown from one of two experiments for a total N=4-5 recipients.

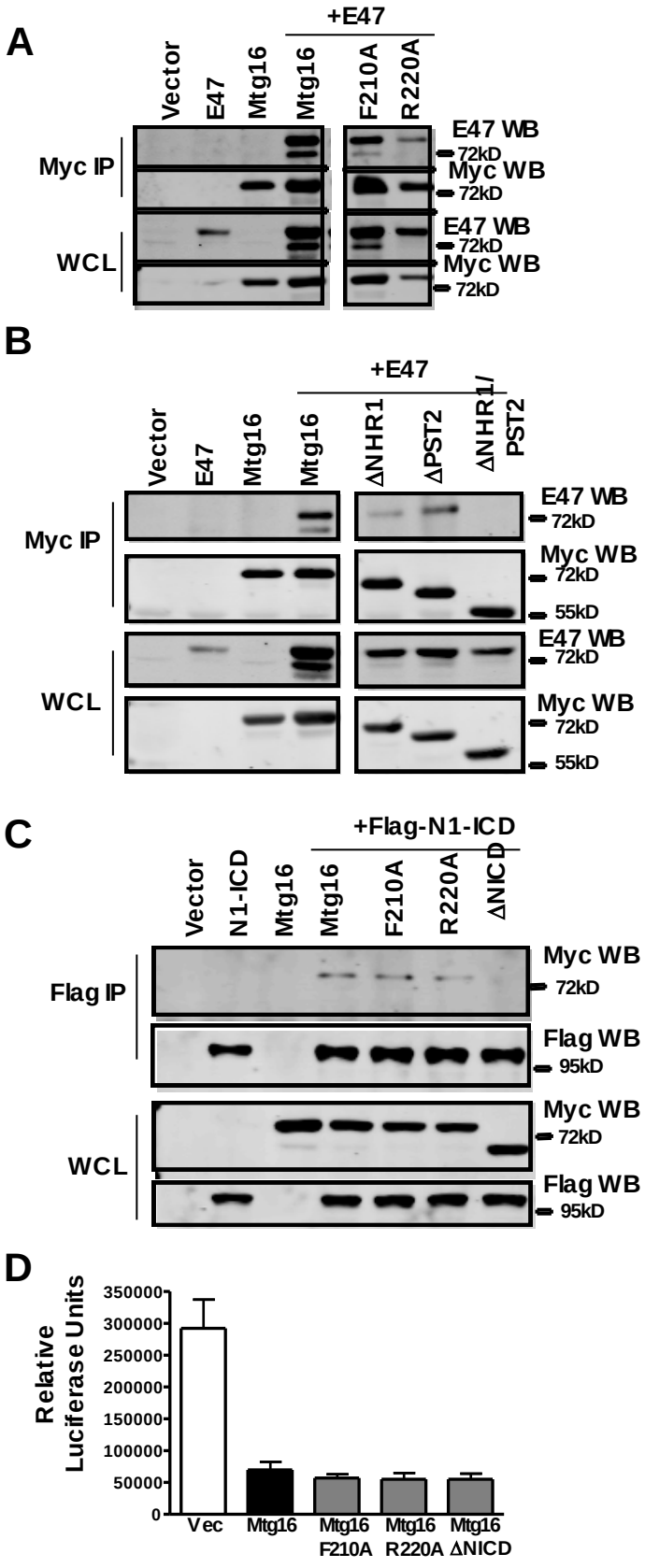
A
+E47
Vector
E47
Mtg16
Mtg16
F210A
R220A
Myc IP
WCL
E47 WB
72kD
Myc WB
72kD
E47 WB
72kD
Myc WB
72kD
B
+E47
Vector
E47
Mtg16
Mtg16
ΔNHR1
ΔPST2
ΔNHR1/PST2
Myc IP
WCL
E47 WB
72kD
Myc WB
72kD
55kD
E47 WB
72kD
Myc WB
72kD
55kD
C
+Flag-N1-ICD
Vector
N1-ICD
Mtg16
Mtg16
F210A
R220A
ΔNICD
Flag IP
WCL
Myc WB
72kD
Flag WB
95kD
Myc WB
72kD
Flag WB
95kD
D
Relative Luciferase Units
350000
300000
250000
200000
150000
100000
50000
0
Vec
Mtg16
Mtg16 F210A
Mtg16 R220A
Mtg16 ΔNICD

Figure 26. Mtg16 associates with E47 and the Notch Intracellular Domain. (A) Mtg16 F210A retains binding to E47 by co-immunoprecipitation. The indicated proteins were co-expressed and association measured by immunoprecipitation followed by western blot analysis. Positions of molecular weight markers are indicated to the right. (B) Deletion of NHR1 is not sufficient to remove the interaction between Mtg16 and E47. The indicated proteins were co-expressed and association measured by immunoprecipitation (IP) followed by western blot analysis (WB). Positions of molecular weight markers are indicated to the right. (C) Mtg16 F210A and R220A retain associating with the Notch1-Intracellular Domain by co-immunoprecipitation, while the DNICD no longer binds. The indicated proteins were co-expressed and association measured by immunoprecipitation (IP) followed by western blot analysis (WB). Positions of molecular weight markers are indicated to the right. (D) F210A, R220A, and ΔNICD do not affect Mtg16-dependent repression. Mtg16 and the indicated mutants were fused in frame with the GAL4 DNA binding domain and tested for repression using a Gal4-luciferase reporter construct. Graph shows the average relative luciferase values from an Gal4 reporter plasmid co-transfected with vector control or the indicated Mtg16 or mutant thereof. The values were normalized to a renilla-luciferase plasmid to control for specificity and transfection efficiency. The experiment was performed twice in triplicate.

Table 1. Genes Upregulated in *Mtg16*$^{-/-}$ LSK and Repressed in E47ER Hematopoietic Progenitor Cells			
Asb7	Dntt	Hip1	Myom1
Calcrl	Entpd4	Il18r1	Phf7
Ccl3	Fmn2	Itga6	Sytl4
Ctla2a	Gcnt2	Loxhd1	Tex15
Dlk1	Gem	Lypla3	

Table 2. Genes Upregulated in Both *Mtg16*$^{-/-}$ LSK and OP9-DL1/E47ER Hematopoietic Progenitor Cells			
Arhgef3	Gadd45b	Kif5a	Rassf4
Atp13a2	Galnt2	Ltb	Rps6ka6
Atp2a3	Gata3	Map3k8	Sgsh
CD52	Hcls1	Nnt	Sla
CD80	Hemgn	Nox4	Slc45a4
Celsr1	Hes1	Olfml1	Slco4a1
Csf2rb2	Hsd11d1	P2ry14	Smad7
Ctsl	Id2	Pcmtd2	Socs3
Dcx	Il10ra	Pik3cd	Tcf7l2
Esr1	Il1r1	Plaur	Tcrb-V13
Fyn	Itgam	Ptprc	Tle6

Table 3. Genes Upregulated in *Mtg16*$^{-/-}$ LSK and Repressed in E47ER 1F9 Thymoma Cells			
Adarb1	Gata3	Mbl1	Rasgef1b
Brd8	Gem	Mdga1	Rgs1
Cav2	Hhex	Myom1	Slc16a9
Col18a1	Hivep3	Nrxn1	Tex15
Dlk1	Hoxb2	Pik3r1	Ttr
Dusp18	Lonrf3	Plaur	Xlr3a

Table 4. Genes Upregulated in *Mtg16*$^{-/-}$ LSK and Activated in E47ER 1F9 Thymoma Cells			
Bcl2l1	Galnt2	Irf6	Sytl4
Ctsl	Gimap6	Itga6	Tcfec
Cyfip2	Hemgn	Itpr3	Tle6
Dhx9	Hes1	Jag2	Tmem35
Ebi3	Id1	Mxd4	Tnfrsf22
Efhc2	Id2	Nnt	Tnfrsf23
Esr1	Il10ra	Nsg2	Vegfa
Gadd45b	Il21r	Socs3	Wfdc2

Discussion

Our work indicates that Mtg16 is required for lymphopoiesis after bone marrow transplantation and that it acts in the LSK and DN1 populations (Fig. 13, 16). Surprisingly, 3 highly conserved domains, when deleted individually, were somewhat dispensable for Mtg16 function in T-cell differentiation, even the oligomerization domain (NHR2, Fig. 18). In contrast, the Notch ICD binding domain and the motif that is required for suppression of E protein transactivation within NHR1 were required for Mtg16 action (Fig. 18, 24). Given the intersection between Notch signaling and E protein function in T-cell differentiation, our data suggest that Mtg16 is a key regulator of this process that contributes to maintaining the correct level of several key genes that control lineage allocation and that are coordinately regulated by Notch signaling and E47 activation, including *Gata3*, *Id2*, and *Hes1* (Tables 1-4).

Although the Notch ICD association motif was important for Mtg16 function in T cell development (Fig. 18), it is intriguing to note that *Mtg16*$^{-/-}$ mice display many of the hallmarks of *E2A*-deficiency. In addition to defects in T cells, mice lacking *E2A* contain reduced numbers of B cells, fewer long-term hematopoietic stem cells and multi-potent progenitor cells, and fewer erythropoietic progenitor cells. In addition, stem cells lacking *E2A* showed a considerable defect in competitive repopulation assays[208,279]. Likewise, *Mtg16*$^{-/-}$ mice show defective stress erythropoiesis with few erythropoietic progenitors as measured by colony forming assays[19] and defects in stem cell competitiveness (Fischer et al., submitted). Chromatin immunoprecipitation assays also suggest that the association between Mtg16 and E proteins play an important role in the action of these factors during

hematopoiesis, as the most robust signal for Mtg16 was found near E protein binding sites in E2F2 when probing for direct Mtg16 targets amongst cell cycle genes (Fig. 27).

While the NHR1 domain was essential, the NHR2 domain was not absolutely required for Mtg16 function in the OP9-DL1 assay. NHR2 forms strong homo- and hetero-oligomers with MTG family members[14,40,280]. In fact, other MTG family members were the major associating proteins when MTGs or RUNX1-MTG8 were purified[14,31]. Our analysis suggests that Mtg16 monomers retain function and the observation that ΔNHR1 and ΔNICD impaired Mtg16 functions (Fig. 18), suggests that hetero-oligomers that might be formed with endogenous, wild type Mtgr1 (the other MTG family member widely expressed in hematopoietic cells, Fig. 14) were unable to exert the same functions as Mtg16 and thereby complement this defect. NHR2 is more essential for multipotent progenitor reconstitution after transplant in the CFU-S assay, as the ΔNHR2 construct could not reconstitute *Mtg16*$^{-/-}$ bone marrow function. Similar to NHR2, the NHR3 and NHR4 domains were not absolutely required for Mtg16 to rescue T-cell development (Fig. 4). NHR4 mediates the weaker of the two contacts between Mtg16 and NCoR/SMRT, but is not required for associating with N-CoR or for transcriptional repression[20,23], whereas the NHR3 domain contributes to binding the regulatory subunit of protein kinase A (PKA RII) [42,281]. The NHR3 domain is the most consistently dispensable, as it was not required for reconstitution of the CFU-S assay (Fig. 22). Rather than contributing to the formation of acute leukemia, deletion of these domains has been associated with increasing the activity of the t(8;21) fusion protein[264], suggesting that these domains play a negative regulatory role.

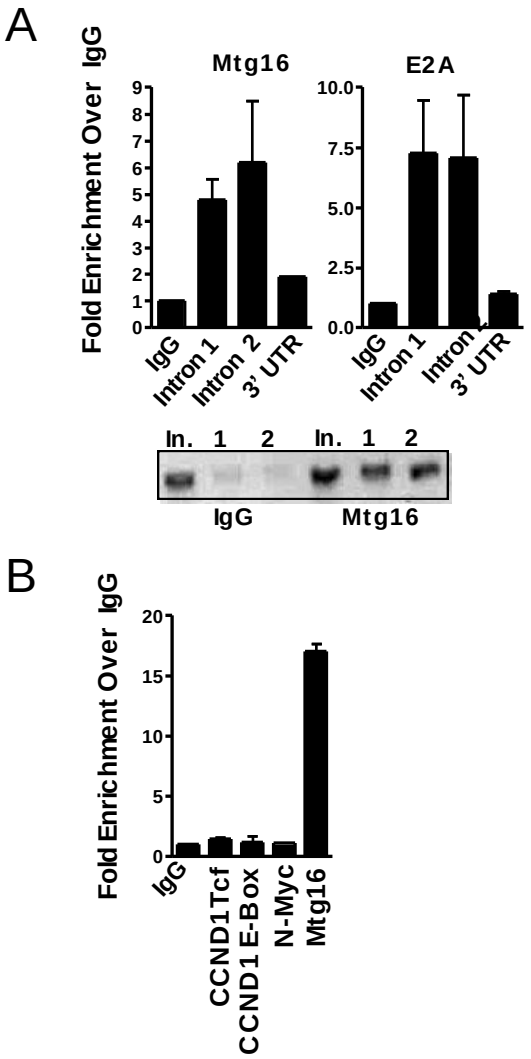

Figure 27. Mtg16 binds an E2A site in the 1st Intron of E2F2 (A) Mtg16 associates with the first intron of *E2F2*. Chromatin immunoprecipitated with either control IgG or anti-Mtg16/Eto2 from lysates of MEL cells was amplified with primers specific to two regions encompassing an E2A binding site in the first intron of *E2F2*, or as a control, the 3Õuntranslated region (UTR) of *E2F2* using quantitative PCR. Graph shows the level of signal relative to IgG set to ÒlÓ The panel at the right shows ChIP using anti-E47 with the same *E2F2* 1st intron primers. The ethidium bromide stained agarose gel shows a representative PCR reaction stopped after 30 cycles; In., input; 1 and 2 designate the duplicate PCR samples from the ChIP reaction using primer set #2 flanking the E2A. (B) Mtg16 associates with a GATA-E-box in the Mtg16 promoter, but not an E2A/CSL site in the CCDN1 promoter or Tcf4 sites in the CCND1 or N-Myc promoters. Experiments performed as in (A) and shown relative to an IgG value of ÒlÓ

Notch signaling is a key determinant in instructing T-cell development, and when coupled with IL7 is sufficient to induce T-lineage development *in vitro*[74,81]. The Notch ICD binds to CSL and recruits Mastermind to activate transcription[274]. The association of MTGs with CSL suggested that Mtg16, like MTG8, acts as a co-repressor to suppress the expression of downstream target genes such as *Hes1*[29]. The discovery of an association between the Notch ICD and Mtg16 furthered this model by suggesting a mechanism by which the Notch ICD impairs the association between Mtg16 and CSL, perhaps allowing Mastermind to bind to CSL[43]. The high levels of expression of the canonical Notch target genes *Hes1* and *Nrap* in *Mtg16*-null LSK cells[43] and the failure of the Mtg16 mutant that lacks the Notch ICD binding motif to complement the null phenotype (Fig. 16), even though this mutant impaired E-protein-dependent transcriptional activation (Fig. 24B), are consistent with this interpretation. Importantly, our mutation data indicate that the loss of *Mtg16* perturbs the function of other necessary factors in T-cell development (e.g., E proteins) that allow the proper integration of Notch signals. Thus, Mtg16 plays a critical role in integrating Notch signals and E protein functions in T cell development, perhaps in the earliest bone marrow progenitor cells.

CHAPTER IV

MYELOID TRANSLOCATION GENE 16 (MTG16) CONTRIBUTES TO MURINE B-CELL DEVELOPMENT

Abstract

Myeloid translocation gene 16 (Mtg16) is a target of the t(16;21) that produces acute myeloid leukemia. Like many targets of leukemia-associated chromosomal translocations, Mtg16 regulates several stages of hematopoiesis, including lineage allocation and stem cell function. Decreased $B220^{+}$ B-cells in the bone marrow of *Mtg16*$^{-/-}$ mice have previously been reported, and we show that this defect is due to decreased B-lineage commitment and an associated decrease in the numbers of Common Lymphoid Progenitor (CLP) cells. The defect in B-cell commitment is magnified after stress such as competitive bone marrow transplant and IL7-dependent methylcellulose colony formation assays. *Mtg16*$^{-/-}$ pre-B colonies have striking growth and survival defects that can be reverted by deletion of *p53*. Defects in B-cell function in the absence of *Mtg16* extend to mature B-cells of the spleen and *Mtg16*$^{-/-}$ splenic B-cells have marginal zone skewing, decreased response to lipopolysaccharide (LPS) *in vitro*, and defective germinal center responses. Therefore, Mtg16 regulates both early B-cell development and mature B-cell function.

Introduction

Chromosomal translocations that lead to leukemia and lymphoma disrupt master regulators of hematopoietic transcription. Originally identified by their role in chromosomal translocations, many of these factors have been subsequently identified as important for facets of hematopoiesis beyond leukemia. One such factor that is emerging in importance in leukemia and general hematopoiesis is Myeloid Translocation Gene 16 (Mtg16) or Cbfa2t3, which is a target of the t(16;21) that produces acute myeloid leukemia when translocated to Runx1 or AML1[12]. Myeloid Translocation Gene 16 is a critical regulator of murine hematopoiesis and affects stem cell function, erythroid development, and lineage fate specification[19] (Chapter III, Fischer et al, in prep). In the absence of *Mtg16* lymphoid lineages are decreased, including a global decrease in $B220^{+}$ cells in the bone marrow and a striking defect in T-cell development[19] (Chapter III). Concurrently, granulocyte/monocyte myeloid lineage commitment is enhanced. The defects seen in T-cell development are attributed to stem and progenitor cell dysfunction, with decreased numbers and impaired function of early T-cell progenitors, including both the Lymphoid Primed Multipotent Progenitor (LMPP) fraction and early thymocyte progenitor (ETP) fraction.

All $Mtg16^{-/-}$ phenotypes are subtle under homeostasis, but become more pronounced after stress such as bone marrow transplant or phenylhydrazine administration[19]. Associated with this stress-related exacerbation is the ability of Mtg16 to regulate cell cycling and survival, which contributes to many of the phenotypes seen after the loss of *Mtg16*[19]. For example, $Mtg16^{-/-}$ hematopoietic progenitor cells were

deficient in spleen colony formation after transplant, but this defect was bypassed with over expression of the cell cycle regulator *Myc,* suggesting that proliferation defects in the absence of *Mtg16* plays a key role in the lack of colony formation[19]. In early developing T-cells, growth and survival defects were seen in OP9-DL1 *in vitro* assays, where increases to apoptosis contribute to decreased cellular expansion in response to IL-7 and Flt3-ligand (Chapter III).

Mtg16 functions by interacting with a number of transcription factors and recruiting transcriptional co-repressors, such as NCoR and HDACs, to repress downstream transcription[20,273]. The transcription factor interacting partners for Mtg16 include many factors that act during hematopoiesis, including Tcf4, CSL, GFI-1, E2A, and Bcl6[25,26,28,31,43]. The interaction between Mtg16 and E2A is exceedingly robust and has been well characterized structurally, though the importance of this interaction was not realized until a novel role for Mtg16 in regulating lymphocyte development, and T-cell development in particular, was discovered[31,270] (Chapter III). E-proteins such as E2A facilitate specification of B-cell fate as well as T-cell fate, and also regulates the function of mature B-cells, including marginal zone vs. follicular zone decisions and germinal center reactions[97,122,148,149,189,198,203].

BCL6, another important transcription factor binding partner for Mtg16, also regulates both immature and mature B-cell development[25,142,282-284]. While the most well-understood role for Bcl6 in hematopoiesis is in regulating the germinal center response associated with mature B-cell immune function, it also regulates immature B-cell survival during V(D)J recombination[142,282-284]. Histone deacetylases, such as HDAC3, also regulate lymphocyte development and conditional deletion of *Hdac3* in early B-cells

(using *Mb1-Cre*) led to an accumulation of early $B220^{+}CD43^{+}$ cells at the expense of mature cells (Bhaskara et al, in prep). This defect appears to be due to defects in V(D)J recombination, though the mechanism is under further investigation. Recent data suggests that conditional deletion *Hdac3* in later B-cells using *CD19-Cre* bypasses the defect in early B-cell development. Mature $Hdac3^{-/-}$ B-cells were defective in germinal center reactions as well, likely reflecting the capacity of Hdac3 to facilitate Bcl6 mediated repression (Bhaskara in prep). Therefore, multiple Mtg16 interacting partners regulate B-cell development and do so at a variety of stages.

Given that Mtg16 is highly expressed in murine $B220^{+}$ populations in both the bone marrow and spleen, that it associates with transcription factors and co-repressors that are important to B-cell development, and that $Mtg16^{-/-}$ display decreased percentages of $B220^{+}$ cells, we further explored the role of Mtg16 in regulating B-cell development[19,25,31] (Chapter III). $Mtg16^{-/-}$ mice showed decreases in cell numbers throughout early B-cell development, with the most striking changes coming in early progenitor populations including Common Lymphoid Progenitors (CLPs) and in mature re-circulating cells. The progenitor defects were made more severe under stress using both bone marrow transplant and *in vitro* methylcellulose colony formation assays supplemented with 10 ng/ml IL-7. Methylcellulose assays also unearthed a striking deficit in cell growth and survival in early B-cells in the absence of *Mtg16*. Furthermore, *Mtg16* appears to be critical for mature B-cell function, with altered marginal zone vs. follicular zone cell fate decisions, defective LPS stimulation responses, and impaired germinal center formation in $Mtg16^{-/-}$ mice. Therefore, Mtg16 is a critical regulator of multiple stages of B-cell development.

Results

Mtg16$^{-/-}$ mice are lymphopenic

Initial analysis of *Mtg16*$^{-/-}$ mice showed changes across hematopoiesis in response to stress, including profound defects in erythropoiesis[19]. In addition, *Mtg16*$^{-/-}$ hematopoiesis produces decreased total thymocytes as well as decreases in total bone marrow B220^{+} developing B-cells[19]. To assess whether this decrease in developing lymphoid cells affects peripheral lymphocytes, we began with complete blood counts and found that these mice are significantly lymphopenic throughout early adulthood (Fig. 28A). Surprisingly, flow cytometric analysis of peripheral hematopoietic organs from 6-8 week old adult mice showed that CD3^{+} T-cells did not contribute significantly to the peripheral lymphopenia, and, while they do show a decrease in total cell number, CD3^{+} T-cells are not decreased as a percentage of total splenic cells (Fig. 28B). This suggests that while T-cell development in the thymus is severely impaired, by 6 weeks of age and under homeostatic conditions, T-cell development can achieve near-normal levels in the peripheral blood system.

On the other hand, *Mtg16*$^{-/-}$ mice showed decreased B220^{+} B-cells in the spleen, both as a percentage of total splenic cells and as a total number of cells, likely accounting for the peripheral lymphopenia (Fig. 28B). As previously published, myeloid development was enhanced, as *Mtg16*$^{-/-}$ mice have increased absolute and relative numbers of Gr1^{+}/Mac1^{+} myeloid cells in the spleen (Fig. 28B). Flow cytometric analysis of the bone marrow showed decreases in total B220^{+} cells in both relative and absolute

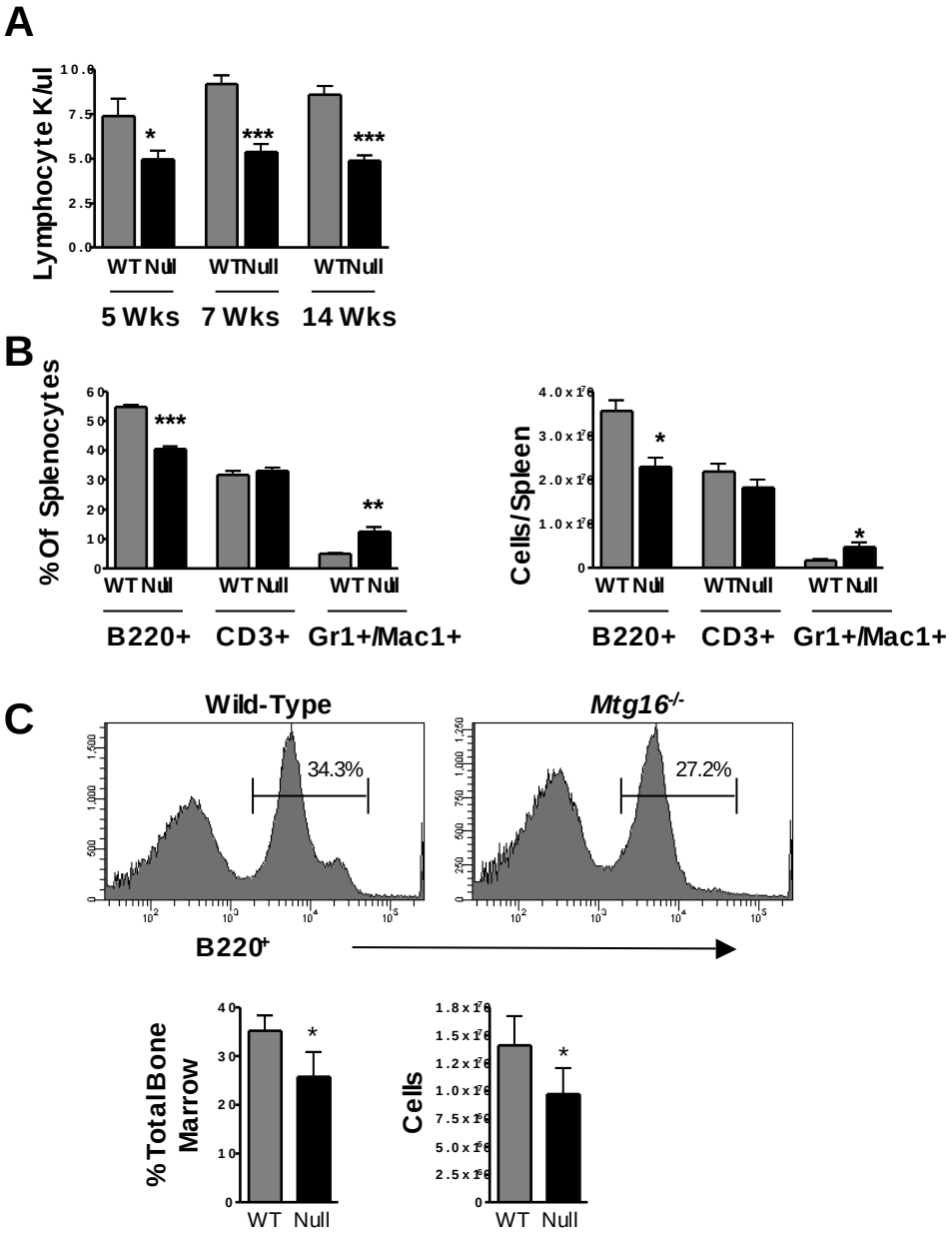

Figure 28. *Mtg16*$^{-/-}$mice are lymphopenic (A) Complete blood counts of wild-type and *Mtg16*$^{-/-}$mice from peripheral blood throughout adulthood. Graph depicts lymphocytes per (B) Flow cytometric analysis of total splenocytes from wild-type and Mtg16$^{-/-}$mice show increased Gr1^{+}/Mac1^{+}myeloid cells and decreased B220^{+} B-cells. Graphs depict Mean $\pm$SD from one of two experiments. *, p<0.05, **p<0.01, ***,p<0.001. (C)Representative plots from flow cytometric analysis of total bone marrow B220^{+} populations. Graphs depict mean $\pm$ SD from one of three independent experiments. *, p<0.05

numbers of total bone marrow cells per femur (Fig. 28C.) The increase in $Gr1^+/Mac1^+$ cells in the absence of *Mtg16* persisted in the bone marrow as well (Chapter III).

Lymphopenia is more severe after competitive bone marrow transplant

Given that many of the *Mtg16*$^{-/-}$ phenotypes are more severe after stress, we sought to assess lymphopenia and lineage allocation after competitive bone marrow transplantation. *Mtg16*$^{-/-}$ defects in erythropoiesis make traditional bone marrow transplant lethal, so all bone marrow transplant assays to assess stem cell function and differentiation were performed with 90% $CD45.2^+$ wild-type or *Mtg16*$^{-/-}$ marrow supplemented with 10% $CD45.1^+$ wild-type bone marrow to provide the necessary erythrocytes for survival (Fischer et al, in prep). By following $CD45.2^+$ cell surface labeling of peripheral blood, competitive reconstitution was monitored. Peripheral reconstitution by *Mtg16*$^{-/-}$ $CD45.2^+$ cells was severely impaired over time (Fischer et al, in prep and Fig. 29A). The defect seen in the peripheral blood was more severe than the defect seen in total bone marrow and hematopoietic stem cells, and given that peripheral blood is comprised primarily of lymphocytes, we hypothesized that the lymphopenia seen in the absence of *Mtg16* was an exacerbated after transplant (Fig. 29A). When lineage contribution in the peripheral blood was assessed following competitive transplant bleeds, most of the wild-type $CD45.2^+$ cells were B and T-cells, while *Mtg16*$^{-/-}$ $CD45.2^+$ peripheral blood showed decreased B-cells and a higher relative proportion of myeloid cells (Fig. 29A).

We next assessed the contribution of $CD45.2^+$ *Mtg16*$^{-/-}$ cells to B-cell development and myeloid development in the bone marrow of recipient mice. Within the

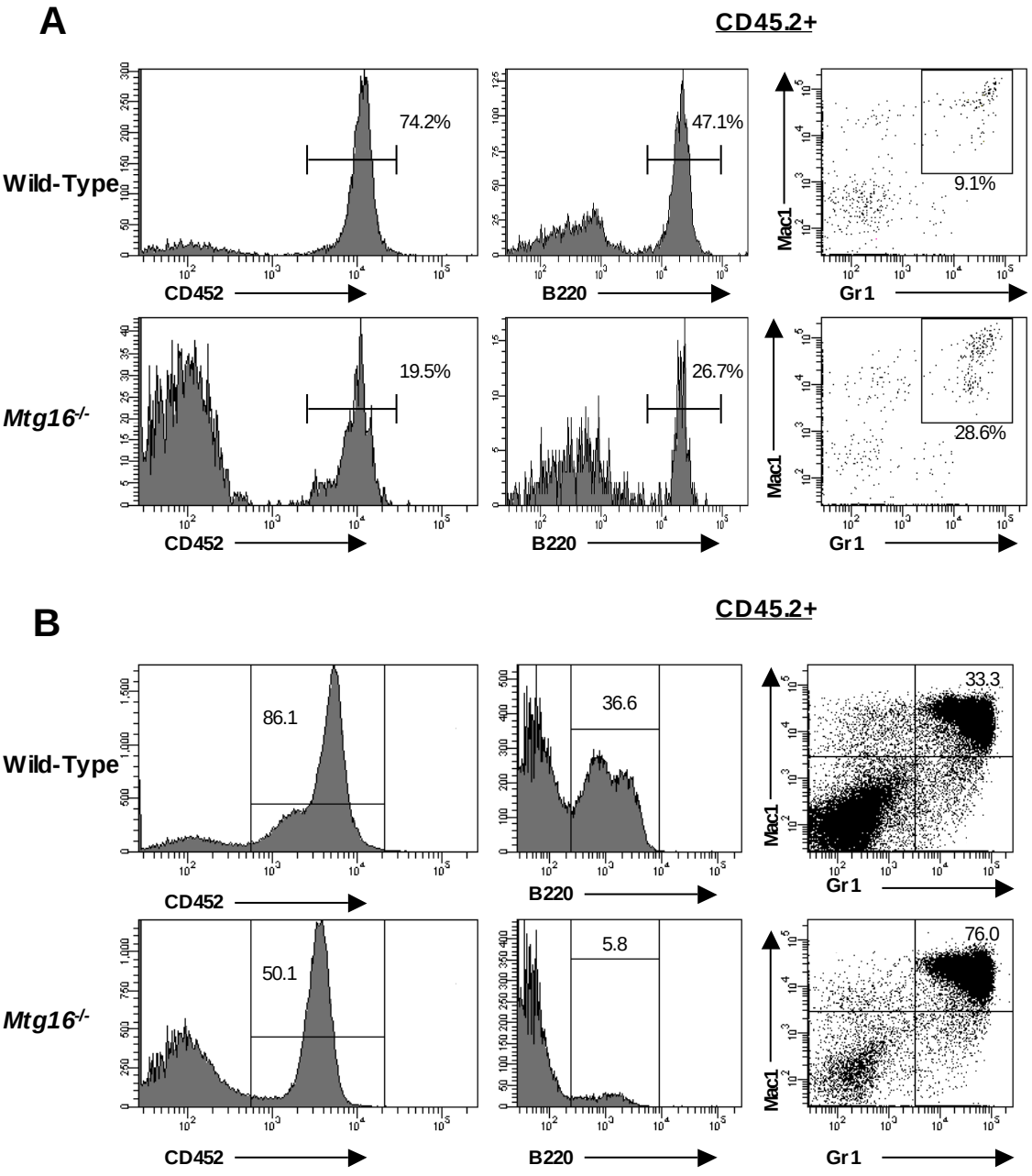

Figure 29. Impaired B-cell and enhanced myeloid development from *Mtg16*$^{-/-}$ bone marrow is more severe after transplant (A) Decreased B-cell contribution and increased myeloid contribution to the peripheral blood from *Mtg16*$^{-/-}$ marrow transplants. Representative plots show flow cytometric labeling of peripheral blood 12 weeks after transplant with 10% CD45.1^{+} wild-type marrow and 90% CD45.2^{+} wild-type or *Mtg16*$^{-/-}$ test marrow. B220 and Gr1/Mac1 plots show CD45.2^{+} cells. (B) Flow cytometric analysis of bone marrow from the same competitive transplant confirm decreased B-cell development and increased Gr1^{+}/Mac1^{+} myeloid development. CD45.2^{+} events are shown.

CD45.2^{+} population, there was little to no contribution to B-cell lineages and an exaggerated Gr1^{+}/Mac1^{+} myeloid population (Fig. 29B). This corresponds well with the defect in thymus reconstitution seen in the absence of *Mtg16*, where virtually no CD45.2^{+} thymocytes remained from *Mtg16*$^{-/-}$ donor cells (Chapter III). Much like other phenotypes, the lymphopenia and decreased B-cell development seen in the absence of *Mtg16* becomes much more dramatic under stress, highlighting the importance of *Mtg16* in regulating B-cell development.

Defects in early B-cell development in the absence of *Mtg16*

To analyze B-cell development in greater detail and pinpoint the mechanism for Mtg16 involvement, we used flow cytometry to detect cells expressing the B220, CD43, BP-1, CD24, IgM, and IgD cell surface markers to identify seven distinct stages labeled A through F^{120}. *Mtg16*$^{-/-}$ developing B-cells show little change in early B-cell stages, or "Hardy Fractions" A through C (Fig. 30.) The most striking changes were in the more mature, CD43^{+} fractions D, E, and F, with a significant relative increase in non-Ig expressing Fraction D at the expense of more mature Ig-expressing B-cells, or Hardy Fractions E and F (Fig. 30). When taking into account the overall decrease in B220^{+} cells, though, the percent of total bone marrow cells in each stage remained lower in the absence of *Mtg16*. As the decrease in mature cells is not accompanied by an increase in immature cells, we ruled out an overt block to development. Instead, it is likely that the decrease seen in Fraction F reflects the decrease in re-circulating peripheral lymphocytes, as they will return to the bone marrow as Fraction F cells.

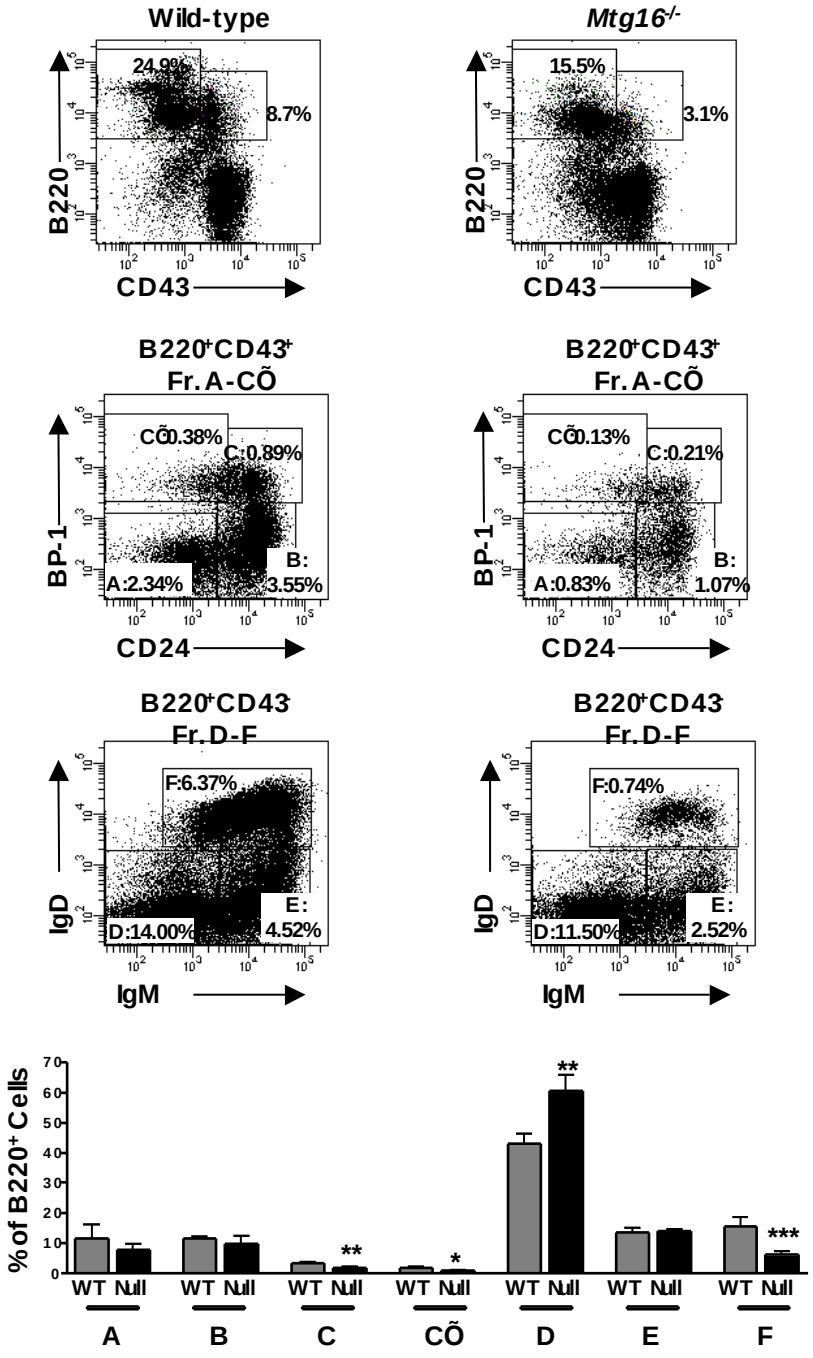

Figure 30. Analysis of *Mtg16*$^{-/-}$ B-cell development. Flow cytometric labeling of wild-type and *Mtg16*$^{-/-}$ bone marrow using the Hardy Fractions A-F. Percentages listed on plots reflect percent*of total bone marrow. Graph depicts percent of total B220^{+} cells. *p<0.05, **p<0.01, ***p<0.001

To further confirm the absence of blocks in early maturation of B-cells in the absence of *Mtg16*, we probed V(D)J IgH recombination in total $B220^+$ populations. Using three different sets of primers to assess D_H to J_H recombination and both proximal and distal V_H to DJ_H recombination, we found normal V(D)J recombination in *Mtg16*$^{-/-}$ $B220^+$ cells when compared to wild-type controls (Fig. 31). While inactivation of *Hdac3*, an Mtg16 binding partner, impaired V(D)J recombination, this phenotype is likely due to a more global effect on chromatin structure (Bhaskara et al, in prep).

Given the small changes seen in B-cell development, the absence of a block to development in the more mature stages of lymphopoiesis after lineage commitment, and the increase in myeloid development, we hypothesized that the source of the lymphopenia preceded lineage commitment into stem and progenitor stages of hematopoiesis. This has previously been characterized in the context of T-cell development, as *Mtg16*$^{-/-}$ cells show enhanced granulocyte and monocyte development in *in vitro* T-cell assays (Chapter III). To address this hypothesis, we first turned to flow cytometric analysis of B-cell progenitors, namely the $Lin^-IL7\text{-}R^+Sca\text{-}1^{lo}c\text{-}Kit^{lo}$ Common Lymphoid Progenitor (CLP) that is though to contribute primarily to B-cell development[62,66]. We observed a significant though relatively subtle decrease in CLPs as a percentage of total bone marrow (Fig. 32). This corresponded to the two-fold decrease seen in the lymphoid primed multipotent progenitor (LMPP) cells that precede CLP development and further confirms decreased lymphoid commitment from early progenitor populations.

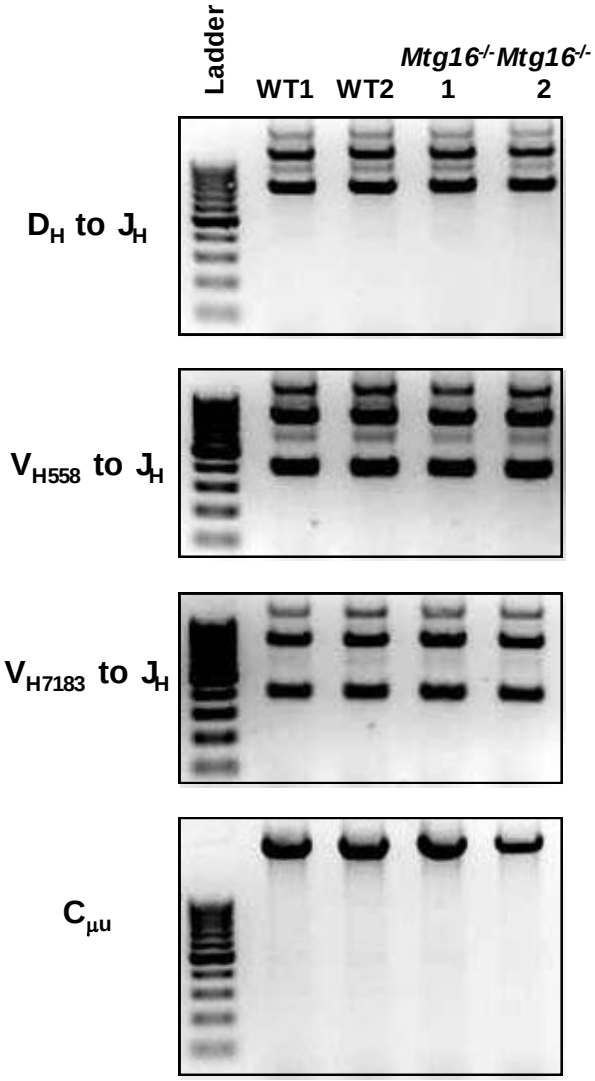

Figure 31. V(D)J Recombination is unperturbed in *Mtg16*$^{-/-}$ B220^{+} Cells V(D)J recombination of the IgH locus in B220^{+} cells was assessed by PCR. V_{H558} to J_H measures proximal V to DJ recombination while V_{H7183} to J_H measures distal V to DJ recombination. $C_{\mu u}$ serves as a control.

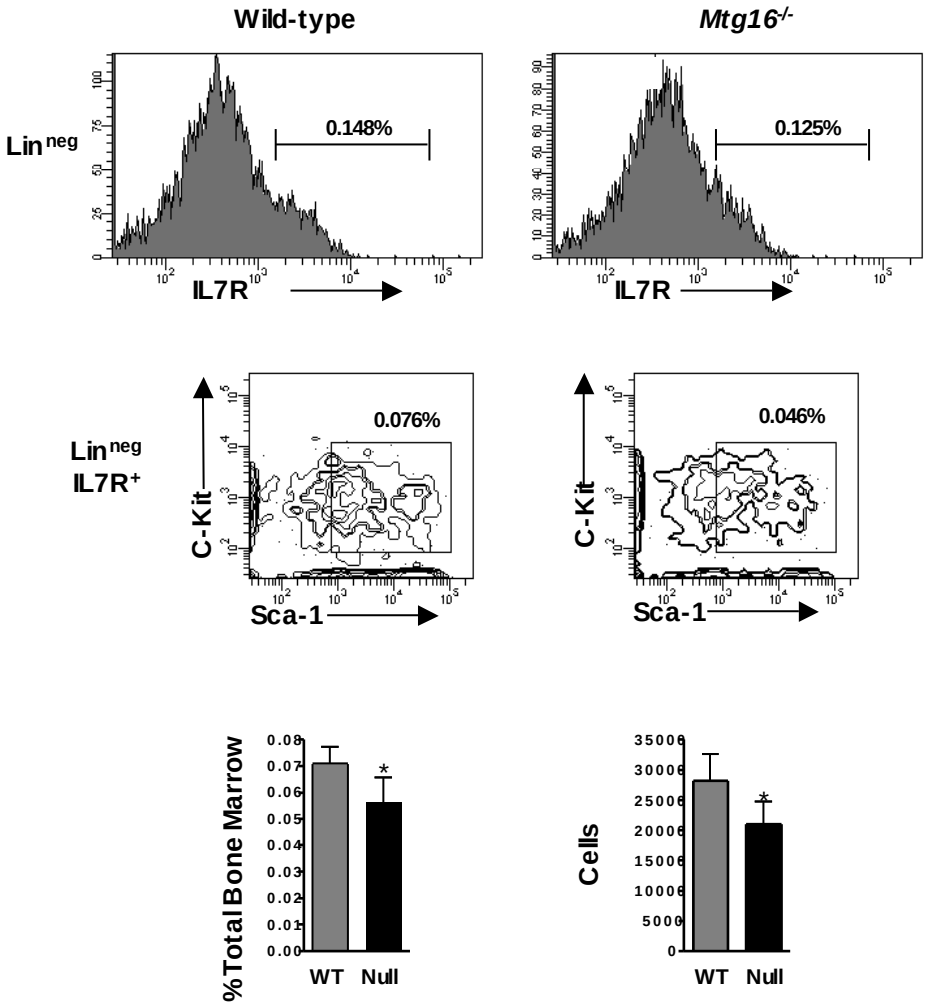

Figure 32. Common Lymphoid Progenitor Cell (CLPs) are decreased in the absence of *Mtg16* $Lin^{neg}IL7R^{+}c\text{-}Kit^{lo}sca\text{-}1^{lo}$ Common Lymphoid Progenitors were assessed by flow cytometry. Representative flow cytometry plots shown from one of two experiments. Percents noted on plots represent percent of total bone marrow. Graphs depict Mean $\pm$ SD, with *$p<0.05$.

Mtg16 is required for normal B-cell methylcellulose colony formation

To assess the functional quality of *Mtg16*$^{-/-}$ progenitor cells in the formation of B-cell lineages, we used *in vitro* differentiation assays. One of the most commonly used assays is the Methylcellulose assay which determines the relative number and quality of progenitor cells by their ability to produce clonogenic colonies of mature cells when plated in a semi-solid media with specific growth factors. To address the ability of *Mtg16*$^{-/-}$ bone marrow to produce early pre-B-cell colonies, we plated 7.5 x 10^4 total bone marrow cells from either wild type or *Mtg16*$^{-/-}$ mice in M3630 methylcellulose containing 10ng/ml rhIL-7. The *Mtg16*$^{-/-}$ colonies were distinctly smaller by visual inspection (Fig. 33A). As expected from the decrease in CLPs and early B-cells in the *Mtg16*$^{-/-}$ marrow, we found a significantly decreased number of pre-B cell colonies at day 7 (Fig. 33B).

While it is recommended that the colony number be counted at day 7, we also allowed our plates to incubate until day 14 to further assess cell growth in what should become nutrient depleted conditions. The wild-type colonies continued to respond to the presence of IL-7, and expanded in size from day 7 to day 14, while the *Mtg16*$^{-/-}$ colonies failed to expand, and in fact appeared to contract in size (Fig. 33A). Colony formation appeared to be complete by day 7, as wild-type plates contained the same or fewer numbers of colonies at day 14 (Fig. 33B). Harvesting the plates and counting total numbers of cells per plate confirmed that *Mtg16*$^{-/-}$ colonies failed to expand over this 14-day period as compared to wild type colonies, leading to a disparity in the total number of cells per plate by day 10; this disparity was significantly larger by day 14 (Fig. 33C).

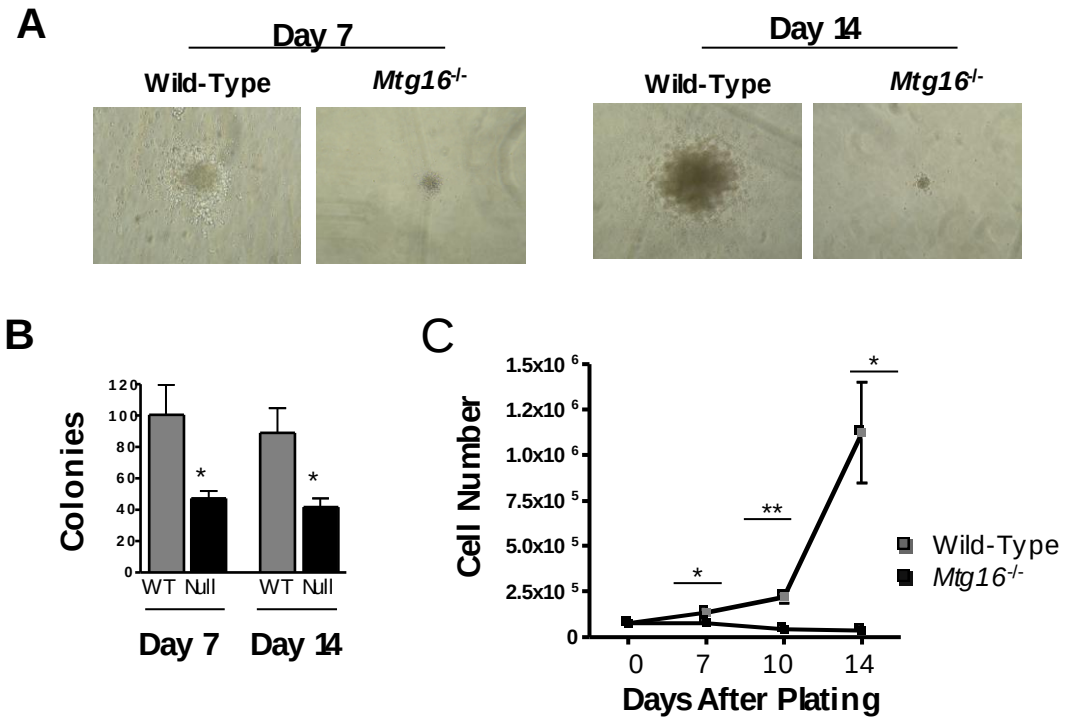

Figure 33. Decreased *Mtg16*$^{-/-}$ Pre-B colony number associated with an expansion deficit (A) Representative pictures of wild-type and *Mtg16*$^{-/-}$ M3630 methylcellulose colonies at both Day 7 and Day 14. The same colony is represented in each picture. 4x magnification. (B) Graphs depict colony counts on Day 7 and Day 14. Mean $\pm$ SD, with *$p<0.05$. (C) Growth curves of total cells per M3630 plate over the 14 day time course. *$p<0.05$, **$p<0.01$.

The natural culprit for the decreased expansion of pre-B colonies in IL7-containing methylcellulose would be decreased cell proliferation. To assess the cell cycle status of pre-B colonies, methylcellulose plates were harvested at day 7 and the DNA stained using propidium iodide to identify cells as 2N (G_o/G_1), 4N (G_2/M), or S-phase. While wild type cells were actively cycling, *Mtg16*$^{-/-}$ pre-B cells accumulated in the 2N G_0/G_1 stage (Fig. 34A). To investigate changes to cell death within the *Mtg16*$^{-/-}$ colonies, methylcellulose plates were harvested and total cells were stained with Annexin V, which showed a statistically significant increase in Annexin V^+ cells in the absence of *Mtg16* (Fig. 34B). Lack of cell-cycle entry and increased apoptosis likely accounts for the small size and decreased expansion of these more mature, B-lineage committed cells. Lack of response to IL-7 driven growth is a possible mechanism for the lack of cell-cycle entry, but colonies do form, and thus *Mtg16*$^{-/-}$ progenitor cells are able to respond to IL-7 and contribute to B-cell development, albeit in a reduced capacity. Furthermore, increasing the concentration of IL-7 had a similar dose-dependent effect on WT and *Mtg16*$^{-/-}$ colony expansion, confirming that *Mtg16*$^{-/-}$ progenitor cells are capable of responding to IL-7 cytokine stimulation (Fig. 34C).

Altered DNA damage in IL7-dependent colonies in the absence of *Mtg16*

Increased DNA damage has been found in several *Mtg*-deficient cell populations, most notably *Mtg8*$^{-/-}$ murine embryonic fibroblasts (MEFs) and *Mtg16*$^{-/-}$ hematopoietic progenitor cells, particularly those that are rapidly cycling in *in vitro* culture assays (DeBusk et al, in prep, Fischer et al, in prep). Collectively, these data suggest a role for Mtg family members in regulating DNA damage and/or DNA damage responses.

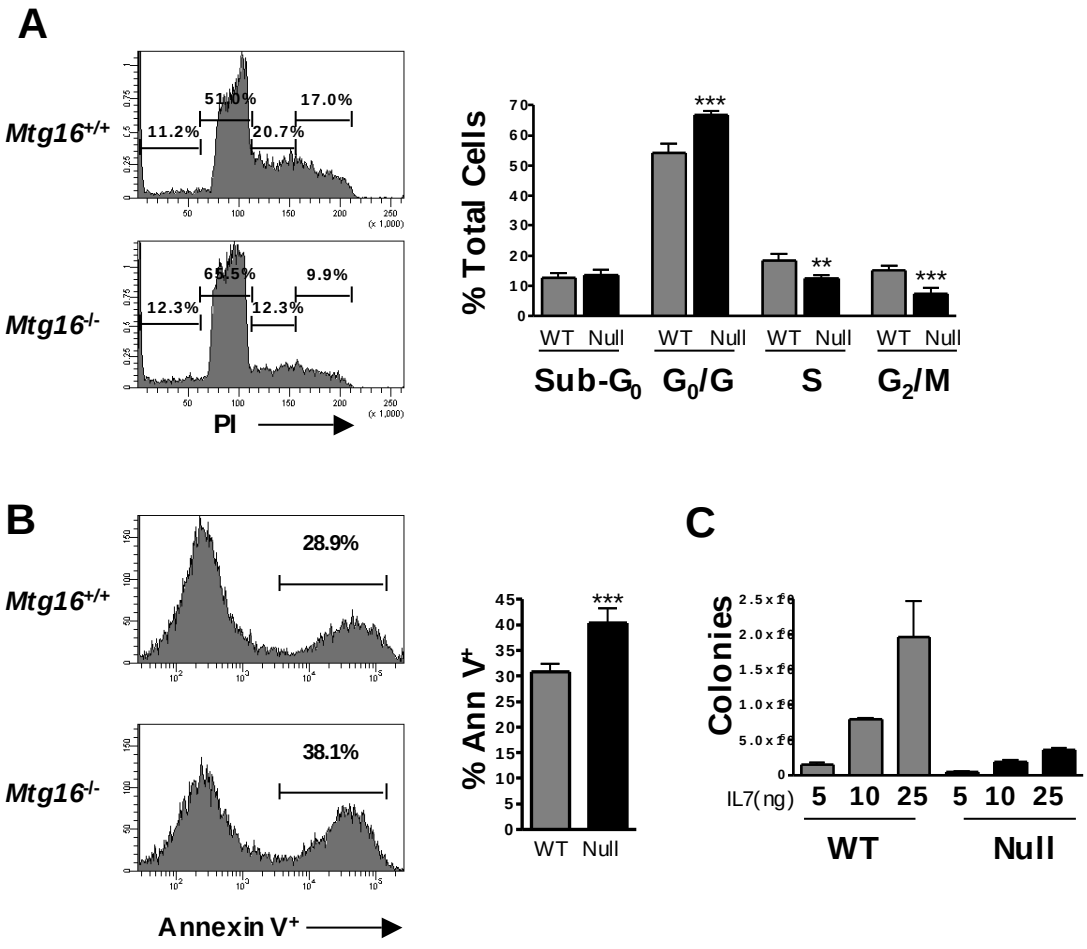

Figure 34. Decreased *Mtg16*$^{-/-}$ Pre-B colony size is due to altered cell cycle and increased apoptosis (A) Representative flow cytometry plots from Propidium idoide staining of wild-type and *Mtg16*$^{-/-}$ M3630 methylcellulose colonies Day 7. Percent of total cells in each population depicted graphically with Mean ± SD. **p<0.01, ***p<0.001 Data from one of two experiments for a total N=7 (B) Representative flow cytometry plots from Annexin V apoptosis staining of Day 7 M3630 colonies. Percent of total positive cells depicted graphically with mean ± SD ***p<0.001. Data from one of two experiments for a total N=7 (C) Colony counts from methylcellulose plated with increasing IL7 concentration. Data from one experiment performed in triplicate.

Given the cell cycle arrest and increased apoptosis seen in *Mtg16*$^{-/-}$ B-cell colonies, we asked if an increase in DNA damage contributed to the defect in growth and survival in colonies grown in IL7-dependent methylcellulose. Using intracellular γH2aX staining, we found a two-fold increase in cells with a high level of γH2aX staining by flow cytometry (Fig. 35).

To further probe the importance of DNA damage in the absence of *Mtg16*, we crossed the *Mtg16*$^{-/-}$ mice with *p53*$^{-/-}$ mice, with the hypothesis that removing a critical DNA damage checkpoint would restore cell cycle entry, block apoptosis, and increase colony growth and formation. In the IL7-containing methylcellulose assays deletion of *p53* in the context of wild-type *Mtg16* caused an increase in colony size and number and an overall decrease in apoptosis, consistent with changes in early B-cell development in the absence of *p53* (Fig. 36A, B). *Mtg16*$^{-/-}$*p53*$^{-/-}$ bone marrow had a subtle increase in colony formation relative to *Mtg16*$^{-/-}$*p53*$^{+/+}$, but a more dramatic increase in the size and cell number of colonies (Fig. 36A, B) that surpassed *Mtg16*$^{+/+}$*p53*$^{+/+}$ controls at day 7, but did not approach the changes seen in *Mtg16*$^{+/+}$*p53*$^{-/-}$. The *Mtg16*$^{-/-}$*p53*$^{-/-}$ colonies displayed a decrease in Annexin V staining that restored the levels to those of *Mtg16*$^{+/+}$*p53*$^{-/-}$ colonies, further confirming that decreased cell survival contributed to the changes in colony number and size seen in the absence of *Mtg16* (Fig. 36C). Given the relatively subtle increase in DNA damage seen in the *Mtg16*$^{-/-}$ colonies, we hypothesize that these changes seen in *Mtg16*$^{-/-}$*p53*$^{-/-}$ primarily reflect a decrease in apoptosis and that other functions of Mtg16, such as lymphoid progenitor specification through transcription factors like E2A, may lead to an intermediate phenotype compared to wild-type and *p53*$^{-/-}$ control cells.

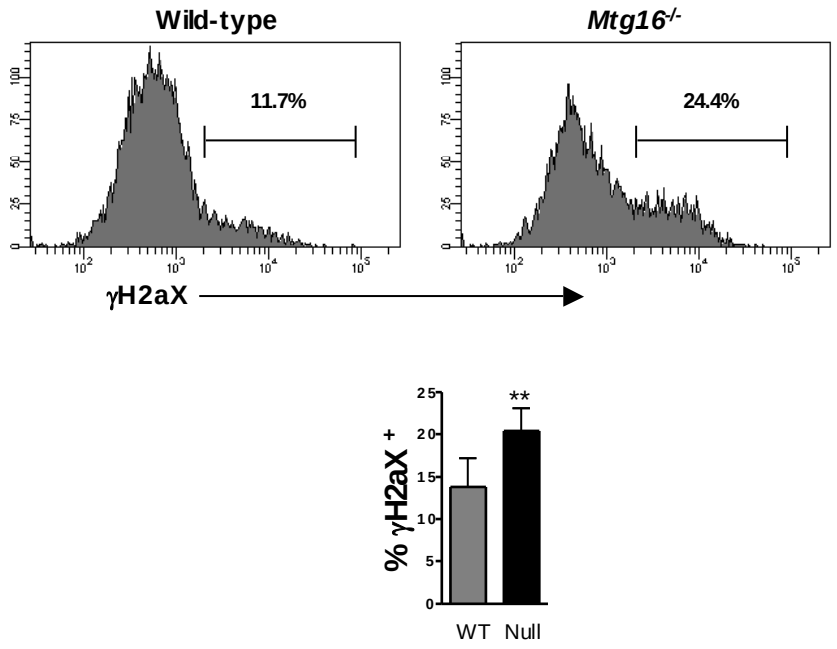

Figure 35. *Mtg16*$^{-/-}$ Pre-B colonies have Increased γH2aX staining by flow cytometry Representative flow cytometry plots from γH2aX staining of Day 7 M3630 cultures. Graph depicts Mean ± SD from one of two experiments with a total N=7. **p<0.01

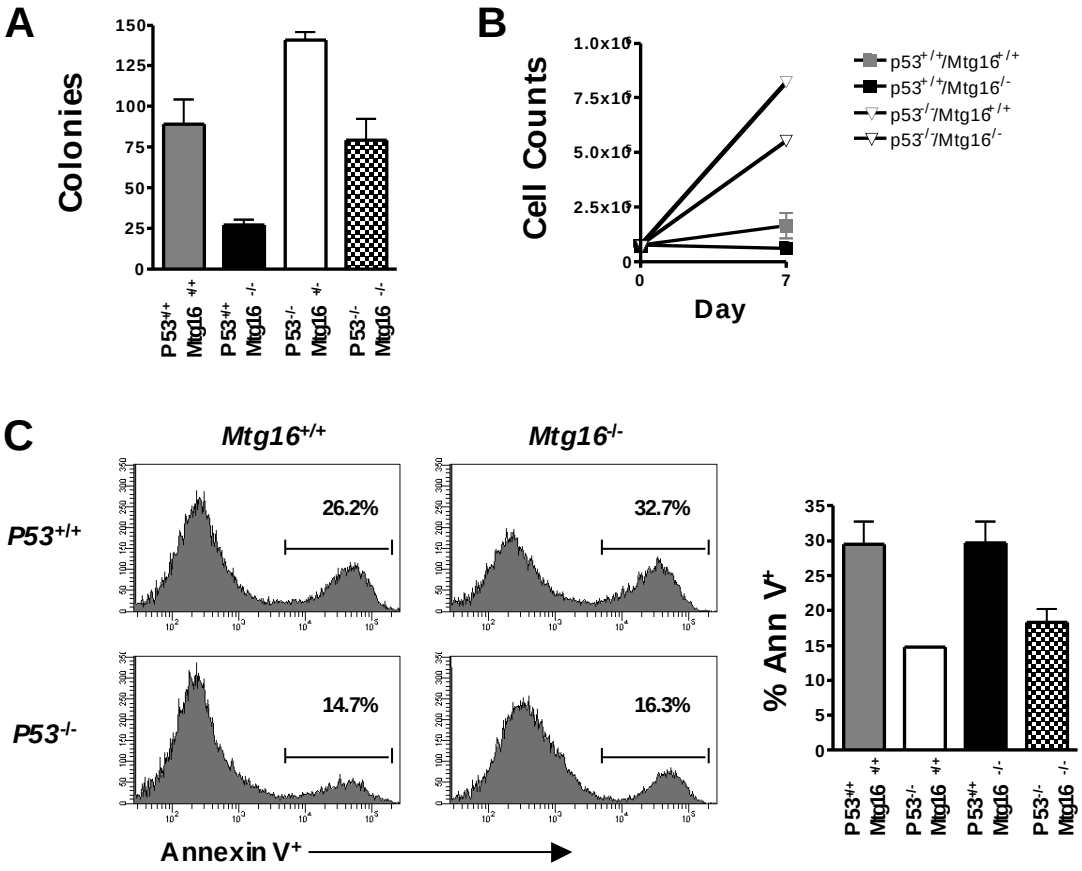

Figure 36. Deletion of *p53* rescues *Mtg16*$^{-/-}$Pre-B colony defects (A) Deletion of p53 rescues colony formation from *Mtg16*$^{-/-}$ bone marrow. Colony counts from one of two experiments. (B) Deletion of *p53* increases colony expansion by total plate cell counts at day 7. Growth curves from one of two experiments. (C) Representative flow cytometry plots from Annexin V staining of Day 7 M3630 colonies. Percent Annexin V^{+} depicted graphically with Mean $\pm$ SEM.

Mtg16 regulates gene expression in early B-cells

To further probe the important molecular functions of Mtg16 that contribute to initial B-cell commitment, we performed microarray analysis on wild type and *Mtg16*$^{-/-}$ B220^{+}CD43^{+}CD24^{-}BP-1^{-} Fraction A cells, or the earliest cells of the B-cell lineage. Many common Mtg16 targets were up regulated, such as *E2F2* and *Id2*, further confirming these as critical Mtg16-regulated genes (Table 5). Increased expression of *Id2* suggests that E-protein mediated transcription may be disrupted, not only by inactivation of Mtg16, but also by the inhibitory action of Id2, as over expression of Id2 disrupted early B-cell development[139].

Also up regulated in the absence of *Mtg16* were several genes that are myeloid specific, such as *myeloperoxidase*(*Mpo*) and *Itgam*, or *Mac1*, suggesting that Mtg16 is necessary to repress certain myeloid gene expression programs. Perhaps most interesting were the changes to cell growth and survival genes, including *Ccnb1* (*Cyclin B1*), which was one of the most affected targets, *Myc*, and *Bcl2*. Several Bcl6 regulated genes were up regulated, including *p21* and *Bcl6* itself, which was particularly interesting given that Bcl6 was more recently found to play a role in early B-cell survival[142].

Altered cell fate decisions in mature *Mtg16*$^{-/-}$ B-cells

Decreases in early B-cell development and lymphoid lineage commitment contribute to peripheral B-cell lymphopenia in *Mtg16*$^{-/-}$ mice, and the factors that we hypothesize contribute to this phenotype, such as Bcl6 and E2A, also regulate mature B-cell development and function in the periphery[148,149]. Therefore, we measured the

Gene	Fold Up
Cr1	15.0546
Gpr141	8.10952
Igkv1-135	7.89093
Pak1	7.32331
Igk-V1	7.23294
Igk-V38	6.40471
Igh-6	5.86083
Igj	5.74372
Gm1502	5.60583
Cd209e	5.29719
Aif1	4.69217
Cd22	4.67798
Gm1419	4.62944
L1cam	4.16947
Mpo	4.1433
Prg2	4.1095
Ighv1-26	3.97359
Igh	3.9466
S100a4	3.94629
S100a8	3.88452
Id2	3.6943
Itgam	3.59454
Ms4a6c	3.36885
Bub1	3.35946
Ngp	3.32772
Kif4	3.31904
Cep55	3.27842
Hist1h2ab	3.2562
Ccnb1	3.24209
Ccnb1	3.23768
Lyzs	3.22142
Dlg2	3.1883
Cenpf	3.14759
Klrb1b	3.12343
Gcnt2	3.10256
Ccnb1	3.08589
Cd33	3.04808
Ifi205	3.01973
Nuf2	3.01537
Klrc1	2.99321
Ifitm6	2.99203
Kif11	2.98547
Shcbp1	2.97952
S100a9	2.96921
Anln	2.95091
Prr11	2.93143

Gene	Fold Up
Gria2	2.9309
Ttk	2.91325
Kif23	2.90409
Igh	2.8012
Bub1b	2.78061
Kif15	2.77385
Ltf	2.75469
Hmmr	2.74494
Hist1h2bp	2.73435
Cenpe	2.73145
Dlg7	2.72742
E2f8	2.72085
Tpcn1	2.71236
Ncr1	2.69831
Hist1h2bp	2.69452
Nusap1	2.66856
Top2a	2.66453
Il18r1	2.64612
Hist1h1b	2.64262
Dock5	2.64109
Ccna2	2.63405
Neil3	2.62119
Gins1	2.61712
Fgl2	2.60991
Cdc2a	2.60284
Hist1h2bp	2.60204
Hist1h2bp	2.60032
Atp8b4	2.59693
Rad51	2.5957
Cd226	2.58117
Clnk	2.57677
Tpx2	2.56645
Aspm	2.54819
Prc1	2.54376
Rragd	2.53425
Rrm2	2.49046
Klrb1a	2.4893
Hist1h4d	2.48205
Gpr114	2.48108
Mmp8	2.46807
Hist1h2bp	2.45619
Hist1h2bm	2.44754
Bcl6	2.44529
Kif14	2.43266
Stil	2.43239
Smc2	2.43106

Gene	Fold Up
Sema4a	2.41242
Il18rap	2.40897
Cdca8	2.40572
Bex6	2.40161
Ncaph	2.39734
Cdc25c	2.39351
Sgol2	2.38841
Heyl	2.38139
Hist1h4b	2.37739
Hist2h3b	2.37717
Kpna2	2.37333
Il2rb	2.37319
Tcrg-C	2.37175
St3gal5	2.36695
Plk1	2.35971
Clspn	2.34205
Kpna2	2.33474
C79407	2.33175
Hist1h3c	2.32775
Hist1h3g	2.32771
Chi3l3	2.32336
Itgax	2.3126
Pmch	2.30101
Kit	2.29783
Txk	2.29456
Retnlg	2.29145
Kpna2	2.29132
4930547N16Rik	2.28981
Depdc1a	2.28786
Klri2	2.28614
Esco2	2.28515
Il13ra1	2.28251
Hist2h3b	2.27719
Cenpk	2.27714
Hist1h3h	2.27343
Cd9	2.27204
BC023892	2.26806
Cdca2	2.26617
A630038E17Rik	2.26349
Tpst2	2.25039
Prelid2	2.2486
Mphosph1	2.24747
Hist1h4b	2.24698
Thy1	2.24379

Gene	Fold Up
Hpgd	2.24264
Raph1	2.23768
Casc5	2.23734
Tacc3	2.23509
Hist1h4m	2.23493
Hist1h4m	2.23493
Ndc80	2.22828
Hist1h3i	2.22681
Ercc6l	2.22626
Hist1h4f	2.22599
Klrk1	2.22214
Cdca3	2.22059
Myc	2.2149
Igh	2.21131
Ccnb2	2.20654
Ect2	2.20418
Pole	2.20309
Anxa1	2.19709
Spc25	2.19568
Arhgap19	2.17976
Klrc2	2.16977
Sh2d1b1	2.16963
Cd63	2.16806
Lcn2	2.16468
Ncapd2	2.16292
Birc5	2.15974
Flna	2.15967
Hist1h4k	2.15796
Hist1h2ak	2.15769
Eomes	2.15314
Ncapg2	2.14858
Hist2h3b	2.14653
Tm6sf1	2.13862
Chek1	2.13556
Pbk	2.13445
Met	2.134
Mns1	2.13274
Pola1	2.12703
Camp	2.12386
Ms4a4b	2.12372
Btla	2.12323
Klre1	2.12134
Sytl2	2.12115
Kif2c	2.11767
Plk4	2.11593
Klrc3	2.11436

Gene	Fold Up
Sgol1	2.11313
Klrb1f	2.11104
Sh2d1a	2.10961
Rrm1	2.10901
Hist1h3i	2.10795
Kntc1	2.10562
Muc13	2.10098
Wdhd1	2.09614
Ccnf	2.09401
Lig1	2.08915
Hist1h4c	2.08658
H2afx	2.0834
Hells	2.07949
Hist1h4f	2.07052
Sytl3	2.06833
Depdc1a	2.06458
Ifngr1	2.05918
Trip13	2.05391
Sass6	2.05286
Incenp	2.03849
Diap3	2.03716
Serpinb1a	2.03042
Brca1	2.02661
E2f2	2.02484
Arsb	2.02255
Cd200r1	2.02098
Cks2	2.01914
Zap70	2.01764
Nkg7	2.01749
Ube2c	2.01616
Cpd	2.01479
Emb	2.01414
Itga2	2.01213
Ccr2	2.0064
Prkar2a	2.0059
Spag5	2.00533
Fignl1	2.00406
Aurkb	2.00228
Ppbp	2.00192
Cit	1.99881
Ccnd2	1.99319
Hist1h2bh	1.99247
Dusp6	1.9904
Prkcq	1.98576
Cd96	1.98481
Igk-V21-4	1.98226

Gene	Fold Up
Ckap2	1.98132
Fbxo5	1.97828
Lcp2	1.97586
Pde3b	1.97359
Pitpnc1	1.97087
Klra3	1.97002
Melk	1.96999
Cenpi	1.96765
Kif18a	1.96763
Lrrk2	1.9649
Fcgr3	1.96454
Klf12	1.96224
Cenph	1.96175
Dennd4a	1.95688
D2Ertd750e	1.94424
Bcl2	1.9422
Mastl	1.9421
Cfp	1.94155
Pglyrp1	1.93921
Aoah	1.93797
Gramd3	1.93765
S100a10	1.93715
Skap1	1.93418
Cd84	1.93254
Bcl2a1c	1.93246
Klrg1	1.93021
2810457I06Rik	1.92948
Klri1	1.92794
Car2	1.92274
Myo1f	1.92225
Cdkn1a	1.92202
Gm1524	1.91773
Osbpl3	1.91349
Cks2	1.90978
Tuba1b	1.90351
Ptpn7	1.9009
Mylc2pl	1.90044

distribution of B-cell populations in mature splenocytes in wild type and *Mtg16*$^{-/-}$ mice. As B-cells exit the bone marrow and travel to the spleen, they arrive as immature transitional T_1 B-cells[144]. These cells gain the expression of IgD and the ability to recirculate and become T_2 transitional cells. T_2 cells then make a cell-fate decision that is regulated by Notch signaling and E-proteins, choosing between a marginal zone and a follicular zone fate[146]. Marginal zone cells function in innate immune responses and remain in the spleen throughout their lifespan, undergoing self-renewal but not entering the circulation. On the other hand, follicular zone cells are re-circulating B-cells that are the critical mediators of the adaptive immune response.

In the absence of *Mtg16*, more splenic B-cells adopt a marginal zone fate (Fig. 37). All B-cell populations in the *Mtg16*$^{-/-}$ spleen are decreased as a percentage of total splenocytes, except for marginal zone cells. In fact, there are equivalent or slightly elevated numbers of marginal zone B-cells in the absence of *Mtg16*. This is not surprising given the roles for Mtg16 in both Notch signaling and E-protein mediated transcription and the consistent up regulation of *Id2* in multiple hematopoietic populations, a protein whose expressions favors the marginal zone fate[148,149,188]. Interestingly, follicular populations are not correspondingly decreased as a proportion of total B-cells (Fig. 37, lower panel). Collectively these data suggest that decreases in mature B-cells in the spleen and the peripheral lymphopenia are exacerbated due to cell fate choices towards non-circulating marginal zone B-cells.

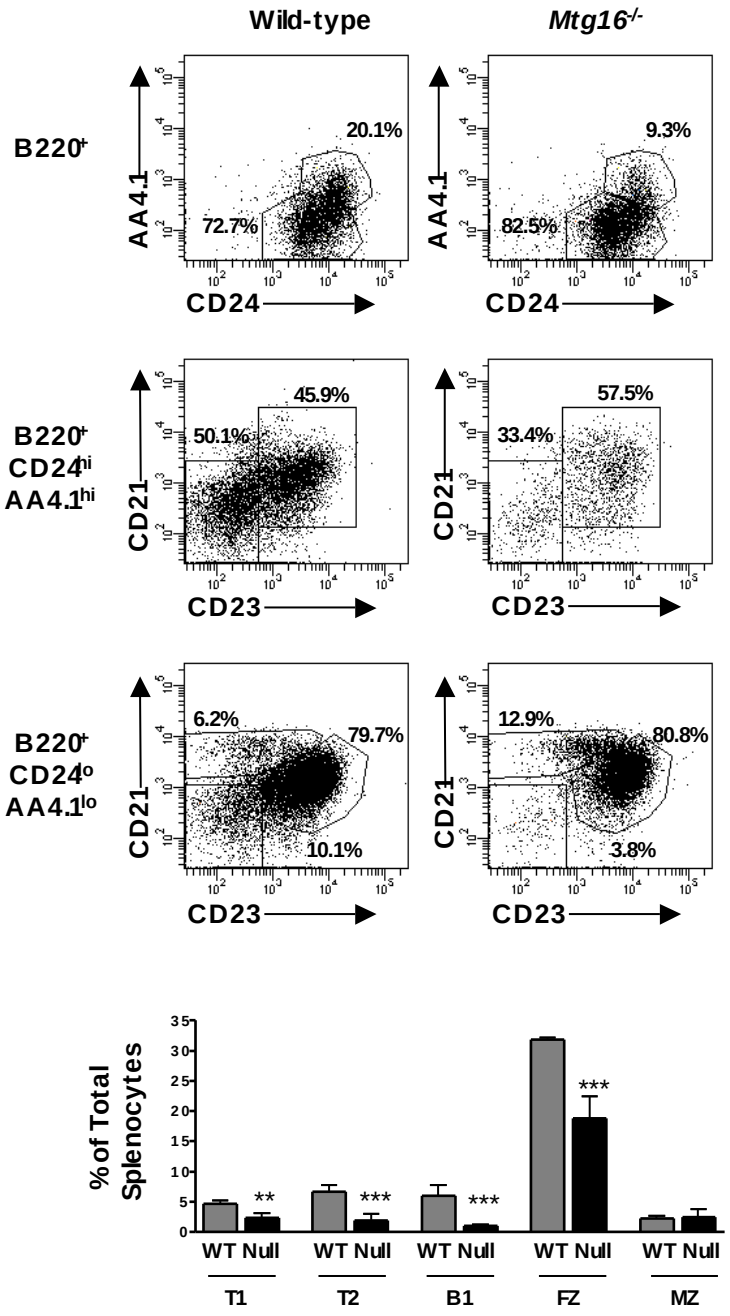

Figure 37. Altered lineage allocation of *Mtg16*$^{-/-}$ splenic B-cells Representative flow cytometry plots depicting populations of B220^{+} B-cells in the spleen. B220^{+} cells were divided into Immature CD24^{hi}AA4.1^{hi} and mature CD24^{lo}AA4.1^{lo} populations. Middle plots depict Immature cells and are divided into T1 CD21^{hi}CD23^{hi} and T2 CD21^{lo}CD23^{lo} cells. Lower plots depict mature cells divided into B1 CD21^{lo}CD23^{lo}, Follicular CD21^{hi}CD23^{hi} and Marginal Zone CD21^{hi}CD23^{lo} populations. Graph shows the percent of total splenocytes from one of two experiments for a total N=7. **p<0.01, ***p<0.001

Defective response to LPS following *In Vitro* stimulation of *Mtg16*$^{-/-}$ B-cells

Given the decrease in peripheral B-cells, we next assessed mature B-cell function as the decrease in cell number could have effects on immune function. To investigate the capacity for *Mtg16*$^{-/-}$ mice to respond to infection, we first began with *in vitro* mitogen response assays using LPS stimulation. Total splenic populations were responsive to LPS at higher levels in *Mtg16*$^{-/-}$ samples (Fig. 38A). This response may primarily reflect the increased proportion of Gr1^{+}/Mac1^{+} cells in *Mtg16*$^{-/-}$ spleens, as macrophages respond robustly to LPS stimulation. Indeed, isolation of B220^{+} populations showed that *Mtg16*$^{-/-}$ B-cells failed to respond (Fig. 38B). This likely reflects a global impairment of *Mtg16*$^{-/-}$ cells to rapidly proliferate in response to stress, though other mechanisms are possible.

Decreased germinal center response in the absence of *Mtg16*

LPS stimulation *in vitro* provides a measure of the ability of cells to proliferate in response to a mitogen, which is a critical part of the immune response, but does not replicate an immune challenge. Therefore, we performed *in vivo* germinal center assays. Bcl6 is a critical determinant of the germinal center reaction, and forms a complex with Mtg family members and Hdac3 to repress the DNA damage response in activated B-cells that are undergoing somatic hypermutation and antibody class-switch recombination. Both *Bcl6*$^{-/-}$ and *Hdac3*$^{-/-}$ mice have defects in germinal center formation. Wild-type and *Mtg16*$^{-/-}$ mice were injected with PBS, Alum, and 4-Hydroxy-3-nitrophenylacetyl Chicken gamma globulin (NP(59)-CGG) supplemented with Alum to

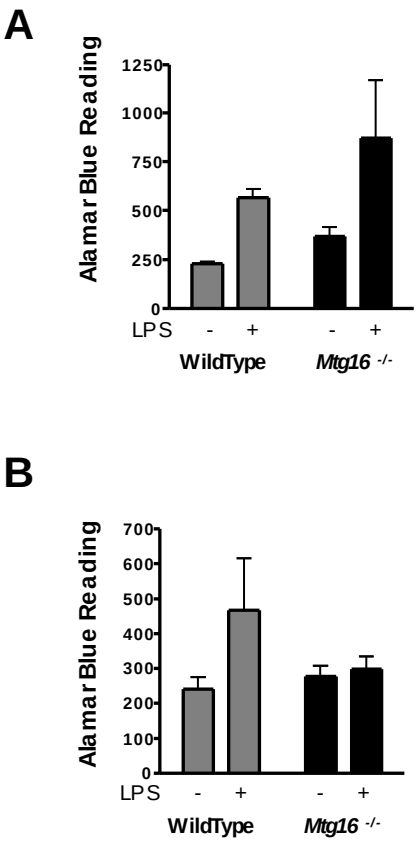

Figure 38. Defective *in vitro* LPS response from *Mtg16*$^{-/-}$ splenic B-cells
(A) Alamar blue cell viability readings from wild-type and *Mtg16*$^{-/-}$ total spleen cells after 72 hours of culture untreated or stimulated with LPS. Mean $\pm$ SD from one of two experiments for a total N=6. (B) Alamar blue cell viability readings from wild-type and *Mtg16*$^{-/-}$ B220^{+} splenocytes after 72 hours of culture untreated or stimulated with LPS. Mean $\pm$ SD from one of two experiments for a total N=6.

and stained with Peanut Agglutinin to visualize activated germinal centers. In the absence of *Mtg16*, there were decreased total follicular B-cells in the spleen, providing fewer cells capable of mounting a reaction (Fig. 39). The B-cells that were present did not contribute to the immune response in this context, as germinal centers were dramatically decreased after injection of NP-CGG + alum (Fig. 39). Decreased proliferative capacity may contribute to this phenotype, and this hypothesis is under further investigation. Ultimately, Mtg16 plays a crucial role in the development of immature B-cells as well as the function of mature splenic B-cells, likely through the interaction with both E-proteins and Bcl6.

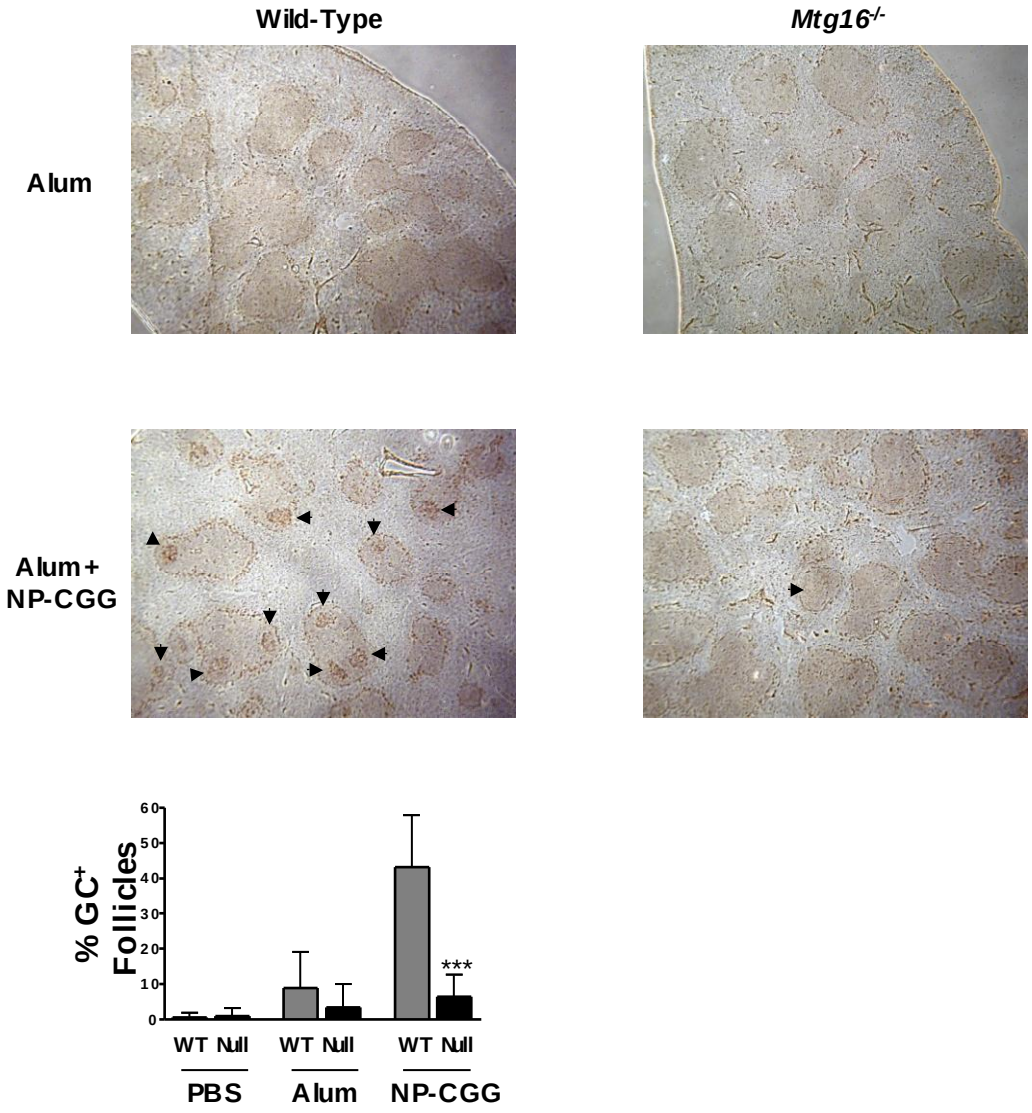

Figure 39. Decreased germinal center response after immunization in the absence of *Mtg16* Representative pictures of total spleen sections from wild-type or *Mtg16*$^{-/-}$ mice injected with Alum or Alum + NP-(CGG) stained with Peanut Agglutinin to identify germinal centers. Positive germinal centers denoted by arrow head. 2x magnification. Germinal centers were quantified manually and graphed as a percent of total follicles. Data from three experiments with a total NP-CGG injected of N=9 for wild-type and N=10 for *Mtg16*$^{-/-}$***p<0.001

Discussion

Mtg16 has been identified as the critical myeloid translocation gene family member in hematopoiesis, as it is the most highly expressed family member and the only family member to exhibit hematopoietic defects in knock-out mouse models[19,47,48]. Much like other targets of chromosomal translocations that produce leukemia, Mtg16 functions across hematopoiesis and serves as a master regulator of lineage commitment and survival. Previous studies have shown defects in *Mtg16*$^{-/-}$ hematopoietic cell development and lineage allocation, particularly in myeloid versus lymphoid cell fate decisions. Here, we show that B-cell development was impaired in the absence of *Mtg16* and this impairment led to lymphopenia (Fig. 28). This defect was more severe after stress, such as bone marrow transplant or in *in vitro* differentiation assays, and *Mtg16*$^{-/-}$ B-cells have deficits in growth and survival *in vitro* (Fig. 29, 33, 34). In addition to impaired development of maturing B-cells, *Mtg16*$^{-/-}$ mice displayed immune function defects, including decreased proliferation in response to a mitogen and a defect in germinal center reactions (Fig. 38, 39). Collectively, these data suggest that Mtg16 is a critical regulator of not only immature B-cell development, but also mature immune function.

Decreases to early B-cells are not surprising, given that immature progenitor cells with lymphoid potential, namely LMPP cells (Chapter III) and CLP cells (Fig. 32), are consistently decreased in the absence of *Mtg16*. Microarray analysis of early B-cell progenitors showed increased expression of myeloid specific genes such as *Itgam* and *MPO*. In T-cell specific assays, myeloid development occurred at the expense of lymphoid development, and *Mtg16*$^{-/-}$ stem cells preferentially gave rise to Gr1^{+}/Mac1^{+}

cells after competitive bone marrow transplant (Fig. 29). Very little myeloid development can occur in the context of IL7-containing methylcellulose and these assays do not directly test the potential of sorted stem cell populations, but instead reflect the decrease in total progenitor cells with B-cell potential from *Mtg16*$^{-/-}$ bone marrow. Nonetheless, increased myeloid commitment and decreased lymphoid commitment contributed to the loss of B-cells in the absence of *Mtg16*.

Much like the phenotype seen in T-cell development, the phenotypes shown here are also likely related to disruption of the bHLH E-protein family. While expression of E-proteins such as E2A are not disrupted in early *Mtg16*$^{-/-}$ B-cells, *Id2* expression was increased. Id2 functions as a negative regulator of E-proteins, and its expression impairs the ability of E2A to function in early B-cell specification[224]. Furthermore, over-expression of *Id2* leads to increased marginal zone commitment, a phenotype seen in the absence of *Mtg16* as well[149]. *Id2* expression is regulated by E2A and Gfi1, which are both binding partners of Mtg16. Moreover, *Gfi1*$^{-/-}$ mice have increased expression of *Id2* across several hematopoietic populations, much like *Mtg16*$^{-/-}$ mice. Deletion of one allele of *Id2* rescued B-cell development from *Gfi1*$^{-/-}$ mice, and it is possible that it would have similar effects in the context of *Mtg16*[285].

One of the most striking phenotypes seen in the *Mtg16*$^{-/-}$ mouse is an impaired response to stress, such as the replication stress associated with rapid proliferation in *in vitro* assays. While *Mtg16*$^{-/-}$ mice are capable of making the necessary erythrocytes for survival, they cannot make any BFU-E colonies methylcellulose supplemented with erythropoietin[19]. Similarly, B-cell development occurred at a reduced rate in the absence of *Mtg16*, but was severely impaired in IL7-containing methylcellulose colony formation

assays. This defect was associated with a severe impairment in cell proliferation and survival (Fig. 34) that was alleviated by deletion of *p53* (Fig. 36). Data is accumulating that suggests MTGs are necessary for appropriate cell cycle control, cell survival, and DNA damage control, potentially through indirect transcriptional effects or potentially from a to-be-determined direct role in cell cycle progression.

The work shown here is the first report of Mtg16 functioning in mature immune responses. Inactivation of *Mtg16* led to a significant lymphopenia, and we hypothesized that decreases to peripheral lymphocytes caused impaired immune function. The two-fold decrease in splenic B-cells was unlikely to cause a significant decrease in germinal center response, though, and it is possible that Mtg16 plays a direct role in the germinal center. The loss of a germinal center reaction in the absence of both *Bcl6* and *Hdac3,* suggests that at least three of the components of the Bcl6-Mtg-NCoR-Hdac3 complex are necessary for germinal centers to form. Bcl6 is capable of interacting with several different co-repressors, but it appears that the NCoR/SMRT interaction is primarily responsible for repression of DNA damage targets such as $p53^{156}$. Future work will focus on locating Mtg16 at Bcl6-regulated promoters in the spleen and identifying direct targets of Mtg16-dependent repression. *CDKN1A* (*p21*) is an attractive target, as it is up regulated in early $Mtg16^{-/-}$ B-cells and repression of *p21* is an important function for Bcl6 in the germinal center.

CHAPTER V

DISCUSSION

Myeloid translocation genes are uniquely situated as transcriptional corepressors to regulate multiple different transcription factors that are critical for hematopoiesis. As such, they can act as master regulators of growth and development, integrating signals into transcriptional programs that define cell fate and growth/survival. Previous work had defined roles for Mtg16 in regulating transcription in erythropoiesis and stem cell homeostasis and, for the first time, we have shown that Mtg16 regulates transcription in the context of lymphoid development. Therefore, much like other targets of chromosomal translocations that lead to leukemia, Mtg16 is an important modulator of hematopoiesis including and beyond the myeloid progenitor population that results from leukemic transformation.

In the absence of *Mtg16* both B- and T-cell development are perturbed. Given that B- and T-cell development diverge beyond the LMPP population and rely upon different combinations of transcription factors to facilitate lineage commitment, we divided our analysis into two parts. It is likely, though, that changes to early lymphoid commitment up to and including the LMPP population affect B- and T-cell development equivalently. Therefore, the work in Chapter III that suggests increased myeloid commitment in the absence of *Mtg16* also affects our interpretation of the data in Chapter

IV. Single-cell lineage potential assays, where sorted single cells are cultured in the presence of IL7, Flt3L, and SCF to support both myeloid and lymphoid commitment would help address the possibility that *Mtg16*$^{-/-}$ LT-HSCs or LMPP cells have increased myeloid and decreased lymphoid potential[51]. Ultimately, gene expression analysis of LMPP cells at the single cell level would define the relative percentage of myeloid and lymphoid primed cells and the relative percentage of priming within a given cell[59]. Given that myeloid lineage genes are upregulated in early B-cells and *Mtg16*$^{-/-}$ cells have increased myeloid capacity after transplant, I hypothesize that more *Mtg16*$^{-/-}$ LMPP cells will be strictly myeloid primed.

In Chapter III, we show that Mtg16 can regulate T-cell development and does so by interacting with both the Notch intracellular domain and E2A, two factors that are known to intersect in critical regulation steps for T-cell development. While previous data suggested that Notch and E-proteins regulate many of the same targets, this is the first work that shows that they share a common interacting partner that facilitates their ability to regulate T-cell development[9]. While NICD and E-protein interaction are necessary functions for Mtg16 in regulating T-cell development, Mtg16 is capable of interacting with other factors that play important roles in T-cell development, namely Gfi1, and the list of Mtg16-interacting factors continues to expand[26,98]. Given that Mtg16 can interact with Gata factors such as Gata1 in erythroid and megakaryocyte development, it is interesting to hypothesize that it can also interact with Gata3 and regulate that T-cell specific factor, though no such interaction has been previously demonstrated[32]. Nonetheless, Mtg16 potentially serves as a master regulator of early T-cell development through the NICD, E-proteins, and Gfi1.

In addition to regulating early T-cell development, Mtg16 can affect both early and late B-cell development and function. In Chapter IV, we show that the role of Mtg16 in early B-cell development is twofold: one, regulating early cell fate choices towards lymphoid lineages and the concurrent production of early B-cell progenitors, namely LMPP cells and CLP cells and two, regulating the growth and survival of early $B220^{+}$ cells under the stress conditions of *in vitro* differentiation assays. Mtg16 also regulates the expansion and survival of immature T-cells in culture, adding further evidence to the hypothesis that MTGs are important regulators of cell growth.

One question raised for ongoing analysis is how mechanistically MTGs are regulating cellular expansion. There are several hypotheses to be tested, and it is likely that they are inter-related and not mutually exclusive. The most obvious answer is that MTGs directly regulate the expression of specific genes that are involved in cell growth and survival, further supported by expression changes in genes such as *p21* and *Bcl2* in *Mtg16*$^{-/-}$ B-cells. This hypothesis has been difficult to test directly in B-cell assays, as *in vitro* complementation or rescue experiments cannot be performed in the context of the methylcellulose assay as the infection conditions disrupt development within this very sensitive experiment.

Therefore, our next step will be to attempt to generate pre-B cultures. These cultures allow expansion and development of B-cells through the full range of early B-cell populations. In the absence of both E2A and Bcl-6, two Mtg16 interacting proteins, pre-B cells cannot grow in culture without transformation by an oncogene such as v-Abl[142,207]. Even in the context of transformation, *E2A*$^{-/-}$ and *Bcl-6*$^{-/-}$ pre-B cultures have deficits in cell growth and survival. While *Mtg16*$^{-/-}$ pre-B colonies are generated in

M3630 methylcellulose, they exhibit many of these same growth and survival defects. Therefore, while we do not anticipate needing to transform early B-cells to facilitate culture initiation, we do anticipate that *Mtg16*$^{-/-}$ pre-B cultures will exhibit growth defects. Complementation of these defects with retroviral reintroduction of Mtg16 will allow structure-function analysis and we anticipate that both E2A and Bcl6 will contribute to Mtg16 function in early B-cell survival.

Alternatively, it is becoming apparent that MTGs may function outside of the canonical role in transcriptional repression. For example, MTGs may regulate transcriptional elongation, most likely of specific genes involved in cell differentiation but potentially as part of a global phenomenon. We and others have data that shows MTGs are capable of binding components of the transcriptional elongation machinery, including MLL, Tif1γ, and Dot1L, and phenotypes generated by the loss of other components of the transcriptional elongation machinery match well with some *Mtg16*$^{-/-}$ phenotypes[286]. It is possible that by disrupting transcriptional elongation, loss of MTGs leads to stalled RNA Pol II, which stalls replication forks and increases DNA damage, producing cell cycle arrest and apoptosis. This idea is further supported by data from both Chapter IV and *Mtg8*$^{-/-}$ MEFs that show increases in DNA damage in the absence of MTGs.

Additionally, in Chapter IV we show for the first time an important role for Mtg16 in regulating the immune response, and specifically the germinal center response. Mtg16 interacts with Bcl6, a critical determinant of germinal center reactions, and, like Bcl6$^{-/-}$ mice, *Mtg16*$^{-/-}$ mice have drastically decreased germinal center formation[282,283]. This result was somewhat surprising given that Bcl6 interacts with several different

corepressors in regulating the germinal center reaction[156]. The impact of Mtg16 on germinal centers may be magnified due to its ability to regulate proliferation of splenic B-cells in response to a mitogen and its ability to interact with E2A, which also contributes to the germinal center response[137]. Repression of the p53 DNA damage response is an important mediator of Bcl6 function in germinal centers, and in the absence of Bcl6, increases to DNA damage lead to apoptosis and loss of germinal centers[151]. Given that deletion of p53 rescues in vitro methylcellulose colony formation from *Mtg16*$^{-/-}$ bone marrow, we hypothesize that it will also rescue formation of the germinal center response.

The interaction between Mtg16 and E-proteins is one of the most robust and reproducible interactions of Mtg family members, but prior to this work, a function for this interaction was unknown. Recent work by our group suggests that the interaction between Mtg16 and E-proteins is also an important component of stem cell regulation. *E2A*$^{-/-}$ mice have decreased stem cell self-renewal, a phenotype that matches closely with the loss of *Mtg16*[208,209]. Both phenotypes result from increased cell cycle entry, and Mtg16 binds to an E2A binding site in the first intron of E2F2, potentially providing a target for repression. The E2A binding site in E2F2 was identified as positively regulated in early B-cells but it is possible that in the context of LT-HSCs that need to restrict cell cycle entry, E2A functions as a repressor for this specific gene[121]. Alternatively, Mtg16 can negatively regulate E2A activation targets as a mechanism for more precise modulation of E2A mediated gene expression. The F210A mutant generated in Chapter III fails to reconstitute *Mtg16*$^{-/-}$ cell function in not only the CFU-S assay, but also in stem cell self-renewal assays such as the LTC-IC assay (Fischer et al, in prep).

Therefore, the Mtg16-E-protein interaction is important for T-cell development, hematopoietic stem cell function, and potentially B-cell function as well.

MTGs were first discovered for their role in chromosomal translocations that lead to Acute Myeloid Leukemia. In attempting to better understand how these translocations lead to leukemia, we and other groups have created knock-out mouse models for each of the three family members. Initial hypotheses theorized that Mtg8 would serve a critical role in regulating hematopoiesis, as this is the family member that is most frequently disrupted with the AML1-ETO fusion protein translocation. Surprisingly, *Mtg8*$^{-/-}$ mice have no discernable hematopoietic phenotypes[45]. Instead, Mtg16 appears to be the critical family member for regulating hematopoiesis. Not only is it the most highly expressed, but it also has the most severe hematopoietic phenotypes[19,47]. These phenotypes overlap with some of the phenotypes found with over-expression of the AML1-ETO fusion protein, including increased granulocyte/monocyte skewing and impaired lymphoid development[257,258]. Both AML1-ETO and Mtg16 regulate cell growth and survival, though the effect of *Mtg16* deletion on cell cycle status appears to be population specific[238].

Dimerization with other Mtg family members is a critical function of the AML1-ETO fusion protein[236]. When combined with the emerging role for Mtg16 in hematopoiesis, this fact suggests that disruption of Mtg16 by the fusion protein, effectively creating *Mtg16*$^{-/-}$ hematopoietic cells, is a significant mechanism of action for the AML1-ETO fusion protein. In fact, previous work has shown that the fusion protein acts in part by disrupting the ability of Mtg16 to interact with NCoR and our own group has shown that the fusion protein is capable of activating transcription by certain factors

primarily by titrating away repressors such as NCoR[237] (Moore in revision). This information leads to a new model for AML1-ETO mediated disruption of transcription (Fig. 40). In this model, the fusion protein tethers ETO to Runx1 targets, recruiting other MTG family members to repress Runx1 transcription (Fig. 40B). In addition, AML1-ETO de-represses MTG targets, potentially by titrating away NCoR and other corepressors from MTGs bound at their appropriate promoters (Fig. 40C). Alternatively, AML1-ETO may disrupt the ability of Mtg16 to bind target transcription factors, effectively creating an *Mtg16*$^{-/-}$ cell (Fig. 40D). In the absence of normal Mtg16 function, differentiation patterns are disrupted, with loss of lymphoid lineages and skewing towards myeloid development. DNA damage increases, by a to-be-determined mechanism, and cell cycle kinetics are disrupted, common features in *Mtg16*$^{-/-}$ populations identified here. Ultimately, in the presence of a second hit mutation, leukemia develops.

Future studies addressing the localization of Mtg16 on chromatin in the presence of the fusion protein will be very useful in addressing this hypothesis. Does Mtg16 travel to Runx1 targets as a dimerization partner of AML1-ETO, removing it from endogenous targets? Does the presence of the fusion protein impair the ability of Mtg16 to interact with other binding partners, namely transcription factors such as E2A? We have very preliminary results to suggest that expression of AML1-ETO may impair the ability of Mtg16 to repress E-protein mediated transcription, though the effect is subtle by luciferase assay. Finally, work is currently underway to determine if loss of *Mtg16* itself is sufficient to predispose cells to transformation. The incidence of *Mtg16* mutations in other cancers would suggest that such a phenomenon is likely.

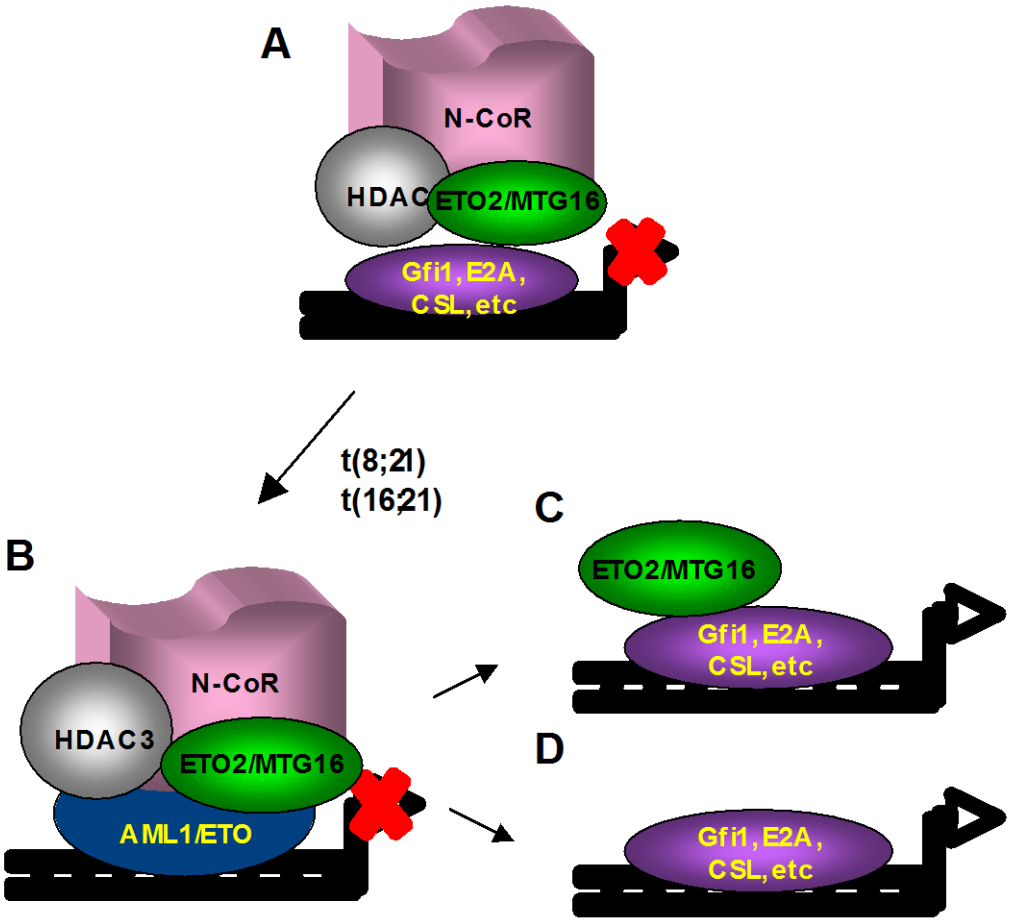

Figure 40. A Model for AML1-ETO mediated disruption of transcription (A) Endogenous MTG family members function as transcriptional corepressors bound to DNA-binding transcription factors and corepressors such as NCoR. (B) Expression of the AML1-ETO fusion protein represses Runx1 targets that are otherwise activated. (C) The AML1-ETO fusion protein disrupts the ability of Mtg16 to interact with NCoR, potentially de-repressing Mtg16 targets. (D) Alternatively, the fusion protein may remove Mtg16 from promoters, effectively creating a *Mtg16*$^{-/-}$ cell.

REFERENCES

1. Ernst P, Wang J, Korsmeyer SJ. The role of MLL in hematopoiesis and leukemia. Curr Opin Hematol. 2002;9:282-287.

2. Fenrick R, Hiebert SW. Role of histone deacetylases in acute leukemia. J Cell Biochem Suppl. 1998;30-31:194-202.

3. Begley CG, Aplan PD, Davey MP, et al. Chromosomal translocation in a human leukemic stem-cell line disrupts the T-cell antigen receptor delta-chain diversity region and results in a previously unreported fusion transcript. Proc Natl Acad Sci U S A. 1989;86:2031-2035.

4. Erickson P, Gao J, Chang KS, et al. Identification of breakpoints in t(8;21) acute myelogenous leukemia and isolation of a fusion transcript, AML1/ETO, with similarity to Drosophila segmentation gene, runt. Blood. 1992;80:1825-1831.

5. Golub TR, Barker GF, Bohlander SK, et al. Fusion of the TEL gene on 12p13 to the AML1 gene on 21q22 in acute lymphoblastic leukemia. Proc Natl Acad Sci U S A. 1995;92:4917-4921.

6. Inaba T, Roberts WM, Shapiro LH, et al. Fusion of the leucine zipper gene HLF to the E2A gene in human acute B-lineage leukemia. Science. 1992;257:531-534.

7. Baron BW, Nucifora G, McCabe N, Espinosa R, 3rd, Le Beau MM, McKeithan TW. Identification of the gene associated with the recurring chromosomal translocations t(3;14)(q27;q32) and t(3;22)(q27;q11) in B-cell lymphomas. Proc Natl Acad Sci U S A. 1993;90:5262-5266.

8. Ellisen LW, Bird J, West DC, et al. TAN-1, the human homolog of the Drosophila notch gene, is broken by chromosomal translocations in T lymphoblastic neoplasms. Cell. 1991;66:649-661.

9. Ikawa T, Kawamoto H, Goldrath AW, Murre C. E proteins and Notch signaling cooperate to promote T cell lineage specification and commitment. J Exp Med. 2006;203:1329-1342.

10. Osada H, Grutz G, Axelson H, Forster A, Rabbitts TH. Association of erythroid transcription factors: complexes involving the LIM protein RBTN2 and the zinc-finger protein GATA1. Proc Natl Acad Sci U S A. 1995;92:9585-9589.

11. Miyoshi H, Kozu T, Shimizu K, et al. The t(8;21) translocation in acute myeloid leukemia results in production of an AML1-MTG8 fusion transcript. Embo J. 1993;12:2715-2721.

12. Gamou T, Kitamura E, Hosoda F, et al. The partner gene of AML1 in t(16;21) myeloid malignancies is a novel member of the MTG8(ETO) family. Blood. 1998;91:4028-4037.

13. Fracchiolla NS, Colombo G, Finelli P, Maiolo AT, Neri A. EHT, a new member of the MTG8/ETO gene family, maps on 20q11 region and is deleted in acute myeloid leukemias. Blood. 1998;92:3481-3484.

14. Kitabayashi I, Ida K, Morohoshi F, et al. The AML1-MTG8 leukemic fusion protein forms a complex with a novel member of the MTG8(ETO/CDR) family, MTGR1. Mol Cell Biol. 1998;18:846-858.

15. Sjoblom T, Jones S, Wood LD, et al. The consensus coding sequences of human breast and colorectal cancers. Science. 2006;314:268-274.

16. Wood LD, Parsons DW, Jones S, et al. The genomic landscapes of human breast and colorectal cancers. Science. 2007;318:1108-1113.

17. Kan Z, Jaiswal BS, Stinson J, et al. Diverse somatic mutation patterns and pathway alterations in human cancers. Nature;466:869-873.

18. Kochetkova M, McKenzie OL, Bais AJ, et al. CBFA2T3 (MTG16) is a putative breast tumor suppressor gene from the breast cancer loss of heterozygosity region at 16q24.3. Cancer Res. 2002;62:4599-4604.

19. Chyla BJ, Moreno-Miralles I, Steapleton MA, et al. Deletion of Mtg16, a target of t(16;21), alters hematopoietic progenitor cell proliferation and lineage allocation. Mol Cell Biol. 2008;28:6234-6247.

20. Amann JM, Nip J, Strom DK, et al. ETO, a target of t(8;21) in acute leukemia, makes distinct contacts with multiple histone deacetylases and binds mSin3A through its oligomerization domain. Mol Cell Biol. 2001;21:6470-6483.

21. Gelmetti V, Zhang J, Fanelli M, Minucci S, Pelicci PG, Lazar MA. Aberrant recruitment of the nuclear receptor corepressor-histone deacetylase complex by the acute myeloid leukemia fusion partner ETO. Mol Cell Biol. 1998;18:7185-7191.

22. Hildebrand D, Tiefenbach J, Heinzel T, Grez M, Maurer AB. Multiple regions of ETO cooperate in transcriptional repression. J Biol Chem. 2001;276:9889-9895.

23. Lutterbach B, Westendorf JJ, Linggi B, et al. ETO, a target of t(8;21) in acute leukemia, interacts with the N-CoR and mSin3 corepressors. Mol Cell Biol. 1998;18:7176-7184.

24. Wang J, Hoshino T, Redner RL, Kajigaya S, Liu JM. ETO, fusion partner in t(8;21) acute myeloid leukemia, represses transcription by interaction with the human N-CoR/mSin3/HDAC1 complex. Proc Natl Acad Sci U S A. 1998;95:10860-10865.

25. Chevallier N, Corcoran CM, Lennon C, et al. ETO protein of t(8;21) AML is a corepressor for Bcl-6 B-cell lymphoma oncoprotein. Blood. 2004;103:1454-1463.

26. McGhee L, Bryan J, Elliott L, et al. Gfi-1 attaches to the nuclear matrix, associates with ETO (MTG8) and histone deacetylase proteins, and represses transcription using a TSA-sensitive mechanism. J Cell Biochem. 2003;89:1005-1018.

27. Melnick AM, Westendorf JJ, Polinger A, et al. The ETO protein disrupted in t(8;21)-associated acute myeloid leukemia is a corepressor for the promyelocytic leukemia zinc finger protein. Mol Cell Biol. 2000;20:2075-2086.

28. Moore AC, Amann JM, Williams CS, et al. Myeloid translocation gene family members associate with T-cell factors (TCFs) and influence TCF-dependent transcription. Mol Cell Biol. 2008;28:977-987.

29. Salat D, Liefke R, Wiedenmann J, Borggrefe T, Oswald F. ETO, but not leukemogenic fusion protein AML1/ETO, augments RBP-Jkappa/SHARP-mediated repression of notch target genes. Mol Cell Biol. 2008;28:3502-3512.

30. Schuh AH, Tipping AJ, Clark AJ, et al. ETO-2 associates with SCL in erythroid cells and megakaryocytes and provides repressor functions in erythropoiesis. Mol Cell Biol. 2005;25:10235-10250.

31. Zhang J, Kalkum M, Yamamura S, Chait BT, Roeder RG. E protein silencing by the leukemogenic AML1-ETO fusion protein. Science. 2004;305:1286-1289.

32. Hamlett I, Draper J, Strouboulis J, Iborra F, Porcher C, Vyas P. Characterization of megakaryocyte GATA1-interacting proteins: the corepressor ETO2 and GATA1 interact to regulate terminal megakaryocyte maturation. Blood. 2008;112:2738-2749.

33. Amann JM, Chyla BJ, Ellis TC, et al. Mtgr1 is a transcriptional corepressor that is required for maintenance of the secretory cell lineage in the small intestine. Mol Cell Biol. 2005;25:9576-9585.

34. Martinez JA, Williams CS, Amann JM, et al. Deletion of Mtgr1 sensitizes the colonic epithelium to dextran sodium sulfate-induced colitis. Gastroenterology. 2006;131:579-588.

35. Aaker JD, Patineau AL, Yang HJ, et al. Feedback regulation of NEUROG2 activity by MTGR1 is required for progression of neurogenesis. Mol Cell Neurosci. 2009;42:267-277.

36. Koyano-Nakagawa N, Kintner C. The expression and function of MTG/ETO family proteins during neurogenesis. Dev Biol. 2005;278:22-34.

37. Aaker JD, Patineau AL, Yang HJ, et al. Interaction of MTG family proteins with NEUROG2 and ASCL1 in the developing nervous system. Neurosci Lett;474:46-51.

38. Davis JN, McGhee L, Meyers S. The ETO (MTG8) gene family. Gene. 2003;303:1-10.

39. Erickson PF, Robinson M, Owens G, Drabkin HA. The ETO portion of acute myeloid leukemia t(8;21) fusion transcript encodes a highly evolutionarily conserved, putative transcription factor. Cancer Res. 1994;54:1782-1786.

40. Lutterbach B, Sun D, Schuetz J, Hiebert SW. The MYND motif is required for repression of basal transcription from the multidrug resistance 1 promoter by the t(8;21) fusion protein. Mol Cell Biol. 1998;18:3604-3611.

41. Zhang J, Hug BA, Huang EY, et al. Oligomerization of ETO is obligatory for corepressor interaction. Mol Cell Biol. 2001;21:156-163.

42. Fukuyama T, Sueoka E, Sugio Y, et al. MTG8 proto-oncoprotein interacts with the regulatory subunit of type II cyclic AMP-dependent protein kinase in lymphocytes. Oncogene. 2001;20:6225-6232.

43. Engel ME, Nguyen HN, Mariotti J, Hunt A, Hiebert SW. Myeloid translocation gene 16 (MTG16) interacts with Notch transcription complex components to integrate Notch signaling in hematopoietic cell fate specification. Mol Cell Biol;30:1852-1863.

44. Wang J, Saunthararajah Y, Redner RL, Liu JM. Inhibitors of histone deacetylase relieve ETO-mediated repression and induce differentiation of AML1-ETO leukemia cells. Cancer Res. 1999;59:2766-2769.

45. Calabi F, Pannell R, Pavloska G. Gene targeting reveals a crucial role for MTG8 in the gut. Mol Cell Biol. 2001;21:5658-5666.

46. Morohoshi F, Mitani S, Mitsuhashi N, et al. Structure and expression pattern of a human MTG8/ETO family gene, MTGR1. Gene. 2000;241:287-295.

47. Lindberg SR, Olsson A, Persson AM, Olsson I. The Leukemia-associated ETO homologues are differently expressed during hematopoietic differentiation. Exp Hematol. 2005;33:189-198.

48. Okumura AJ, Peterson LF, Lo MC, Zhang DE. Expression of AML/Runx and ETO/MTG family members during hematopoietic differentiation of embryonic stem cells. Exp Hematol. 2007;35:978-988.

49. Reya T, Morrison SJ, Clarke MF, Weissman IL. Stem cells, cancer, and cancer stem cells. Nature. 2001;414:105-111.

50. Orkin SH, Zon LI. Hematopoiesis: an evolving paradigm for stem cell biology. Cell. 2008;132:631-644.

51. Adolfsson J, Mansson R, Buza-Vidas N, et al. Identification of Flt3+ lympho-myeloid stem cells lacking erythro-megakaryocytic potential a revised road map for adult blood lineage commitment. Cell. 2005;121:295-306.

52. Adolfsson J, Borge OJ, Bryder D, et al. Upregulation of Flt3 expression within the bone marrow Lin(-)Sca1(+)c-kit(+) stem cell compartment is accompanied by loss of self-renewal capacity. Immunity. 2001;15:659-669.

53. Luc S, Buza-Vidas N, Jacobsen SE. Delineating the cellular pathways of hematopoietic lineage commitment. Semin Immunol. 2008;20:213-220.

54. Ceredig R, Rolink AG, Brown G. Models of haematopoiesis: seeing the wood for the trees. Nat Rev Immunol. 2009;9:293-300.

55. Purton LE, Scadden DT. Limiting factors in murine hematopoietic stem cell assays. Cell Stem Cell. 2007;1:263-270.

56. Benveniste P, Frelin C, Janmohamed S, et al. Intermediate-term hematopoietic stem cells with extended but time-limited reconstitution potential. Cell Stem Cell;6:48-58.

57. Challen GA, Boles N, Lin KK, Goodell MA. Mouse hematopoietic stem cell identification and analysis. Cytometry A. 2009;75:14-24.

58. Akashi K, Traver D, Miyamoto T, Weissman IL. A clonogenic common myeloid progenitor that gives rise to all myeloid lineages. Nature. 2000;404:193-197.

59. Mansson R, Hultquist A, Luc S, et al. Molecular evidence for hierarchical transcriptional lineage priming in fetal and adult stem cells and multipotent progenitors. Immunity. 2007;26:407-419.

60. Li LX, Goetz CA, Katerndahl CD, Sakaguchi N, Farrar MA. A Flt3- and Ras-dependent pathway primes B cell development by inducing a state of IL-7 responsiveness. J Immunol;184:1728-1736.

61. Sitnicka E, Bryder D, Theilgaard-Monch K, Buza-Vidas N, Adolfsson J, Jacobsen SE. Key role of flt3 ligand in regulation of the common lymphoid progenitor but not in maintenance of the hematopoietic stem cell pool. Immunity. 2002;17:463-472.

62. Kondo M, Weissman IL, Akashi K. Identification of clonogenic common lymphoid progenitors in mouse bone marrow. Cell. 1997;91:661-672.

63. Schwarz BA, Bhandoola A. Circulating hematopoietic progenitors with T lineage potential. Nat Immunol. 2004;5:953-960.

64. Schwarz BA, Sambandam A, Maillard I, Harman BC, Love PE, Bhandoola A. Selective thymus settling regulated by cytokine and chemokine receptors. J Immunol. 2007;178:2008-2017.

65. Lai AY, Kondo M. Identification of a bone marrow precursor of the earliest thymocytes in adult mouse. Proc Natl Acad Sci U S A. 2007;104:6311-6316.

66. Allman D, Sambandam A, Kim S, et al. Thymopoiesis independent of common lymphoid progenitors. Nat Immunol. 2003;4:168-174.

67. Benz C, Martins VC, Radtke F, Bleul CC. The stream of precursors that colonizes the thymus proceeds selectively through the early T lineage precursor stage of T cell development. J Exp Med. 2008;205:1187-1199.

68. Peschon JJ, Morrissey PJ, Grabstein KH, et al. Early lymphocyte expansion is severely impaired in interleukin 7 receptor-deficient mice. J Exp Med. 1994;180:1955-1960.

69. von Freeden-Jeffry U, Vieira P, Lucian LA, McNeil T, Burdach SE, Murray R. Lymphopenia in interleukin (IL)-7 gene-deleted mice identifies IL-7 as a nonredundant cytokine. J Exp Med. 1995;181:1519-1526.

70. Miller JP, Izon D, DeMuth W, Gerstein R, Bhandoola A, Allman D. The earliest step in B lineage differentiation from common lymphoid progenitors is critically dependent upon interleukin 7. J Exp Med. 2002;196:705-711.

71. Carvalho TL, Mota-Santos T, Cumano A, Demengeot J, Vieira P. Arrested B lymphopoiesis and persistence of activated B cells in adult interleukin 7(-/)- mice. J Exp Med. 2001;194:1141-1150.

72. Taghon TN, David ES, Zuniga-Pflucker JC, Rothenberg EV. Delayed, asynchronous, and reversible T-lineage specification induced by Notch/Delta signaling. Genes Dev. 2005;19:965-978.

73. Kondo M, Akashi K, Domen J, Sugamura K, Weissman IL. Bcl-2 rescues T lymphopoiesis, but not B or NK cell development, in common gamma chain-deficient mice. Immunity. 1997;7:155-162.

74. Schmitt TM, Zuniga-Pflucker JC. Induction of T cell development from hematopoietic progenitor cells by delta-like-1 in vitro. Immunity. 2002;17:749-756.

75. Sitnicka E, Brakebusch C, Martensson IL, et al. Complementary signaling through flt3 and interleukin-7 receptor alpha is indispensable for fetal and adult B cell genesis. J Exp Med. 2003;198:1495-1506.

76. Mombaerts P, Iacomini J, Johnson RS, Herrup K, Tonegawa S, Papaioannou VE. RAG-1-deficient mice have no mature B and T lymphocytes. Cell. 1992;68:869-877.

77. Shinkai Y, Rathbun G, Lam KP, et al. RAG-2-deficient mice lack mature lymphocytes owing to inability to initiate V(D)J rearrangement. Cell. 1992;68:855-867.

78. Jung D, Alt FW. Unraveling V(D)J recombination; insights into gene regulation. Cell. 2004;116:299-311.

79. Igarashi H, Gregory SC, Yokota T, Sakaguchi N, Kincade PW. Transcription from the RAG1 locus marks the earliest lymphocyte progenitors in bone marrow. Immunity. 2002;17:117-130.

80. Sambandam A, Maillard I, Zediak VP, et al. Notch signaling controls the generation and differentiation of early T lineage progenitors. Nat Immunol. 2005;6:663-670.

81. Radtke F, Wilson A, Stark G, et al. Deficient T cell fate specification in mice with an induced inactivation of Notch1. Immunity. 1999;10:547-558.

82. Godfrey DI, Kennedy J, Suda T, Zlotnik A. A developmental pathway involving four phenotypically and functionally distinct subsets of CD3-CD4-CD8- triple-negative adult mouse thymocytes defined by CD44 and CD25 expression. J Immunol. 1993;150:4244-4252.

83. Porritt HE, Rumfelt LL, Tabrizifard S, Schmitt TM, Zuniga-Pflucker JC, Petrie HT. Heterogeneity among DN1 prothymocytes reveals multiple progenitors with different capacities to generate T cell and non-T cell lineages. Immunity. 2004;20:735-745.

84. Bell JJ, Bhandoola A. The earliest thymic progenitors for T cells possess myeloid lineage potential. Nature. 2008;452:764-767.

85. Wada H, Masuda K, Satoh R, et al. Adult T-cell progenitors retain myeloid potential. Nature. 2008;452:768-772.

86. Shen HQ, Lu M, Ikawa T, et al. T/NK bipotent progenitors in the thymus retain the potential to generate dendritic cells. J Immunol. 2003;171:3401-3406.

87. Ikawa T, Kawamoto H, Fujimoto S, Katsura Y. Commitment of common T/Natural killer (NK) progenitors to unipotent T and NK progenitors in the murine fetal thymus revealed by a single progenitor assay. J Exp Med. 1999;190:1617-1626.

88. Masuda K, Kakugawa K, Nakayama T, Minato N, Katsura Y, Kawamoto H. T cell lineage determination precedes the initiation of TCR beta gene rearrangement. J Immunol. 2007;179:3699-3706.

89. Tabrizifard S, Olaru A, Plotkin J, Fallahi-Sichani M, Livak F, Petrie HT. Analysis of transcription factor expression during discrete stages of postnatal thymocyte differentiation. J Immunol. 2004;173:1094-1102.

90. Mombaerts P, Clarke AR, Rudnicki MA, et al. Mutations in T-cell antigen receptor genes alpha and beta block thymocyte development at different stages. Nature. 1992;360:225-231.

91. Saint-Ruf C, Ungewiss K, Groettrup M, Bruno L, Fehling HJ, von Boehmer H. Analysis and expression of a cloned pre-T cell receptor gene. Science. 1994;266:1208-1212.

92. Godfrey DI, Kennedy J, Mombaerts P, Tonegawa S, Zlotnik A. Onset of TCR-beta gene rearrangement and role of TCR-beta expression during CD3-CD4-CD8-thymocyte differentiation. J Immunol. 1994;152:4783-4792.

93. Dudley EC, Petrie HT, Shah LM, Owen MJ, Hayday AC. T cell receptor beta chain gene rearrangement and selection during thymocyte development in adult mice. Immunity. 1994;1:83-93.

94. Nossal GJ. Negative selection of lymphocytes. Cell. 1994;76:229-239.

95. Guidos CJ. Positive selection of CD4+ and CD8+ T cells. Curr Opin Immunol. 1996;8:225-232.

96. Laiosa CV, Stadtfeld M, Graf T. Determinants of lymphoid-myeloid lineage diversification. Annu Rev Immunol. 2006;24:705-738.

97. Bain G, Engel I, Robanus Maandag EC, et al. E2A deficiency leads to abnormalities in alphabeta T-cell development and to rapid development of T-cell lymphomas. Mol Cell Biol. 1997;17:4782-4791.

98. Yucel R, Karsunky H, Klein-Hitpass L, Moroy T. The transcriptional repressor Gfi1 affects development of early, uncommitted c-Kit+ T cell progenitors and CD4/CD8 lineage decision in the thymus. J Exp Med. 2003;197:831-844.

99. Taghon T, Yui MA, Rothenberg EV. Mast cell lineage diversion of T lineage precursors by the essential T cell transcription factor GATA-3. Nat Immunol. 2007;8:845-855.

100. Ting CN, Olson MC, Barton KP, Leiden JM. Transcription factor GATA-3 is required for development of the T-cell lineage. Nature. 1996;384:474-478.

101. Hendriks RW, Nawijn MC, Engel JD, van Doorninck H, Grosveld F, Karis A. Expression of the transcription factor GATA-3 is required for the development of the earliest T cell progenitors and correlates with stages of cellular proliferation in the thymus. Eur J Immunol. 1999;29:1912-1918.

102. Ichikawa M, Asai T, Saito T, et al. AML-1 is required for megakaryocytic maturation and lymphocytic differentiation, but not for maintenance of hematopoietic stem cells in adult hematopoiesis. Nat Med. 2004;10:299-304.

103. Growney JD, Shigematsu H, Li Z, et al. Loss of Runx1 perturbs adult hematopoiesis and is associated with a myeloproliferative phenotype. Blood. 2005;106:494-504.

104. Anderson MK, Weiss AH, Hernandez-Hoyos G, Dionne CJ, Rothenberg EV. Constitutive expression of PU.1 in fetal hematopoietic progenitors blocks T cell development at the pro-T cell stage. Immunity. 2002;16:285-296.

105. Gonzalez-Garcia S, Garcia-Peydro M, Martin-Gayo E, et al. CSL-MAML-dependent Notch1 signaling controls T lineage-specific IL-7R{alpha} gene expression in early human thymopoiesis and leukemia. J Exp Med. 2009;206:779-791.

106. Yamamoto M, Ko LJ, Leonard MW, Beug H, Orkin SH, Engel JD. Activity and tissue-specific expression of the transcription factor NF-E1 multigene family. Genes Dev. 1990;4:1650-1662.

107. Pandolfi PP, Roth ME, Karis A, et al. Targeted disruption of the GATA3 gene causes severe abnormalities in the nervous system and in fetal liver haematopoiesis. Nat Genet. 1995;11:40-44.

108. Hosoya T, Kuroha T, Moriguchi T, et al. GATA-3 is required for early T lineage progenitor development. J Exp Med. 2009;206:2987-3000.

109. Pai SY, Truitt ML, Ting CN, Leiden JM, Glimcher LH, Ho IC. Critical roles for transcription factor GATA-3 in thymocyte development. Immunity. 2003;19:863-875.

110. Okuda T, van Deursen J, Hiebert SW, Grosveld G, Downing JR. AML1, the target of multiple chromosomal translocations in human leukemia, is essential for normal fetal liver hematopoiesis. Cell. 1996;84:321-330.

111. Wang Q, Stacy T, Binder M, Marin-Padilla M, Sharpe AH, Speck NA. Disruption of the Cbfa2 gene causes necrosis and hemorrhaging in the central nervous system and blocks definitive hematopoiesis. Proc Natl Acad Sci U S A. 1996;93:3444-3449.

112. Miyoshi H, Shimizu K, Kozu T, Maseki N, Kaneko Y, Ohki M. t(8;21) breakpoints on chromosome 21 in acute myeloid leukemia are clustered within a limited region of a single gene, AML1. Proc Natl Acad Sci U S A. 1991;88:10431-10434.

113. Taniuchi I, Osato M, Egawa T, et al. Differential requirements for Runx proteins in CD4 repression and epigenetic silencing during T lymphocyte development. Cell. 2002;111:621-633.

114. Huang G, Zhang P, Hirai H, et al. PU.1 is a major downstream target of AML1 (RUNX1) in adult mouse hematopoiesis. Nat Genet. 2008;40:51-60.

115. Scott EW, Simon MC, Anastasi J, Singh H. Requirement of transcription factor PU.1 in the development of multiple hematopoietic lineages. Science. 1994;265:1573-1577.

116. McKercher SR, Torbett BE, Anderson KL, et al. Targeted disruption of the PU.1 gene results in multiple hematopoietic abnormalities. Embo J. 1996;15:5647-5658.

117. Anderson MK, Hernandez-Hoyos G, Diamond RA, Rothenberg EV. Precise developmental regulation of Ets family transcription factors during specification and commitment to the T cell lineage. Development. 1999;126:3131-3148.

118. Laiosa CV, Stadtfeld M, Xie H, de Andres-Aguayo L, Graf T. Reprogramming of committed T cell progenitors to macrophages and dendritic cells by C/EBP alpha and PU.1 transcription factors. Immunity. 2006;25:731-744.

119. Jepsen K, Hermanson O, Onami TM, et al. Combinatorial roles of the nuclear receptor corepressor in transcription and development. Cell. 2000;102:753-763.

120. Hardy RR, Hayakawa K. B cell development pathways. Annu Rev Immunol. 2001;19:595-621.

121. Lin YC, Jhunjhunwala S, Benner C, et al. A global network of transcription factors, involving E2A, EBF1 and Foxo1, that orchestrates B cell fate. Nat Immunol;11:635-643.

122. Kee BL, Murre C. Induction of early B cell factor (EBF) and multiple B lineage genes by the basic helix-loop-helix transcription factor E12. J Exp Med. 1998;188:699-713.

123. Bhalla S, Spaulding C, Brumbaugh RL, et al. differential roles for the E2A activation domains in B lymphocytes and macrophages. J Immunol. 2008;180:1694-1703.

124. Pongubala JM, Northrup DL, Lancki DW, et al. Transcription factor EBF restricts alternative lineage options and promotes B cell fate commitment independently of Pax5. Nat Immunol. 2008;9:203-215.

125. Nutt SL, Heavey B, Rolink AG, Busslinger M. Commitment to the B-lymphoid lineage depends on the transcription factor Pax5. Nature. 1999;401:556-562.

126. Rolink A, Nutt S, Busslinger M, et al. Differentiation, dedifferentiation, and redifferentiation of B-lineage lymphocytes: roles of the surrogate light chain and the Pax5 gene. Cold Spring Harb Symp Quant Biol. 1999;64:21-25.

127. Zhang Z, Cotta CV, Stephan RP, deGuzman CG, Klug CA. Enforced expression of EBF in hematopoietic stem cells restricts lymphopoiesis to the B cell lineage. Embo J. 2003;22:4759-4769.

128. Sigvardsson M, O'Riordan M, Grosschedl R. EBF and E47 collaborate to induce expression of the endogenous immunoglobulin surrogate light chain genes. Immunity. 1997;7:25-36.

129. O'Riordan M, Grosschedl R. Coordinate regulation of B cell differentiation by the transcription factors EBF and E2A. Immunity. 1999;11:21-31.

130. Zhuang Y, Jackson A, Pan L, Shen K, Dai M. Regulation of E2A gene expression in B-lymphocyte development. Mol Immunol. 2004;40:1165-1177.

131. Fuxa M, Skok J, Souabni A, Salvagiotto G, Roldan E, Busslinger M. Pax5 induces V-to-DJ rearrangements and locus contraction of the immunoglobulin heavy-chain gene. Genes Dev. 2004;18:411-422.

132. Roessler S, Gyory I, Imhof S, et al. Distinct promoters mediate the regulation of Ebf1 gene expression by interleukin-7 and Pax5. Mol Cell Biol. 2007;27:579-594.

133. Kikuchi K, Lai AY, Hsu CL, Kondo M. IL-7 receptor signaling is necessary for stage transition in adult B cell development through up-regulation of EBF. J Exp Med. 2005;201:1197-1203.

134. Smith EM, Gisler R, Sigvardsson M. Cloning and characterization of a promoter flanking the early B cell factor (EBF) gene indicates roles for E-proteins and autoregulation in the control of EBF expression. J Immunol. 2002;169:261-270.

135. Dias S, Silva H, Jr., Cumano A, Vieira P. Interleukin-7 is necessary to maintain the B cell potential in common lymphoid progenitors. J Exp Med. 2005;201:971-979.

136. Seet CS, Brumbaugh RL, Kee BL. Early B cell factor promotes B lymphopoiesis with reduced interleukin 7 responsiveness in the absence of E2A. J Exp Med. 2004;199:1689-1700.

137. Kwon K, Hutter C, Sun Q, et al. Instructive role of the transcription factor E2A in early B lymphopoiesis and germinal center B cell development. Immunity. 2008;28:751-762.

138. Lin H, Grosschedl R. Failure of B-cell differentiation in mice lacking the transcription factor EBF. Nature. 1995;376:263-267.

139. Thal MA, Carvalho TL, He T, et al. Ebf1-mediated down-regulation of Id2 and Id3 is essential for specification of the B cell lineage. Proc Natl Acad Sci U S A. 2009;106:552-557.

140. Cobaleda C, Schebesta A, Delogu A, Busslinger M. Pax5: the guardian of B cell identity and function. Nat Immunol. 2007;8:463-470.

141. Mikkola I, Heavey B, Horcher M, Busslinger M. Reversion of B cell commitment upon loss of Pax5 expression. Science. 2002;297:110-113.

142. Duy C, Yu JJ, Nahar R, et al. BCL6 is critical for the development of a diverse primary B cell repertoire. J Exp Med;207:1209-1221.

143. Fujita N, Jaye DL, Geigerman C, et al. MTA3 and the Mi-2/NuRD complex regulate cell fate during B lymphocyte differentiation. Cell. 2004;119:75-86.

144. Allman D, Lindsley RC, DeMuth W, Rudd K, Shinton SA, Hardy RR. Resolution of three nonproliferative immature splenic B cell subsets reveals multiple selection points during peripheral B cell maturation. J Immunol. 2001;167:6834-6840.

145. Oracki SA, Walker JA, Hibbs ML, Corcoran LM, Tarlinton DM. Plasma cell development and survival. Immunol Rev;237:140-159.

146. Hozumi K, Negishi N, Suzuki D, et al. Delta-like 1 is necessary for the generation of marginal zone B cells but not T cells in vivo. Nat Immunol. 2004;5:638-644.

147. Saito T, Chiba S, Ichikawa M, et al. Notch2 is preferentially expressed in mature B cells and indispensable for marginal zone B lineage development. Immunity. 2003;18:675-685.

148. Quong MW, Martensson A, Langerak AW, Rivera RR, Nemazee D, Murre C. Receptor editing and marginal zone B cell development are regulated by the helix-loop-helix protein, E2A. J Exp Med. 2004;199:1101-1112.

149. Becker-Herman S, Lantner F, Shachar I. Id2 negatively regulates B cell differentiation in the spleen. J Immunol. 2002;168:5507-5513.

150. Basso K, Dalla-Favera R. BCL6: master regulator of the germinal center reaction and key oncogene in B cell lymphomagenesis. Adv Immunol;105:193-210.

151. Phan RT, Dalla-Favera R. The BCL6 proto-oncogene suppresses p53 expression in germinal-centre B cells. Nature. 2004;432:635-639.

152. Ranuncolo SM, Polo JM, Dierov J, et al. Bcl-6 mediates the germinal center B cell phenotype and lymphomagenesis through transcriptional repression of the DNA-damage sensor ATR. Nat Immunol. 2007;8:705-714.

153. Ranuncolo SM, Wang L, Polo JM, et al. BCL6-mediated attenuation of DNA damage sensing triggers growth arrest and senescence through a p53-dependent pathway in a cell context-dependent manner. J Biol Chem. 2008;283:22565-22572.

154. Ranuncolo SM, Polo JM, Melnick A. BCL6 represses CHEK1 and suppresses DNA damage pathways in normal and malignant B-cells. Blood Cells Mol Dis. 2008;41:95-99.

155. Phan RT, Saito M, Basso K, Niu H, Dalla-Favera R. BCL6 interacts with the transcription factor Miz-1 to suppress the cyclin-dependent kinase inhibitor p21 and cell cycle arrest in germinal center B cells. Nat Immunol. 2005;6:1054-1060.

156. Parekh S, Polo JM, Shaknovich R, et al. BCL6 programs lymphoma cells for survival and differentiation through distinct biochemical mechanisms. Blood. 2007;110:2067-2074.

157. Tunyaplin C, Shaffer AL, Angelin-Duclos CD, Yu X, Staudt LM, Calame KL. Direct repression of prdm1 by Bcl-6 inhibits plasmacytic differentiation. J Immunol. 2004;173:1158-1165.

158. Bray SJ. Notch signalling: a simple pathway becomes complex. Nat Rev Mol Cell Biol. 2006;7:678-689.

159. Wallberg AE, Pedersen K, Lendahl U, Roeder RG. p300 and PCAF act cooperatively to mediate transcriptional activation from chromatin templates by notch intracellular domains in vitro. Mol Cell Biol. 2002;22:7812-7819.

160. Liu H, Chi AW, Arnett KL, et al. Notch dimerization is required for leukemogenesis and T-cell development. Genes Dev;24:2395-2407.

161. Tsunematsu R, Nakayama K, Oike Y, et al. Mouse Fbw7/Sel-10/Cdc4 is required for notch degradation during vascular development. J Biol Chem. 2004;279:9417-9423.

162. Fryer CJ, White JB, Jones KA. Mastermind recruits CycC:CDK8 to phosphorylate the Notch ICD and coordinate activation with turnover. Mol Cell. 2004;16:509-520.

163. Guarani V, Deflorian G, Franco CA, et al. Acetylation-dependent regulation of endothelial Notch signalling by the SIRT1 deacetylase. Nature;473:234-238.

164. Oswald F, Kostezka U, Astrahantseff K, et al. SHARP is a novel component of the Notch/RBP-Jkappa signalling pathway. Embo J. 2002;21:5417-5426.

165. Kao HY, Ordentlich P, Koyano-Nakagawa N, et al. A histone deacetylase corepressor complex regulates the Notch signal transduction pathway. Genes Dev. 1998;12:2269-2277.

166. Nagel AC, Krejci A, Tenin G, et al. Hairless-mediated repression of notch target genes requires the combined activity of Groucho and CtBP corepressors. Mol Cell Biol. 2005;25:10433-10441.

167. Bray S, Furriols M. Notch pathway: making sense of suppressor of hairless. Curr Biol. 2001;11:R217-221.

168. Alcalay M, Meani N, Gelmetti V, et al. Acute myeloid leukemia fusion proteins deregulate genes involved in stem cell maintenance and DNA repair. J Clin Invest. 2003;112:1751-1761.

169. Pui JC, Allman D, Xu L, et al. Notch1 expression in early lymphopoiesis influences B versus T lineage determination. Immunity. 1999;11:299-308.

170. Han H, Tanigaki K, Yamamoto N, et al. Inducible gene knockout of transcription factor recombination signal binding protein-J reveals its essential role in T versus B lineage decision. Int Immunol. 2002;14:637-645.

171. Wilson A, MacDonald HR, Radtke F. Notch 1-deficient common lymphoid precursors adopt a B cell fate in the thymus. J Exp Med. 2001;194:1003-1012.

172. Tanigaki K, Tsuji M, Yamamoto N, et al. Regulation of alphabeta/gammadelta T cell lineage commitment and peripheral T cell responses by Notch/RBP-J signaling. Immunity. 2004;20:611-622.

173. Wolfer A, Wilson A, Nemir M, MacDonald HR, Radtke F. Inactivation of Notch1 impairs VDJbeta rearrangement and allows pre-TCR-independent survival of early alpha beta Lineage Thymocytes. Immunity. 2002;16:869-879.

174. Garbe AI, Krueger A, Gounari F, Zuniga-Pflucker JC, von Boehmer H. Differential synergy of Notch and T cell receptor signaling determines alphabeta versus gammadelta lineage fate. J Exp Med. 2006;203:1579-1590.

175. Hasserjian RP, Aster JC, Davi F, Weinberg DS, Sklar J. Modulated expression of notch1 during thymocyte development. Blood. 1996;88:970-976.

176. Huang EY, Gallegos AM, Richards SM, Lehar SM, Bevan MJ. Surface expression of Notch1 on thymocytes: correlation with the double-negative to double-positive transition. J Immunol. 2003;171:2296-2304.

177. Tsuji M, Shinkura R, Kuroda K, Yabe D, Honjo T. Msx2-interacting nuclear target protein (Mint) deficiency reveals negative regulation of early thymocyte differentiation by Notch/RBP-J signaling. Proc Natl Acad Sci U S A. 2007;104:1610-1615.

178. Aster JC, Pear WS, Blacklow SC. Notch signaling in leukemia. Annu Rev Pathol. 2008;3:587-613.

179. Weng AP, Ferrando AA, Lee W, et al. Activating mutations of NOTCH1 in human T cell acute lymphoblastic leukemia. Science. 2004;306:269-271.

180. Pear WS, Aster JC, Scott ML, et al. Exclusive development of T cell neoplasms in mice transplanted with bone marrow expressing activated Notch alleles. J Exp Med. 1996;183:2283-2291.

181. Bellavia D, Campese AF, Alesse E, et al. Constitutive activation of NF-kappaB and T-cell leukemia/lymphoma in Notch3 transgenic mice. Embo J. 2000;19:3337-3348.

182. Rohn JL, Lauring AS, Linenberger ML, Overbaugh J. Transduction of Notch2 in feline leukemia virus-induced thymic lymphoma. J Virol. 1996;70:8071-8080.

183. Chiang MY, Xu L, Shestova O, et al. Leukemia-associated NOTCH1 alleles are weak tumor initiators but accelerate K-ras-initiated leukemia. J Clin Invest. 2008;118:3181-3194.

184. Kunisato A, Chiba S, Nakagami-Yamaguchi E, et al. HES-1 preserves purified hematopoietic stem cells ex vivo and accumulates side population cells in vivo. Blood. 2003;101:1777-1783.

185. Stier S, Cheng T, Dombkowski D, Carlesso N, Scadden DT. Notch1 activation increases hematopoietic stem cell self-renewal in vivo and favors lymphoid over myeloid lineage outcome. Blood. 2002;99:2369-2378.

186. Maillard I, Koch U, Dumortier A, et al. Canonical notch signaling is dispensable for the maintenance of adult hematopoietic stem cells. Cell Stem Cell. 2008;2:356-366.

187. Mercher T, Cornejo MG, Sears C, et al. Notch signaling specifies megakaryocyte development from hematopoietic stem cells. Cell Stem Cell. 2008;3:314-326.

188. Tanigaki K, Han H, Yamamoto N, et al. Notch-RBP-J signaling is involved in cell fate determination of marginal zone B cells. Nat Immunol. 2002;3:443-450.

189. Bain G, Maandag EC, Izon DJ, et al. E2A proteins are required for proper B cell development and initiation of immunoglobulin gene rearrangements. Cell. 1994;79:885-892.

190. Voronova AF, Lee F. The E2A and tal-1 helix-loop-helix proteins associate in vivo and are modulated by Id proteins during interleukin 6-induced myeloid differentiation. Proc Natl Acad Sci U S A. 1994;91:5952-5956.

191. Miyamoto A, Cui X, Naumovski L, Cleary ML. Helix-loop-helix proteins LYL1 and E2a form heterodimeric complexes with distinctive DNA-binding properties in hematolymphoid cells. Mol Cell Biol. 1996;16:2394-2401.

192. Murre C, McCaw PS, Vaessin H, et al. Interactions between heterologous helix-loop-helix proteins generate complexes that bind specifically to a common DNA sequence. Cell. 1989;58:537-544.

193. Massari ME, Jennings PA, Murre C. The AD1 transactivation domain of E2A contains a highly conserved helix which is required for its activity in both Saccharomyces cerevisiae and mammalian cells. Mol Cell Biol. 1996;16:121-129.

194. Quong MW, Massari ME, Zwart R, Murre C. A new transcriptional-activation motif restricted to a class of helix-loop-helix proteins is functionally conserved in both yeast and mammalian cells. Mol Cell Biol. 1993;13:792-800.

195. Benezra R, Davis RL, Lockshon D, Turner DL, Weintraub H. The protein Id: a negative regulator of helix-loop-helix DNA binding proteins. Cell. 1990;61:49-59.

196. Sun XH, Copeland NG, Jenkins NA, Baltimore D. Id proteins Id1 and Id2 selectively inhibit DNA binding by one class of helix-loop-helix proteins. Mol Cell Biol. 1991;11:5603-5611.

197. Bain G, Quong MW, Soloff RS, Hedrick SM, Murre C. Thymocyte maturation is regulated by the activity of the helix-loop-helix protein, E47. J Exp Med. 1999;190:1605-1616.

198. Dias S, Mansson R, Gurbuxani S, Sigvardsson M, Kee BL. E2A proteins promote development of lymphoid-primed multipotent progenitors. Immunity. 2008;29:217-227.

199. Kee BL, Bain G, Murre C. IL-7Ralpha and E47: independent pathways required for development of multipotent lymphoid progenitors. Embo J. 2002;21:103-113.

200. Engel I, Johns C, Bain G, Rivera RR, Murre C. Early thymocyte development is regulated by modulation of E2A protein activity. J Exp Med. 2001;194:733-745.

201. Engel I, Murre C. E2A proteins enforce a proliferation checkpoint in developing thymocytes. Embo J. 2004;23:202-211.

202. Yashiro-Ohtani Y, He Y, Ohtani T, et al. Pre-TCR signaling inactivates Notch1 transcription by antagonizing E2A. Genes Dev. 2009;23:1665-1676.

203. Borghesi L, Aites J, Nelson S, Lefterov P, James P, Gerstein R. E47 is required for V(D)J recombinase activity in common lymphoid progenitors. J Exp Med. 2005;202:1669-1677.

204. Murre C, McCaw PS, Baltimore D. A new DNA binding and dimerization motif in immunoglobulin enhancer binding, daughterless, MyoD, and myc proteins. Cell. 1989;56:777-783.

205. Romanow WJ, Langerak AW, Goebel P, et al. E2A and EBF act in synergy with the V(D)J recombinase to generate a diverse immunoglobulin repertoire in nonlymphoid cells. Mol Cell. 2000;5:343-353.

206. Greenbaum S, Lazorchak AS, Zhuang Y. Differential functions for the transcription factor E2A in positive and negative gene regulation in pre-B lymphocytes. J Biol Chem. 2004;279:45028-45035.

207. Lazorchak AS, Wojciechowski J, Dai M, Zhuang Y. E2A promotes the survival of precursor and mature B lymphocytes. J Immunol. 2006;177:2495-2504.

208. Yang Q, Esplin B, Borghesi L. E47 regulates hematopoietic stem cell proliferation and energetics but not myeloid lineage restriction. Blood;117:3529-3538.

209. Yang Q, Kardava L, St Leger A, et al. E47 controls the developmental integrity and cell cycle quiescence of multipotential hematopoietic progenitors. J Immunol. 2008;181:5885-5894.

210. Barndt R, Dai MF, Zhuang Y. A novel role for HEB downstream or parallel to the pre-TCR signaling pathway during alpha beta thymopoiesis. J Immunol. 1999;163:3331-3343.

211. Sawada S, Littman DR. A heterodimer of HEB and an E12-related protein interacts with the CD4 enhancer and regulates its activity in T-cell lines. Mol Cell Biol. 1993;13:5620-5628.

212. Takeuchi A, Yamasaki S, Takase K, et al. E2A and HEB activate the pre-TCR alpha promoter during immature T cell development. J Immunol. 2001;167:2157-2163.

213. Wojciechowski J, Lai A, Kondo M, Zhuang Y. E2A and HEB are required to block thymocyte proliferation prior to pre-TCR expression. J Immunol. 2007;178:5717-5726.

214. Cisse B, Caton ML, Lehner M, et al. Transcription factor E2-2 is an essential and specific regulator of plasmacytoid dendritic cell development. Cell. 2008;135:37-48.

215. Zhuang Y, Cheng P, Weintraub H. B-lymphocyte development is regulated by the combined dosage of three basic helix-loop-helix genes, E2A, E2-2, and HEB. Mol Cell Biol. 1996;16:2898-2905.

216. Wikstrom I, Forssell J, Goncalves M, Colucci F, Holmberg D. E2-2 regulates the expansion of pro-B cells and follicular versus marginal zone decisions. J Immunol. 2006;177:6723-6729.

217. Wikstrom I, Forssell J, Penha-Goncalves MN, Bergqvist I, Holmberg D. A role for E2-2 at the DN3 stage of early thymopoiesis. Mol Immunol. 2008;45:3302-3311.

218. Cochrane SW, Zhao Y, Welner RS, Sun XH. Balance between Id and E proteins regulates myeloid-versus-lymphoid lineage decisions. Blood. 2009;113:1016-1026.

219. Leeanansaksiri W, Wang H, Gooya JM, et al. IL-3 induces inhibitor of DNA-binding protein-1 in hemopoietic progenitor cells and promotes myeloid cell development. J Immunol. 2005;174:7014-7021.

220. Kim D, Peng XC, Sun XH. Massive apoptosis of thymocytes in T-cell-deficient Id1 transgenic mice. Mol Cell Biol. 1999;19:8240-8253.

221. Sun XH. Constitutive expression of the Id1 gene impairs mouse B cell development. Cell. 1994;79:893-900.

222. Schotte R, Dontje W, Nagasawa M, et al. Synergy between IL-15 and Id2 promotes the expansion of human NK progenitor cells, which can be counteracted by the E protein HEB required to drive T cell development. J Immunol;184:6670-6679.

223. Morrow MA, Mayer EW, Perez CA, Adlam M, Siu G. Overexpression of the Helix-Loop-Helix protein Id2 blocks T cell development at multiple stages. Mol Immunol. 1999;36:491-503.

224. Ji M, Li H, Suh HC, Klarmann KD, Yokota Y, Keller JR. Id2 intrinsically regulates lymphoid and erythroid development via interaction with different target proteins. Blood. 2008;112:1068-1077.

225. Kee BL, Rivera RR, Murre C. Id3 inhibits B lymphocyte progenitor growth and survival in response to TGF-beta. Nat Immunol. 2001;2:242-247.

226. Goardon N, Lambert JA, Rodriguez P, et al. ETO2 coordinates cellular proliferation and differentiation during erythropoiesis. Embo J. 2006;25:357-366.

227. Hall MA, Curtis DJ, Metcalf D, et al. The critical regulator of embryonic hematopoiesis, SCL, is vital in the adult for megakaryopoiesis, erythropoiesis, and lineage choice in CFU-S12. Proc Natl Acad Sci U S A. 2003;100:992-997.

228. Mikkola HK, Klintman J, Yang H, et al. Haematopoietic stem cells retain long-term repopulating activity and multipotency in the absence of stem-cell leukaemia SCL/tal-1 gene. Nature. 2003;421:547-551.

229. Meyers S, Downing JR, Hiebert SW. Identification of AML-1 and the (8;21) translocation protein (AML-1/ETO) as sequence-specific DNA-binding proteins: the runt homology domain is required for DNA binding and protein-protein interactions. Mol Cell Biol. 1993;13:6336-6345.

230. Frank R, Zhang J, Uchida H, Meyers S, Hiebert SW, Nimer SD. The AML1/ETO fusion protein blocks transactivation of the GM-CSF promoter by AML1B. Oncogene. 1995;11:2667-2674.

231. Zhang DE, Hohaus S, Voso MT, et al. Function of PU.1 (Spi-1), C/EBP, and AML1 in early myelopoiesis: regulation of multiple myeloid CSF receptor promoters. Curr Top Microbiol Immunol. 1996;211:137-147.

232. Petrovick MS, Hiebert SW, Friedman AD, Hetherington CJ, Tenen DG, Zhang DE. Multiple functional domains of AML1: PU.1 and C/EBPalpha synergize with different regions of AML1. Mol Cell Biol. 1998;18:3915-3925.

233. Lutterbach B, Westendorf JJ, Linggi B, Isaac S, Seto E, Hiebert SW. A mechanism of repression by acute myeloid leukemia-1, the target of multiple chromosomal translocations in acute leukemia. J Biol Chem. 2000;275:651-656.

234. Durst KL, Lutterbach B, Kummalue T, Friedman AD, Hiebert SW. The inv(16) fusion protein associates with corepressors via a smooth muscle myosin heavy-chain domain. Mol Cell Biol. 2003;23:607-619.

235. Meyers S, Lenny N, Hiebert SW. The t(8;21) fusion protein interferes with AML-1B-dependent transcriptional activation. Mol Cell Biol. 1995;15:1974-1982.

236. Yan M, Ahn EY, Hiebert SW, Zhang DE. RUNX1/AML1 DNA-binding domain and ETO/MTG8 NHR2-dimerization domain are critical to AML1-ETO9a leukemogenesis. Blood. 2009;113:883-886.

237. Ibanez V, Sharma A, Buonamici S, et al. AML1-ETO decreases ETO-2 (MTG16) interactions with nuclear receptor corepressor, an effect that impairs granulocyte differentiation. Cancer Res. 2004;64:4547-4554.

238. Burel SA, Harakawa N, Zhou L, Pabst T, Tenen DG, Zhang DE. Dichotomy of AML1-ETO functions: growth arrest versus block of differentiation. Mol Cell Biol. 2001;21:5577-5590.

239. Rhoades KL, Hetherington CJ, Harakawa N, et al. Analysis of the role of AML1-ETO in leukemogenesis, using an inducible transgenic mouse model. Blood. 2000;96:2108-2115.

240. Westendorf JJ, Yamamoto CM, Lenny N, Downing JR, Selsted ME, Hiebert SW. The t(8;21) fusion product, AML-1-ETO, associates with C/EBP-alpha, inhibits C/EBP-alpha-dependent transcription, and blocks granulocytic differentiation. Mol Cell Biol. 1998;18:322-333.

241. Krejci O, Wunderlich M, Geiger H, et al. p53 signaling in response to increased DNA damage sensitizes AML1-ETO cells to stress-induced death. Blood. 2008;111:2190-2199.

242. Linggi B, Muller-Tidow C, van de Locht L, et al. The t(8;21) fusion protein, AML1 ETO, specifically represses the transcription of the p14(ARF) tumor suppressor in acute myeloid leukemia. Nat Med. 2002;8:743-750.

243. Yang G, Khalaf W, van de Locht L, et al. Transcriptional repression of the Neurofibromatosis-1 tumor suppressor by the t(8;21) fusion protein. Mol Cell Biol. 2005;25:5869-5879.

244. Zhang DE, Hetherington CJ, Meyers S, et al. CCAAT enhancer-binding protein (C/EBP) and AML1 (CBF alpha2) synergistically activate the macrophage colony-stimulating factor receptor promoter. Mol Cell Biol. 1996;16:1231-1240.

245. Radomska HS, Huettner CS, Zhang P, Cheng T, Scadden DT, Tenen DG. CCAAT/enhancer binding protein alpha is a regulatory switch sufficient for induction of granulocytic development from bipotential myeloid progenitors. Mol Cell Biol. 1998;18:4301-4314.

246. Pabst T, Mueller BU, Harakawa N, et al. AML1-ETO downregulates the granulocytic differentiation factor C/EBPalpha in t(8;21) myeloid leukemia. Nat Med. 2001;7:444-451.

247. Vangala RK, Heiss-Neumann MS, Rangatia JS, et al. The myeloid master regulator transcription factor PU.1 is inactivated by AML1-ETO in t(8;21) myeloid leukemia. Blood. 2003;101:270-277.

248. Shaknovich R, Yeyati PL, Ivins S, et al. The promyelocytic leukemia zinc finger protein affects myeloid cell growth, differentiation, and apoptosis. Mol Cell Biol. 1998;18:5533-5545.

249. Gardini A, Cesaroni M, Luzi L, et al. AML1/ETO oncoprotein is directed to AML1 binding regions and co-localizes with AML1 and HEB on its targets. PLoS Genet. 2008;4:e1000275.

250. Park S, Chen W, Cierpicki T, et al. Structure of the AML1-ETO eTAFH domain-HEB peptide complex and its contribution to AML1-ETO activity. Blood. 2009;113:3558-3567.

251. Peterson LF, Yan M, Zhang DE. The p21Waf1 pathway is involved in blocking leukemogenesis by the t(8;21) fusion protein AML1-ETO. Blood. 2007;109:4392-4398.

252. Viale A, De Franco F, Orleth A, et al. Cell-cycle restriction limits DNA damage and maintains self-renewal of leukaemia stem cells. Nature. 2009;457:51-56.

253. Yergeau DA, Hetherington CJ, Wang Q, et al. Embryonic lethality and impairment of haematopoiesis in mice heterozygous for an AML1-ETO fusion gene. Nat Genet. 1997;15:303-306.

254. Okuda T, Cai Z, Yang S, et al. Expression of a knocked-in AML1-ETO leukemia gene inhibits the establishment of normal definitive hematopoiesis and directly generates dysplastic hematopoietic progenitors. Blood. 1998;91:3134-3143.

255. Yuan Y, Zhou L, Miyamoto T, et al. AML1-ETO expression is directly involved in the development of acute myeloid leukemia in the presence of additional mutations. Proc Natl Acad Sci U S A. 2001;98:10398-10403.

256. Higuchi M, O'Brien D, Kumaravelu P, Lenny N, Yeoh EJ, Downing JR. Expression of a conditional AML1-ETO oncogene bypasses embryonic lethality and establishes a murine model of human t(8;21) acute myeloid leukemia. Cancer Cell. 2002;1:63-74.

257. Schwieger M, Lohler J, Friel J, Scheller M, Horak I, Stocking C. AML1-ETO inhibits maturation of multiple lymphohematopoietic lineages and induces myeloblast transformation in synergy with ICSBP deficiency. J Exp Med. 2002;196:1227-1240.

258. de Guzman CG, Warren AJ, Zhang Z, et al. Hematopoietic stem cell expansion and distinct myeloid developmental abnormalities in a murine model of the AML1-ETO translocation. Mol Cell Biol. 2002;22:5506-5517.

259. Fenske TS, Pengue G, Mathews V, et al. Stem cell expression of the AML1/ETO fusion protein induces a myeloproliferative disorder in mice. Proc Natl Acad Sci U S A. 2004;101:15184-15189.

260. Miyamoto T, Weissman IL, Akashi K. AML1/ETO-expressing nonleukemic stem cells in acute myelogenous leukemia with 8;21 chromosomal translocation. Proc Natl Acad Sci U S A. 2000;97:7521-7526.

261. Yan M, Burel SA, Peterson LF, et al. Deletion of an AML1-ETO C-terminal NcoR/SMRT-interacting region strongly induces leukemia development. Proc Natl Acad Sci U S A. 2004;101:17186-17191.

262. Ahn EY, Yan M, Malakhova OA, et al. Disruption of the NHR4 domain structure in AML1-ETO abrogates SON binding and promotes leukemogenesis. Proc Natl Acad Sci U S A. 2008;105:17103-17108.

263. Ahn EY, Dekelver RC, Lo MC, et al. SON Controls Cell-Cycle Progression by Coordinated Regulation of RNA Splicing. Mol Cell;42:185-198.

264. Yan M, Kanbe E, Peterson LF, et al. A previously unidentified alternatively spliced isoform of t(8;21) transcript promotes leukemogenesis. Nat Med. 2006;12:945-949.

265. Roudaia L, Cheney MD, Manuylova E, et al. CBFbeta is critical for AML1-ETO and TEL-AML1 activity. Blood. 2009;113:3070-3079.

266. Banker DE, Radich J, Becker A, et al. The t(8;21) translocation is not consistently associated with high Bcl-2 expression in de novo acute myeloid leukemias of adults. Clin Cancer Res. 1998;4:3051-3062.

267. Schessl C, Rawat VP, Cusan M, et al. The AML1-ETO fusion gene and the FLT3 length mutation collaborate in inducing acute leukemia in mice. J Clin Invest. 2005;115:2159-2168.

268. Chou FS, Wunderlich M, Griesinger A, Mulloy JC. N-Ras(G12D) induces features of stepwise transformation in preleukemic human umbilical cord blood cultures expressing the AML1-ETO fusion gene. Blood;117:2237-2240.

269. Wang YY, Zhao LJ, Wu CF, et al. C-KIT mutation cooperates with full-length AML1-ETO to induce acute myeloid leukemia in mice. Proc Natl Acad Sci U S A;108:2450-2455.

270. Plevin MJ, Zhang J, Guo C, Roeder RG, Ikura M. The acute myeloid leukemia fusion protein AML1-ETO targets E proteins via a paired amphipathic helix-like TBP-associated factor homology domain. Proc Natl Acad Sci U S A. 2006;103:10242-10247.

271. Rice KL, Hormaeche I, Licht JD. Epigenetic regulation of normal and malignant hematopoiesis. Oncogene. 2007;26:6697-6714.

272. Blobel GA. CREB-binding protein and p300: molecular integrators of hematopoietic transcription. Blood. 2000;95:745-755.

273. Cai Y, Xu Z, Xie J, et al. Eto2/MTG16 and MTGR1 are heteromeric corepressors of the TAL1/SCL transcription factor in murine erythroid progenitors. Biochem Biophys Res Commun. 2009;390:295-301.

274. Kovall RA. More complicated than it looks: assembly of Notch pathway transcription complexes. Oncogene. 2008;27:5099-5109.

275. Ikawa T, Kawamoto H, Wright LY, Murre C. Long-term cultured E2A-deficient hematopoietic progenitor cells are pluripotent. Immunity. 2004;20:349-360.

276. Guo C, Hu Q, Yan C, Zhang J. Multivalent binding of the ETO corepressor to E proteins facilitates dual repression controls targeting chromatin and the basal transcription machinery. Mol Cell Biol. 2009;29:2644-2657.

277. Wei Y, Liu S, Lausen J, et al. A TAF4-homology domain from the corepressor ETO is a docking platform for positive and negative regulators of transcription. Nat Struct Mol Biol. 2007;14:653-661.

278. Schwartz R, Engel I, Fallahi-Sichani M, Petrie HT, Murre C. Gene expression patterns define novel roles for E47 in cell cycle progression, cytokine-mediated signaling, and T lineage development. Proc Natl Acad Sci U S A. 2006;103:9976-9981.

279. Semerad CL, Mercer EM, Inlay MA, Weissman IL, Murre C. E2A proteins maintain the hematopoietic stem cell pool and promote the maturation of myelolymphoid and myeloerythroid progenitors. Proc Natl Acad Sci U S A. 2009;106:1930-1935.

280. Liu Y, Cheney MD, Gaudet JJ, et al. The tetramer structure of the Nervy homology two domain, NHR2, is critical for AML1/ETO's activity. Cancer Cell. 2006;9:249-260.

281. Corpora T, Roudaia L, Oo ZM, et al. Structure of the AML1-ETO NHR3-PKA(RIIalpha) Complex and Its Contribution to AML1-ETO Activity. J Mol Biol.

282. Fukuda T, Yoshida T, Okada S, et al. Disruption of the Bcl6 gene results in an impaired germinal center formation. J Exp Med. 1997;186:439-448.

283. Dent AL, Shaffer AL, Yu X, Allman D, Staudt LM. Control of inflammation, cytokine expression, and germinal center formation by BCL-6. Science. 1997;276:589-592.

284. Ye BH, Cattoretti G, Shen Q, et al. The BCL-6 proto-oncogene controls germinal-centre formation and Th2-type inflammation. Nat Genet. 1997;16:161-170.

285. Li H, Ji M, Klarmann KD, Keller JR. Repression of Id2 expression by Gfi-1 is required for B-cell and myeloid development. Blood;116:1060-1069.

286. Bai X, Kim J, Yang Z, et al. TIF1gamma controls erythroid cell fate by regulating transcription elongation. Cell;142:133-143.